ORNL/TM-2020/1666

Thermal Neutron Scattering Evaluation of Yttrium Hydride: FY20 Progress

Chris W. Chapman
Kemal Ramić
Xunxiang Hu
Jesse M. Brown
Goran Arbanas
Alexander I. Kolesnikov
Douglass L. Abernathy
Luke Daemen
A. (Timmy) J. Ramirez-Cuesta
Yongqiang Cheng
Matthew B. Stone
Li (Emily) Liu
Yaron Danon

August 2020

M2TC-20OR0406014

Approved for public release. Distribution is unlimited.

OAK RIDGE NATIONAL LABORATORY
MANAGED BY UT-BATTELLE FOR THE US DEPARTMENT OF ENERGY

DOCUMENT AVAILABILITY

Reports produced after January 1, 1996, are generally available free via US Department of Energy (DOE) SciTech Connect.

Website www.osti.gov

Reports produced before January 1, 1996, may be purchased by members of the public from the following source:

National Technical Information Service
5285 Port Royal Road
Springfield, VA 22161
Telephone 703-605-6000 (1-800-553-6847)
TDD 703-487-4639
Fax 703-605-6900
E-mail info@ntis.gov
Website http://classic.ntis.gov/

Reports are available to DOE employees, DOE contractors, Energy Technology Data Exchange representatives, and International Nuclear Information System representatives from the following source:

Office of Scientific and Technical Information
PO Box 62
Oak Ridge, TN 37831
Telephone 865-576-8401
Fax 865-576-5728
E-mail reports@osti.gov
Website http://www.osti.gov/contact.html

This report was prepared as an account of work sponsored by an agency of the United States Government. Neither the United States Government nor any agency thereof, nor any of their employees, makes any warranty, express or implied, or assumes any legal liability or responsibility for the accuracy, completeness, or usefulness of any information, apparatus, product, or process disclosed, or represents that its use would not infringe privately owned rights. Reference herein to any specific commercial product, process, or service by trade name, trademark, manufacturer, or otherwise, does not necessarily constitute or imply its endorsement, recommendation, or favoring by the United States Government or any agency thereof. The views and opinions of authors expressed herein do not necessarily state or reflect those of the United States Government or any agency thereof.

ORNL/TM-2020/1666

Transformational Challenge Reactor Program

THERMAL NEUTRON SCATTERING EVALUATION OF YTTRIUM HYDRIDE: FY20 PROGRESS

Chris W. Chapman, Kemal Ramić, Xunxiang Hu, Jesse M. Brown, Goran Arbanas,
Alexander I. Kolesnikov, Douglass L. Abernathy, Luke Daemen, Anibal (Timmy) J. Ramirez-Cuesta,
Yongqiang Cheng, Matthew B. Stone, Li (Emily) Liu, Yaron Danon

Date Published: August 2020

M2TC-20OR0406014

Prepared by
OAK RIDGE NATIONAL LABORATORY
Oak Ridge, TN 37831-6283
managed by
UT-BATTELLE, LLC
for the
US DEPARTMENT OF ENERGY
under contract DE-AC05-00OR22725

CONTENTS

LIST OF FIGURES

LIST OF TABLES

ACKNOWLEDGMENTS

The authors would like to thank Dr. Olle Hellman for the help with s-TDEP method, as well as Victor Fanelli, Bekki Mills, and Andrew Payzant for their help in planning and coordinating the SNS experiments.

This research was sponsored by the TCR program of the US Department of Energy (DOE) Office of Nuclear Energy. This research used resources at Spallation Neutron Source, a DOE Office of Science (SC) user facility operated by ORNL. This research used resources of the National Energy Research Scientific Computing Center, which is a DOE SC user facility operated under Contract No. DE-AC02-05CH11231. Computational resources were also provided by the Rensselaer Polytechnic Institute Center for Computational Innovations, more specifically the Artificial Intelligence Multiprocessing Optimized System supercomputer. This research used resources of the Compute and Data Environment for Science at Oak Ridge National Laboratory, which is supported by DOE SC under Contract No. DE-AC05-00OR22725.

ABBREVIATIONS

AIMD	ab initio molecular dynamics
CCR	close-cycle refrigerator
DDXS	double differential scattering cross section
DFT	density functional theory
DOE	US Department of Energy
IFC	interatomic force constant
INS	inelastic neutron scattering
MD	molecular dynamics
NQE	nuclear quantum effect
ORNL	Oak Ridge National Laboratory
QHA	quasi-harmonic approximation
SNS	Spallation Neutron Source
s-TDEP	stochastic temperature-dependent effective potential
TCR	Transformational Challenge Reactor
TDEP	temperature-dependent effective potential
XRD	x-ray diffractometry

ABSTRACT

This paper details the thermal neutron scattering measurements of yttrium hydride for various hydrogen concentrations and temperatures that were conducted at the Spallation Neutron Source at Oak Ridge National Laboratory. Measurements at a temperature range of 5 to 1,200 K were conducted to determine the change in inelastic scattering as a function of temperature and to probe for any anharmonic effects known to exist in other metallic hydrides. Additionally, hydrogen concentrations of YH_x that range from $x = 1.62$ to 1.90 were measured to determine the effects of varying hydrogen concentration on the inelastic neutron spectra. Changes in temperature affected the inelastic spectra in unanticipated ways, indicating that there are anharmonic effects, whereas hydrogen concentration does not significantly affect the inelastic spectra. These measurements were compared against the ENDF/B-VIII.0 thermal scattering files of hydrogen in YH_2 and yttrium in YH_2, as well as a new thermal scattering file created by using the stochastic temperature-dependent effective potential (s-TDEP). Both libraries were found to be in good agreement with the experimental data at lower temperatures. At higher temperatures, the s-TDEP method is better at predicting the experimentally observed softening of phonon modes in acoustic and optical regions.

1. INTRODUCTION

Hydrogen is an ideal moderator material for use in nuclear reactor applications, and water is the most commonly used moderator. However, its application for high-temperature reactor systems above 400°C is limited to extremely high-pressure systems. In contrast, metal hydrides are uniquely suited for high-temperature reactor systems. Historically, ZrH was the preferred metal hydride for nuclear reactor applications due to its low absorption cross section, negative prompt temperature reactivity coefficient, and general availability. Yttrium hydride was not widely used due to the unavailability of high-purity yttrium and its much higher cost. Today, high-purity yttrium metal is available as an industrial metal, making it attainable. As a result, yttrium hydride has become the moderator of choice for high-temperature reactors due to its superior thermal stability indicated by its lower equilibrium hydrogen partial pressure and the higher attainable hydrogen concentration at high temperature (>1,100 K) [1, 2]. This is why yttrium hydride is being developed under various US Department of Energy (DOE) programs to serve as the moderator for microreactors and small module reactors [3]. One of these programs—the Transformational Challenge Reactor (TCR) program, which launched in 2019 at Oak Ridge National Laboratory (ORNL)—was created to leverage advances in novel materials, processing, and modeling to significantly reduce the time needed to iterate from conceptual design to nuclear regulatory qualification. Yttrium hydride was selected as the moderator material for the TCR program [4].

Moderating materials require special care when simulating thermal neutron scattering in neutron transport codes because, unlike traditional nuclear data that treat the nucleus as an isolated free gas atom, the de Broglie wavelength of the neutron becomes comparable with the interatomic distances of the materials, and crystal structure effects must be considered. Specific files (i.e., thermal scattering libraries) are required to describe these interactions. The ENDF/B-VIII.0 [5] library for yttrium hydride was developed with the implicit assumption that the phonon density of states (DOS) does not significantly change as a function of temperature [6]. This library was found to be in good agreement with room temperature total cross section measurements, but no comparison with differential scattering measurements was made nor were temperatures other than room temperature considered. Additionally, no effort was made to quantify the anharmonic effect known to exist in metallic hydrides [7] or to determine whether this effect would impact differential scattering measurements or the total cross section. Additionally, the hydrogen concentration dependence of the neutron scattering properties of YH_x are unknown, although it is critically important for the optimized design of reactors that use YH_x moderators with various hydrogen concentration.

The purpose of this work is twofold. The first purpose is to provide differential scattering cross section measurements that can be used to compare against the existing ENDF/B-VIII.0 yttrium hydride library. These measurements were obtained at the ORNL Spallation Neutron Source (SNS) at various temperatures by using YH_x with various hydrogen concentrations. The second is to explore new methods for generating a thermal neutron scattering library to account for these anharmonic effects on double differential neutron scattering cross sections. To accomplish this, the stochastic temperature-dependent effective potential (s-TDEP) method [8, 9, 10, 11] was used to calculate these features. A robust thermal neutron scattering library verified by critical experiments will facilitate more accurate neutron transport calculations for optimal reactor core designs.

Section 2 describes the yttrium hydride fabrication process, and Section 3 provides a brief overview of thermal neutron scattering theory, simulation, and experimental techniques. Section 4 discusses the experimental results and their comparison against the available ENDF/B-VIII.0 and s-TDEP simulations. Section 5 presents concluding thoughts and comments about future work.

2. YTTRIUM HYDRIDE FABRICATION

Yttrium hydride samples with various H/Y atomic ratios were fabricated through the direct interaction of ultrahigh purity metallic yttrium (nominal 99.99%, purchased from American Elements) and hydrogen at elevated temperature. Carefully matching the processing temperature and hydrogen partial pressure in the retort gives rise to the desired hydrogen concentration informed by the well-established thermodynamics of the Y-H binary system. Final hydrogen gas pressure was determined based on the desired H/Y atomic ratios of the hydrides. More details regarding the fabrication of the yttrium hydride are available in Schappel, Silva, and Terrani [12]. The hydrogen stoichiometry of the synthesized specimens was determined by using the weight change method. X-ray diffractometry (XRD) was also performed to identify the phases presented within the samples. A representative XRD pattern (i.e., $YH_{1.62}$) is shown in Figure 1. The solid solution of hydrogen in alpha yttrium, $YH_{0.235}$ (hexagonal close-packed crystal structure) [13], and delta-yttrium dihydride, $YH_{\sim 2}$ (face-centered cubic structure) [14] are both found in the fabricated hydride samples. The hydride samples with higher H/Y atomic ratios have a larger weight fraction of delta-phase yttrium hydride. The sample information and XRD results are summarized in Table 1.

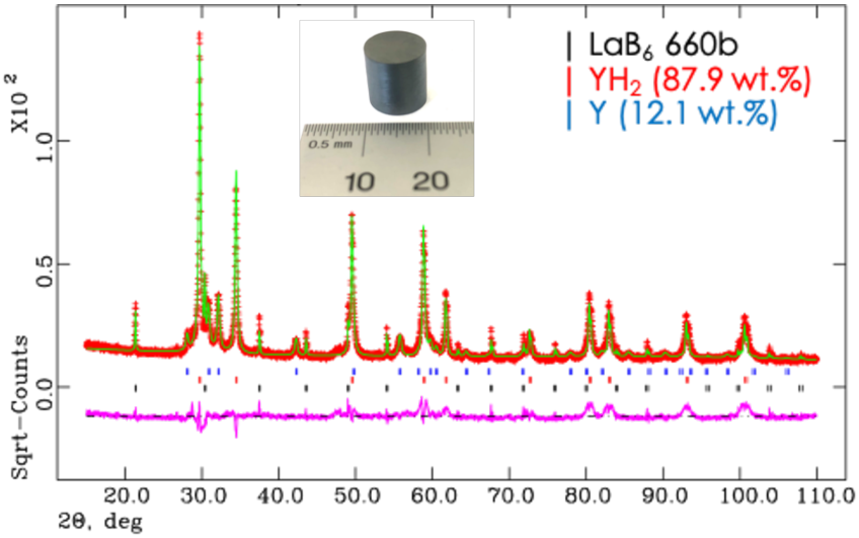

Figure 1. XRD pattern of $YH_{1.62}$ and Rietveld refinement fit. The picture of a $YH_{1.62}$ rod (10 mm in diameter, 15 mm tall) is also shown. LaB_6 is the standard material mixed with hydride powder in XRD and is not included in the yttrium hydride.

Table 1. XRD analysis of yttrium hydride samples for the thermal neutron scattering measurements at room temperature.

Samples	α-Y weight pct (%)	δ-YH_2 weight pct (%)	H concentration in δ-YH
$YH_{1.62}$	12.1	87.9	1.81
$YH_{1.68}$	11.6	88.4	1.87
$YH_{1.74}$	9.0	91.0	1.89
$YH_{1.86}$	4.2	95.8	1.93
$YH_{1.87}$	2.7	97.3	1.91
$YH_{1.90}$	2.1	97.9	1.94

The inelastic neutron scattering (INS) experiments were performed on three instruments at SNS—the Wide Angular-Range Chopper Spectrometer (ARCS) [15], the Fine-Resolution Fermi Chopper Spectrometer (SEQUOIA) [16], and the Vibrational Spectrometer (VISION) [17]—and their descriptions are given in Section 3.2. For SEQUOIA experiments, two bulk yttrium hydride rods that were 10 mm in diameter and 15 mm tall—$YH_{1.62}$ and $YH_{1.86}$—were fabricated first and then crushed into fine powder. To mitigate the hydrogen release at elevated temperature, an aluminum sample holder was used to contain the powder sample. The aluminum sample holder consists of an aluminum plate and cover (Al-6063). A specially designed aluminum gasket was used to enable the gas-tight sealing of the final assembly. The yttrium hydride powder was loaded in the area of 30 × 40 × 0.5 mm. An opening was available at the bottom of the aluminum plate for inserting a heating rod to enable the uniform temperature distribution across the sample holder, which was attached to the hot stage adapter at the bottom-loading close-cycle refrigerator (CCR) at SEQUOIA. During neutron scattering experiments, the sample in the sealed holder and aluminum heat shield were in a vacuum. This setup provides low neutron scattering background and allowed the sample temperature to be controlled from $T = 5$ to 800 K. Figure 2 shows pictures of the sample holder assembly before the holder was sealed. Similar aluminum sample holders were used for VISION measurements. Unlike the SEQUOIA measurements, the bottom heating element attachments were not needed due to the helium exchange gas in the top-loading CCR of VISION in which measurements were done at $T = 5$ and 293 K. These sample holders could be directly mounted to the CCR of the SEQUOIA and VISION instruments.

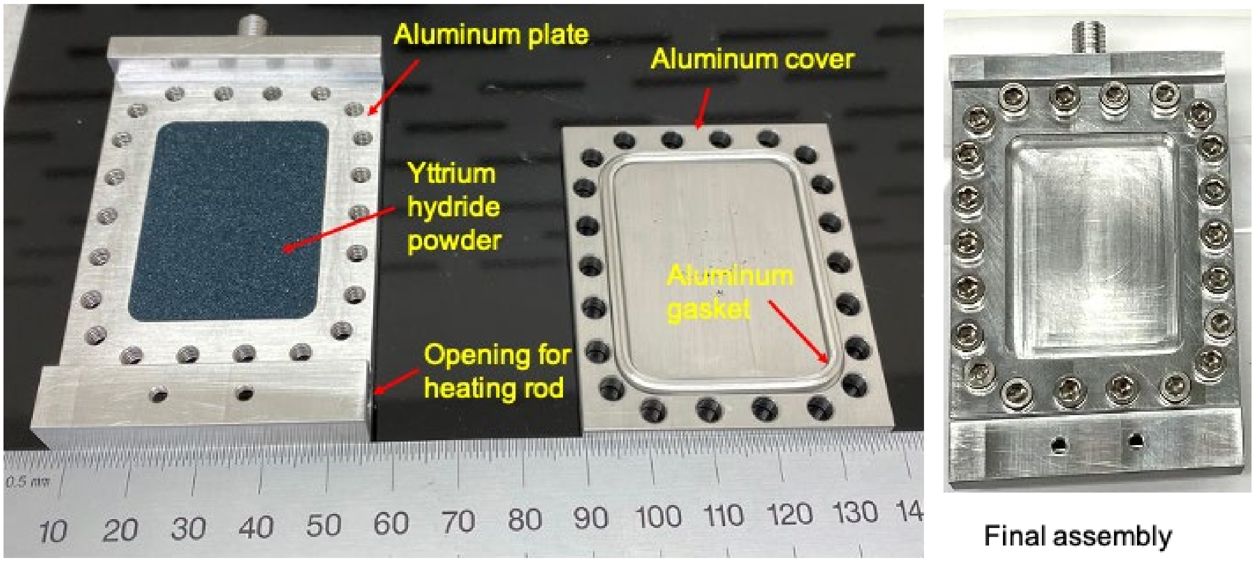

Figure 2. The aluminum sample holder parts and the final assembly.

For the high-temperature ARCS measurement (up to 1,200 K), a thin-wall low boron quartz tube (0.46 mm wall thickness and 9.07 mm inside diameter) was used to contain the 0.11 mm yttrium hydride foil. The 0.1 mm metallic yttrium foil was first loaded in the quartz tube, and then the assembly was placed in the retort of the TCR bulk metal hydriding system for hydrogen loading [12]. The quartz tubes were sealed after the successful fabrication of yttrium hydride. During the measurement, the quartz tube containing yttrium hydride foil was placed in a vanadium sample holder and mounted in the MICAS furnace installed at ARCS [18]. Figure 3 shows the thin-wall quartz tubes that contain yttrium hydride foils.

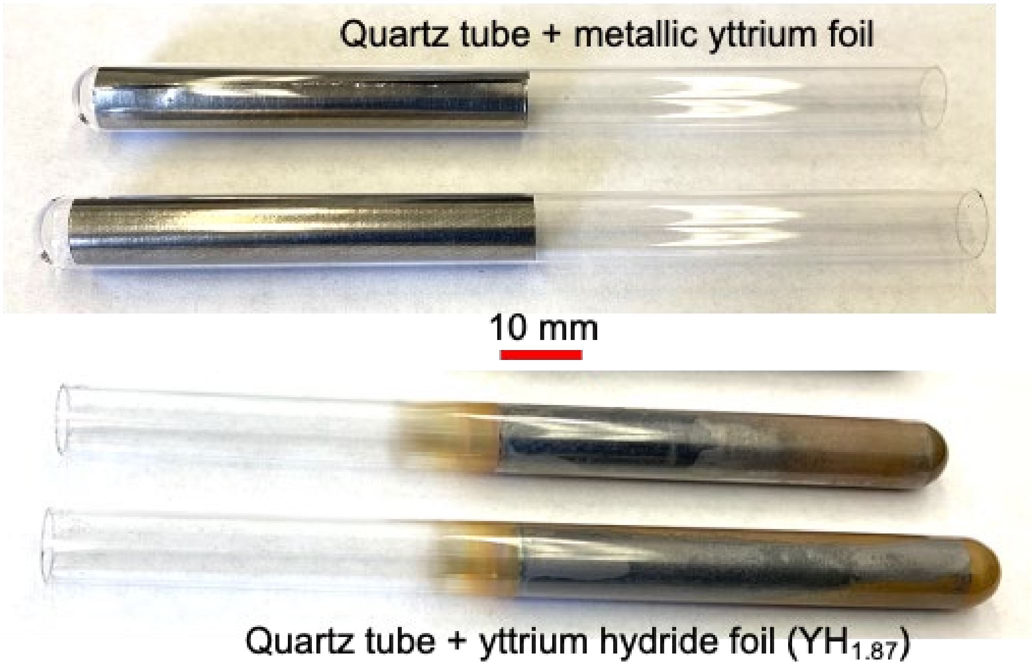

Figure 3. Quartz tubes containing yttrium foils and yttrium hydride foils.

3. THERMAL NEUTRON SCATTERING

3.1 THEORY

The theory of thermal neutron scattering experiments is extensively described in MacFarlane and Kahler [19] and in the authors' previous work [20, 21, 22]. Here, the authors focus on the most important parts of these studies. In the typical neutron scattering experiment, time-of-flight data are transformed to *S(Q,E)*, which is the dynamic structure factor, and *Q* and *E* are the neutron momentum and energy transfer. The double differential scattering cross section (DDXS) can be represented as:

$$\frac{d^2\sigma}{d\Omega dE} = \frac{\sigma_b}{4\pi}\frac{\boldsymbol{k'}}{\boldsymbol{k}} S(Q,E)\,, \qquad (1)$$

where **k'** and **k** are wavevectors of final and initial neutron states, respectively; Ω is the solid angle; and σ_b is the bound scattering cross section. In the ENDF/B-VIII.0 format, DDXS is represented as:

$$\frac{d^2\sigma}{d\mu dE} = \frac{\sigma_b}{2k_BT}\sqrt{\frac{E_f}{E_i}}\, e^{-\frac{\beta}{2}} S(\alpha,\beta), \tag{2}$$

where E_i and E_f are the incident and scattered neutron energies, respectively; μ is the cosine of the scattering angle; k_BT is the equilibrium temperature in electronvolts; α and β are unitless momentum and energy transfer, respectively; and $S(\alpha, \beta)$ is the scattering law. The transformation between $S(Q, E)$ and $S(\alpha, \beta)$ is as follows:

$$S(Q,E) = \frac{S(\alpha,\beta)}{k_BTe^{-T/(2k_BT)}}, \quad \alpha = \frac{\hbar^2Q^2}{2Am_nk_BT}, \quad \beta = -\frac{E}{k_BT}, \tag{3}$$

where m_n is the neutron mass, and A is the ratio of the scattering atom mass to the neutron mass. By using the LEAPR module of NJOY2016 [19], the $S(\alpha, \beta)$ can be calculated from the phonon spectrum, or *DOS*, by using:

$$S(\alpha,\beta) = \frac{1}{2\pi}\int_{-\infty}^{\infty} e^{i\beta\hat{t}} e^{-\gamma(\hat{t})} d\hat{t}, \tag{4}$$

With:

$$e^{-\gamma(\hat{t})} = \alpha \int_{-\infty}^{\infty} P(\beta)\left[1 - e^{i\beta\hat{t}}\right] e^{-\frac{\beta}{2}} d\beta, \tag{5}$$

where t^ is the time measured in units of ¯h/k_BT seconds, and $P(\beta)$ is dependent on the phonon spectrum, $\rho(\beta)$, as follows:

$$P(\beta) = \frac{\rho(\beta)}{2\beta\sinh(\beta/2)}. \tag{6}$$

3.2 EXPERIMENTAL TECHNIQUES

Three instruments—ARCS, SEQUOIA, and VISION—were used to measure the INS of the yttrium hydride samples at SNS. ARCS and SEQUOIA are direct geometry time-of-flight spectrometers in which an incident neutron energy is specified, and a spectra of final energies and scattering angles is measured. Both instruments use a Fermi chopper to define the energy of the incident neutrons. This is done by rotating the chopper at a specific frequency and phase relative to the timing of the pulsed source to allow through only the desired neutron energy. The neutrons then interact with the sample material, and the scattered neutrons are measured downstream at the detector bank.

For both instruments, incident energies of 45, 180, and 600 meV were selected for measurement. The incident energies of 45 and 180 meV were chosen based on previous calculations and measurements of the phonon DOS [23], which show significant contributions below 30 meV and between 100 to 150 meV. The 600 meV incident energy was chosen to measure multiple phonon scattering. For the purposes of these experiments, there are three primary differences between ARCS and SEQUOIA. The detector bank at SEQUOIA covers scattering angles from -30 to 60° in the horizontal plane and ±18° in the vertical plane. By comparison, ARCS covers angles from -28 to 135° in the horizontal plane and -27 to 26° in the vertical plane. Another difference is in the energy range and energy resolution available with these instruments. ARCS allows for incident neutron energies between 20 to 1,500 meV with a resolution at the elastic peak between 3 to 5%, whereas SEQUOIA can measure incident energies between 4 to 6,000 meV with an energy resolution between 1 to 5%. Finally, ARCS allows the high-temperature MICAS furnace to be used for measurements up to 1,600°C.

VISION is an indirect geometry vibrational spectrometer. Unlike a direct geometry spectrometer, VISION shines a white beam of neutrons on the sample, and the final energy is selected by setting detectors at specific angles that correspond to scattered energies of 4 meV. This results in a constant relative energy resolution of $\Delta E/E$ = 1.5%. There are two detector banks at VISION: a forward scattering bank at 45° (low *Q*) and a back scattering bank at 135° (high *Q*). At SEQUOIA, $YH_{1.86}$ was measured at 5, 295, 550, and 800 K. Additionally, $YH_{1.62}$ was also measured at 5 K. This additional measurement was done to investigate the differences in hydrogen concentration on the DDXS. $YH_{1.87}$ was measured at ARCS at temperatures of 295, 550, 800, 900, 1,000, 1,100, and 1,200 K. The higher temperatures represent the range of temperatures expected for normal TCR operations, and a description of any changes as a function of temperature is needed to accurately model the reactor. VISION was used to further analyze the differences in hydrogen concentration and measured $YH_{1.62}$, $YH_{1.74}$, $YH_{1.86}$, and $YH_{1.90}$, all at 5 and 293 K. A table detailing the samples used for each experiment is shown in Table 2.

Table 2. Sample information for thermal neutron scattering measurements.

SNS instrument	Samples	Sample form	Sample fixture	Mass (g)	Temperature (K)
SEQUOIA	$YH_{1.62}$	Powder	Aluminum plate and cover	0.6966	5
	$YH_{1.86}$			0.7020	5, 295, 550, 800
VISION	$YH_{1.62}$			0.6966	5, 293
	$YH_{1.74}$			0.6684	
	$YH_{1.86}$			0.7020	
	$YH_{1.90}$			0.7696	
ARCS	$YH_{1.68}$	0.1 mm hydride foil	Thin-wall quartz tube	1.6681	295, 550, 800, 900, 1,000, 1,100, 1,200
	$YH_{1.87}$			1.8937	

3.3 SIMULATION TECHNIQUES

The calculation of the phonon spectrum is not a straightforward task, and over time, different methodologies that use first principles or molecular dynamics (MD) have been presented. Codes such as PHONON [24] and Phonopy [25] use density functional theory (DFT) to perform lattice dynamics calculations in harmonic and quasi-harmonic approximation. More recently, codes such as MDANSE [26], Alamode [27], and PhononA [28] were developed to address anharmonicity in lattice dynamics calculations. In this work, anharmonicity and the temperature dependence of the phonon spectrum were addressed via the TDEP method [8, 9, 10], which is a collection of tools for finite temperature lattice dynamics. The main algorithm of the code extracts interatomic force constants (IFCs) from sets of displacements and forces them by fitting them to coefficients in an effective lattice dynamical Hamiltonian. Lattice dynamics theory shows that the displacement of the atom from its equilibrium position in the lattice changes the potential energy of the lattice. As the temperature changes, it disorders the lattice, changing the atomic positions of all atoms in the lattice. The total potential energy of the lattice can be modeled as a Taylor expansion of potential energy contributions at each atom's position in the lattice. For an atom *i* whose position is defined as displacement *ui* from an equilibrium position *Ri* + *τi*, in which *Ri* is the lattice vector and *τi* is the position in lattice:

$$\boldsymbol{r}_i = \boldsymbol{R}_i + \boldsymbol{\tau}_i + \boldsymbol{u}_i, \tag{7}$$

and the potential energy can be expended in terms of displacements as:

$$U(\{\boldsymbol{u}\}) = U_o + \sum_i \sum_\alpha \Phi_i^\alpha u_i^\alpha + \frac{1}{2!}\sum_{ij}\sum_{\alpha\beta}\Phi_{ij}^{\alpha\beta} u_i^\alpha u_j^\beta + \frac{1}{3!}\sum_{ijk}\sum_{\alpha\beta\gamma}\Phi_{ijk}^{\alpha\beta\gamma} u_i^\alpha u_j^\beta u_k^\gamma + \frac{1}{4!}\sum_{ijkl}\sum_{\alpha\beta\gamma\delta}\Phi_{ijkl}^{\alpha\beta\gamma\delta} u_i^\alpha u_j^\beta u_k^\gamma u_l^\gamma + \cdots, \tag{8}$$

where U_0 is the potential energy of the static lattice, and $\alpha\beta\gamma\delta$ are Cartesian indices. The coefficients of a Taylor series expansion, denoted by Φ, that are derivatives of potential energy with respect to the displacements of atoms are called *IFCs* or *Born-von Kármán force constants*. The basic idea of effective phonon theories is to sample a Born-Oppenheimer surface and produce an effective Hamiltonian. The crystal Hamiltonian is equal to:

$$\hat{H} = U_o + \sum_i \frac{\boldsymbol{p}_i^2}{2m_i} + \frac{1}{2!}\sum_{ij}\sum_{\alpha\beta}\Phi_{ij}^{\alpha\beta} u_i^\alpha u_j^\beta + \frac{1}{3!}\sum_{ijk}\sum_{\alpha\beta\gamma}\Phi_{ijk}^{\alpha\beta\gamma} u_i^\alpha u_j^\beta u_k^\gamma\ , \tag{9}$$

where p_i is the momentum, Φ_{ij} are the second-order IFCs, and Φ_{ijk} are third-order IFCs. The Born-Oppenheimer surface can be sampled by Born-Oppenheimer MD (i.e., ab initio MD [AIMD]) or by stochastic sampling [11]. Both methods produce displacements and forces that can be fitted to the effective Hamiltonian. For this work, stochastic sampling was used, as introduced in Shulumba, Hellman, and Minnich [11] and described in more detail in Kim et al. [29] in which nuclear quantum effects were also studied. In this work, only phonon spectra from second-order IFCs were studied, but the follow-up paper that is in preparation will study the effects of including third- and fourth- order IFCs while also including nuclear quantum effects, which are highly prevalent for materials that include hydrogen.

The approach to sampling the Born-Oppenheimer surface had two parts. The first part was calculating temperature-dependent lattice constants, and the second part was calculating forces generated from temperature-dependent stochastic samples. In both cases, VASP was used, which is a package for performing ab initio quantum-mechanical MD simulations with pseudopotentials or the projector-augmented wave method and a plane wave basis set [30, 31, 32]. For the force calculations, the GPU port of VASP [33, 34] was used.

A supercell of 96 atoms was used to calculate temperature-dependent lattice constants. Two methods were used; one calculated lattice constants from AIMD, and the second used the quasi-harmonic approximation (QHA), as implemented in Phonopy. Although the obtained values for lattice constants from AIMD were slightly undercalculated, the method served as a check for which the exchange-correlation function should be used for calculating forces. According to the "YH_2 Crystal Structure" data sheet [35], the density of YH_2 at 295 K is 4.27 g/cm^3. A set of 20 picoseconds simulations were performed with a time step of 1 femtosecond and NPT calculations with different exchange-correlation functionals at 295 K. The summary of calculated densities is shown in Table 3.

Table 3. The summary of calculated densities of YH_2 at 295 K using different exchange-correlation functionals.

Functional	Density (*g/cm^3*)	Standard deviation
LDA	4.42252	0.02712
GGA-PBE	4.19189	0.03206
GGA-PBE DFT-D2	4.37922	0.02813
GGA-PBE DFT-D3-BJ	4.33043	0.03189
GGA-rPBE	4.09662	0.02924
GGA-rPBE DFT-D3-BJ	4.35327	0.02978
GGA-BLYP	4.06174	0.02819
GGA-BLYP DFT-D2	4.36413	0.03151
GGA-PBEsol	4.32336	0.02729
GGA-AM05	4.30513	0.02871

The GGA-AM05 functional was chosen for subsequent calculations. To calculate the lattice constant at 5 K, the system was cooled over a period of 10 picoseconds, equilibriated for an initial 2 picoseconds, and then further equilibriated for 20 picoseconds to calculate the lattice constant. The lattice constant at 550 K was calculated by heating the 295 K structure over 10 picoseconds, with an initial equailibriation over 2 picoseconds followed by 20 picoseconds to calculate the lattice constant. Then, by using the same procedure, the lattice constant at 800 K was determined by heating from 550 to 800 K. The summary of lattice constants obtained from AIMD and QHA is shown in Table 4.

Table 4. The summary of lattice constants for YH_2 obtained from AIMD and QHA. The units are in Å.

Method	5 K	295 K	550 K	800 K
AIMD	5.16407782	5.18855749	5.2090923300	5.23391035
QHA	5.20380930	5.21000170	5.22406131	5.24407152

Lattice constants calculated via the QHA method—for which the value at 5 K was in line with the experimentally obtained value of 5.2032 Å at 90 K in Daou and Vajda [36]—were used to generate stochastic samples by the "canonical_configuration" module of TDEP at temperatures that correspond to the measurements. For force calculations, a 4 × 4 × 4 supercell was used with a primitive unit cell that had three atoms—one yttrium and two hydrogen atoms—for a total of 192 atoms. Force calculations were performed using a 5 × 5 × 5 k-points grid in VASP with the following parameters: IBRION = -1, ISIF = 2, Prec = Accurate, ENCUT = 500, EDIFF = 1.0E-9, ISMEAR = 2 with SIGMA = 0.01, IALGO = 38, ADDGRID = .TRUE., and LREAL = Auto flags. For the most accurate force calculation, it is desirable to use the LREAL = .FALSE. flag, but due to the use of a GPU VASP port, which only accepts LREAL = Auto or .TRUE., the authors had to settle with slightly less precise force calculations. They tried to compensate for this by performing an extra iteration of s-TDEP force calculations. *s-TDEP* is an iterative procedure that continues until the IFCs are converged. The authors started with two samples generated by the "canonical_configuration" module of TDEP, performed VASP forces calculations, and extracted IFCs by using TDEP. This was followed by generating four new stochastic samples by "canonical_configuration" with the IFCs from the two samples in a previous iteration. After VASP force calculations, 4 + 2 IFCs were extracted, eight new stochastic samples were generated, and this procedure was repeated until the IFCs converged. Complete IFC convergence was observed on the seventh iteration (i.e., 254 VASP force calculations).

Phonon dispersion relations can be calculated by using the "phonon_dispersion_relations" module of TDEP from second-order IFCs by calculating the eigenvalues and eigenvectors of the dynamical matrix over the Brillouin zone:

$$\omega_{\boldsymbol{q}}^2 \boldsymbol{\epsilon}_{\boldsymbol{q}} = \boldsymbol{\Phi}(\boldsymbol{q}) \boldsymbol{\epsilon}_{\boldsymbol{q}}, \tag{10}$$

where $\omega_{\boldsymbol{qs}}^2$ are the eigenvalues, $\boldsymbol{\epsilon}_{\boldsymbol{qs}}$ are eigenvectors, and the partial derivatives of the dynamical matrix are equal to:

$$\frac{\partial \boldsymbol{\Phi}(\boldsymbol{q})}{\partial q_\alpha} = \sum_{\boldsymbol{R}} \frac{i R_\alpha \boldsymbol{\Phi}_{\mathrm{ij}}(\boldsymbol{R})}{\sqrt{m_i m_j}} e^{i\boldsymbol{q}\cdot\boldsymbol{R}} \,. \tag{11}$$

The calculated phonon dispersion lines along the high symmetry points in the first Brillouin zone are shown in Figure 4. There are three lower energy acoustic modes and six higher energy optical modes. Vibrations of yttrium atoms are mostly responsible for acoustic modes, and vibrations of hydrogen atoms are dominant for optical modes.

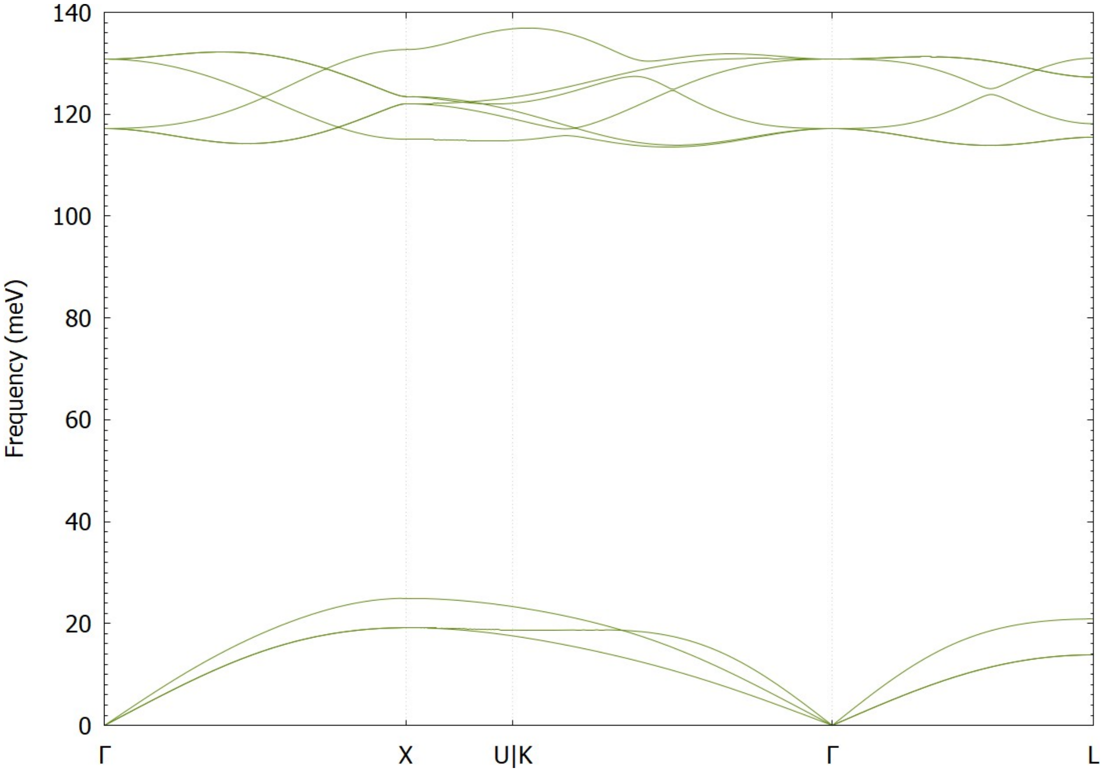

Figure 4.The calculated phonon dispersion lines at 5 K for YH$_2$ from the "phonon_dispersion_relations" module of TDEP. The symbols on the *x*-axis represent the high symmetry points in the first Brillouin zone.

The phonon DOS can also be calculated with the "phonon_dispersion_relations" module of TDEP by using:

$$g_s(\omega) = \frac{(2\pi)^3}{V}\int_{BZ}\delta\big(\omega - \omega_{\boldsymbol{q}s}\big)d\boldsymbol{q}\ , \tag{12}$$

for each vibrational mode, *s*. The atomic contribution for each atom *i* is:

$$g_i(\omega) = \frac{(2\pi)^3}{V}\sum_s\int_{BZ}\left|\epsilon_{\boldsymbol{q}s}^i\right|^2\delta\big(\omega - \omega_{\boldsymbol{q}s}\big)d\boldsymbol{q}, \tag{13}$$

which can be summed up to the total DOS. The total phonon spectrum with contributions from each vibrational mode (i.e., different colored lines under the total DOS curve) can be observed in Figure 5(a).

a) Total DOS with vibrational mode-projections

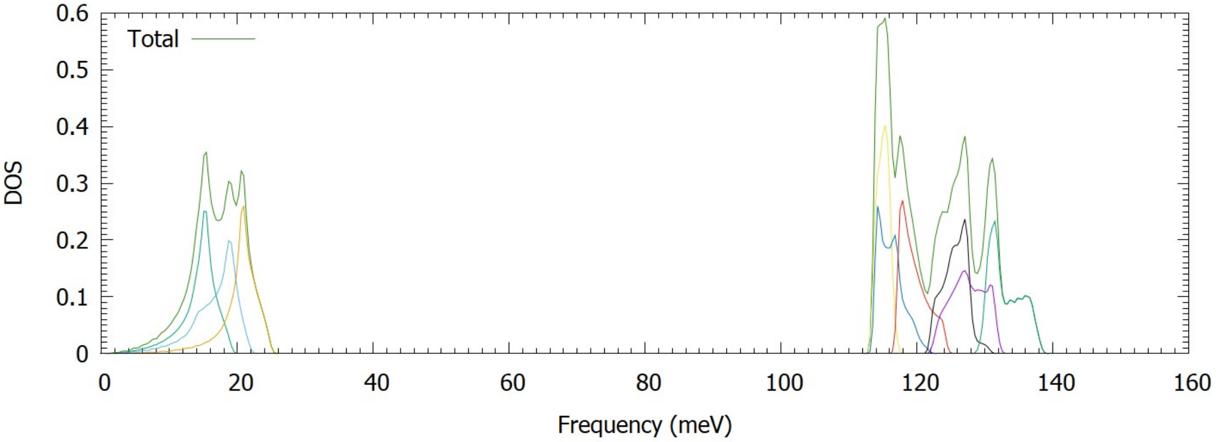

b) Total DOS comparison

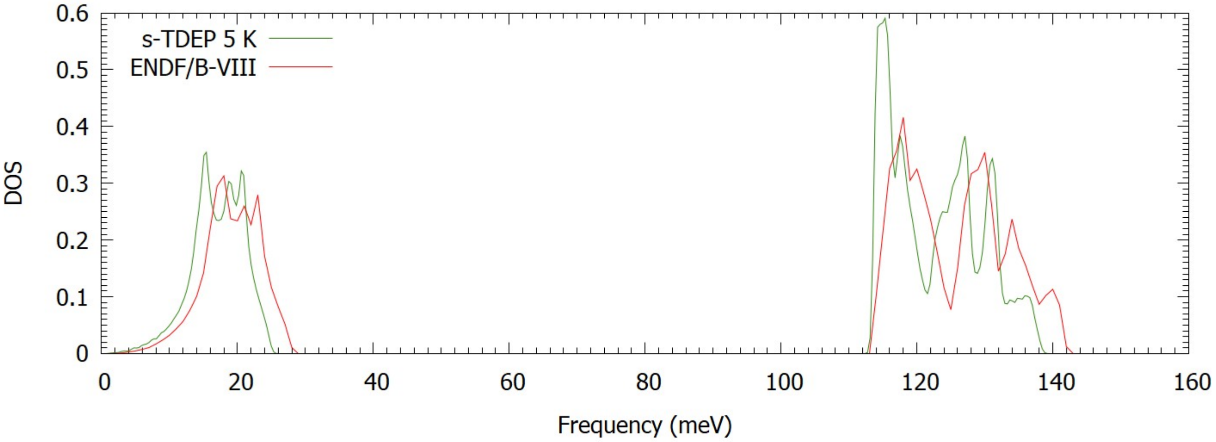

c) Total DOS comparison at different temperatures

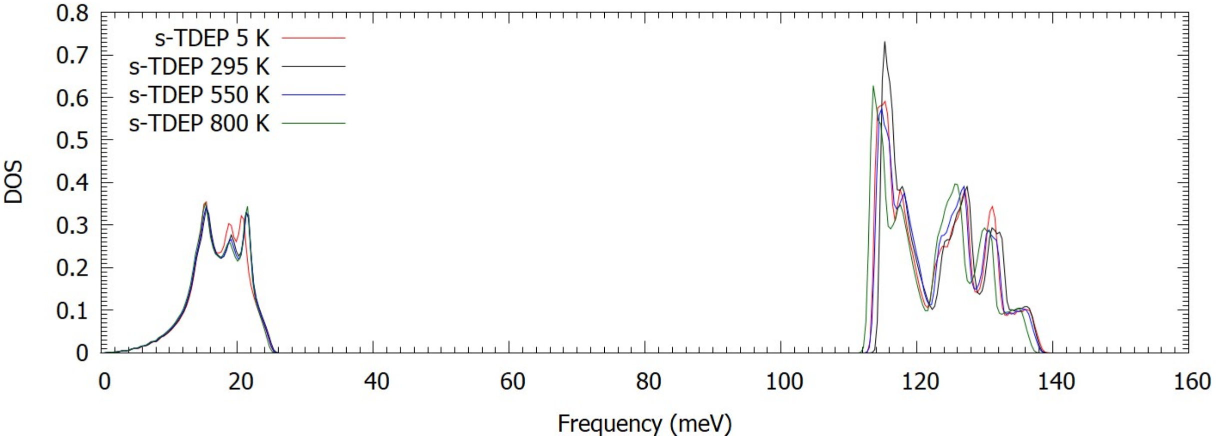

Figure 5. (a) The calculated phonon spectrum at 5 K. The green line corresponds to the total phonon density of states, and the other lines correspond to each vibrational mode. (b) The comparison between ENDF/B-VIII.0 phonon spectrum and s-TDEP phonon spectrum at 5 K. (c) The temperature dependence of s-TDEP-calculated phonon spectra.

The comparison between the current ENDF/B-VIII.0 library for YH_2 [6] and the s-TDEP-calculated phonon spectrum can be observed in Figure 5(b). The ENDF/B-VIII.0 phonon spectrum was notably calculated by using VASP and PHONON codes with a lattice constant of 5.2032 Å. The ENDF/B-VIII.0 library uses the same phonon spectrum to generate the thermal scattering law at different temperatures from 293.6 to 1,600 K. The goal of this work is to use TDEP to calculate the temperature dependence of the phonon spectrum and compare it with the experiments. s-TDEP-calculated phonon spectra at different temperatures can be observed in Figure 5(c).

Section 4.1.2 details the discussion regarding the differences between s-TDEP phonon spectra at different temperatures and the comparison with ENDF/B-VIII.0 phonon spectrum, aided by comparison with the measurements.

4. RESULTS

4.1 SEQUOIA AND ARCS

4.1.1 Experimental Data

A plot that shows the effect of temperature on the inelastic spectra of $YH_{1.86}$ is shown in Figure 6. To better compare multiple experiments in one plot, the dynamic structure factor is integrated over *Q*-space and normalized to unity. The large peak at energy transfer = 0 represents the elastic peak and is an expected feature. For all of these plots, the experimental uncertainties are too small to be displayed on the plots unless stated otherwise and thus are not shown. Additionally, plots of the 2D dynamic structure factor at each incident energy at 5 K are shown in Figure 7.

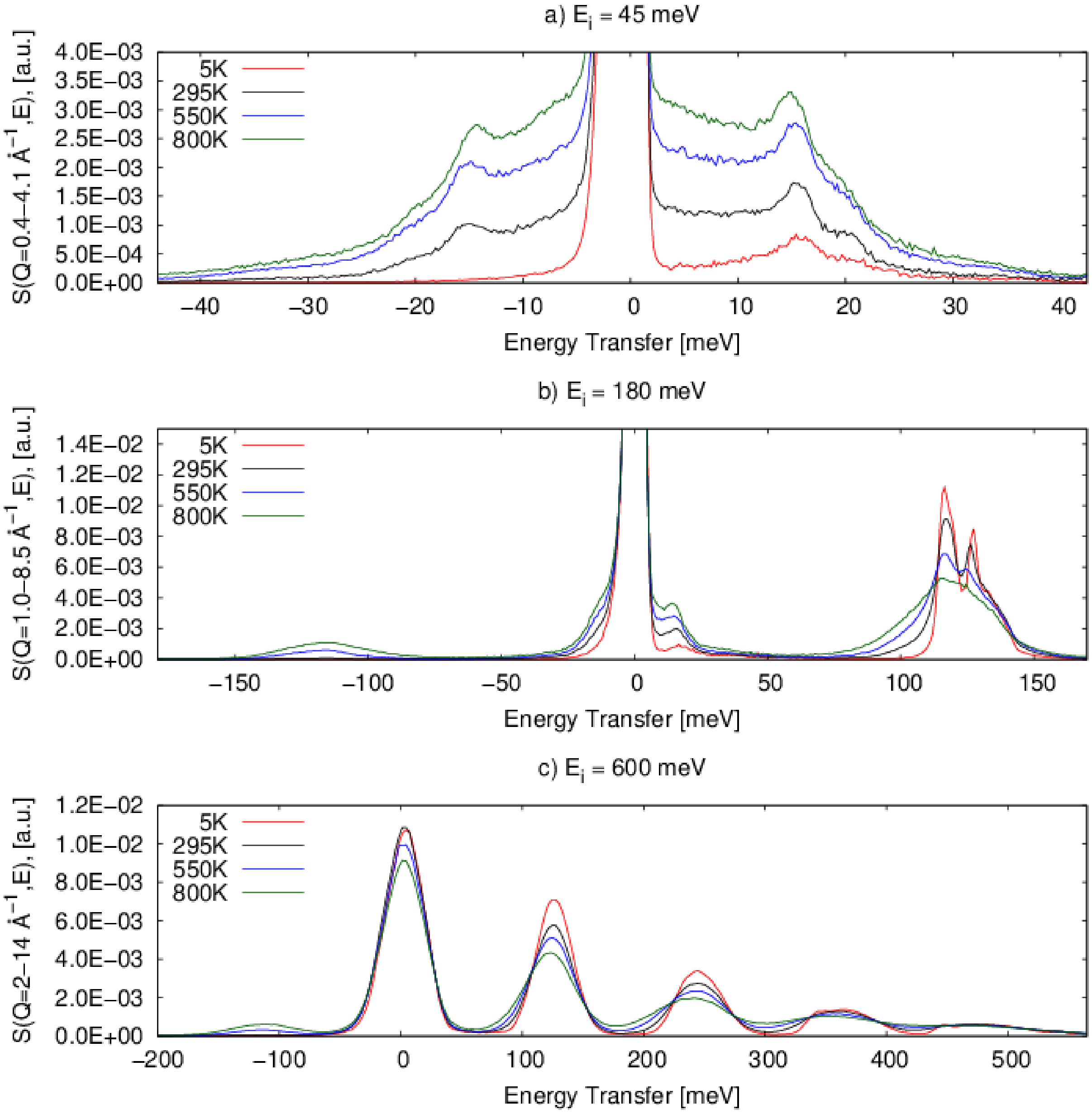

Figure 6. Temperature comparison of *Q*-integrated dynamic structure factor of $YH_{1.86}$ measured at SEQUOIA: (a) E_i = 45 meV, (b) E_i = 180 meV, and (c) E_i = 600 meV.

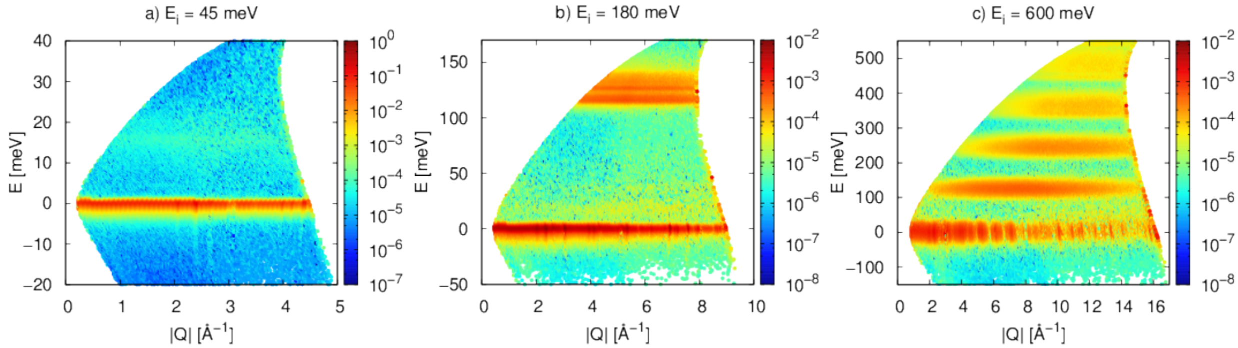

Figure 7. 2D mesh of the dynamic structure factors of $YH_{1.86}$ measured at SEQUOIA at 5 K for three incident energy measurements.

This work shows the expected features of the dynamic structure factor as temperature is increased, primarily that the higher temperature modes broaden out at positive energy transfer and a more pronounced mode at negative energy transfer. This is due to the difference in one-phonon scattering as a function of positive or negative energy transfer, described by:

$$S(Q,E>0) \sim e^{-\langle u_H^2(T)\rangle Q^2}[n(E,T)+1],$$
$$S(Q,E<0) \sim e^{-\langle u_H^2(T)\rangle Q^2}[n(E,T)], \qquad (14)$$

where $\langle u_H^2(T)\rangle$ is the mean squared displacement of hydrogen atoms, $e^{-\langle u_H^2(T)\rangle Q^2}$ is the Debye Waller factor, and $n(E,T)$ is the Bose population factor defined by:

$$n(E,T) = \left[e^{\frac{E}{k_B T}} - 1\right]^{-1}. \qquad (15)$$

The Bose population factor increases with temperature, but $n(E, T)$ will increase relatively more for neutron energy gain sites ($E < 0$) than $[n(E, T) + 1]$ for neutron energy lost sites ($E > 0$) because $n(E, T)$ is almost zero at low temperature ($T = 5$ K).

Figures 6(a) and 6(b) also show how the peak between 10 to 20 meV (i.e., the yttrium contribution to the spectra) increases as temperature increases, whereas the peaks between 100 to 150 meV (i.e., hydrogen contributions) decrease. Since the bound scattering cross section of hydrogen is much larger than for yttrium (82.02 b vs. 7.7 b), the spectra is mainly due to the scattering off of hydrogen. The 10–20 meV peak corresponds to yttrium vibrations, which cause hydrogen atoms to vibrate, whereas the 100–150 meV range corresponds solely to hydrogen vibrations. Since the Debye Waller factor for hydrogen is almost the same for all energies, this also due to the Bose population factor contributions because the Bose population factor has a larger impact on the 10–20 meV range than on the 100–150 meV range. All three plots also show that increasing temperature changes the location of some of the peaks. This is most noticeable in the 600 meV plot between 100 to 150 meV. This is due to changes in the lattice constants as a function of temperature, as discussed in Section 3.3.

A plot showing the Q-integrated spectra as a function of hydrogen concentration at 180 meV and 5 K is shown in Figure 8. From this plot, there appears to be only a small difference between the two different hydrogen concentrations. There could be a difference between the two in that the $YH_{1.62}$ has a larger peak around the 10–15 meV range and smaller peaks in the 100–150 meV range compared with $YH_{1.86}$. Since the spectra are both normalized to unity, this indicates that the alpha yttrium contribution is more prominent in samples with smaller hydrogen concentration. Also, since hydrogen is mostly contained in the delta phase, the real formula for the hydride phase should be delta-$YH_{1.81}$ for $YH_{1.62}$ and delta-$YH_{1.93}$ for $YH_{1.86}$. Therefore, the difference in hydrogen concentrations in the delta phases is 6.6%, as outlined in Table 1.

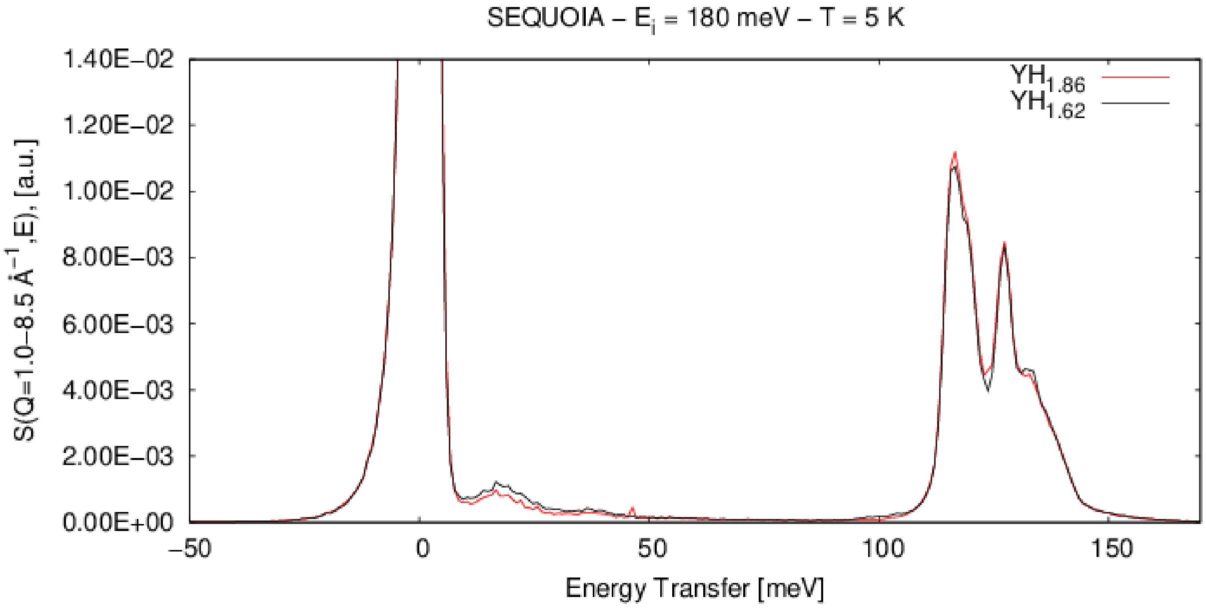

Figure 8. Hydrogen concentration comparison of *Q*-integrated dynamic structure factor of $YH_{1.62}$ and $YH_{1.86}$ for E_i = 180 meV at 5 K measured at SEQUOIA.

The INS spectra from the ARCS beamline as a function of temperature are shown in Figure 9. Again, the shifting of the peak locations noticed from the SEQUOIA measurements is shown, albeit more prominently since the maximum temperature of the ARCS experiments was 1,200 K. A comparison of the ARCS and SEQUOIA data for the same temperature and incident energy is shown in Figure 10 in which the range of *Q*-values available from ARCS are shown to be different compared with the range from SEQUOIA due to the wider angular array of detectors at ARCS. Another plot comparing the spectra measured at the two spectrometers is shown in Figure 11 in which the *Q*-integrated spectra between the two are shown to be comparable with a few exceptions. The elastic peak is wider in the ARCS data because ARCS generally has a broader energy resolution. This can also be seen in the E_i = 180 meV plot at around 20 meV in which the acoustic peak is more noticeable in the SEQUOIA data than the ARCS data.

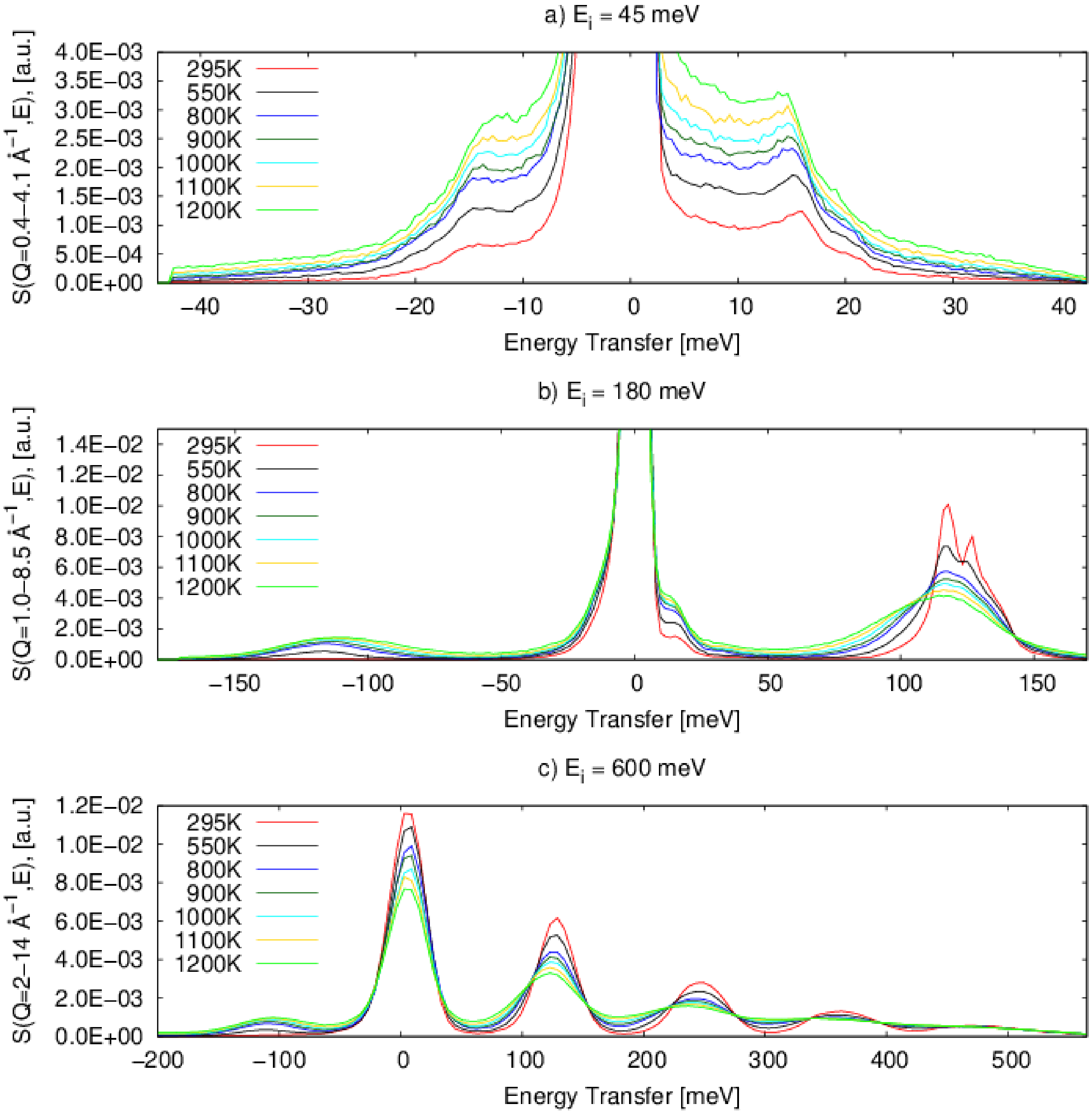

Figure 9. Temperature comparison of *Q*-integrated dynamic structure factor of $YH_{1.87}$ measured at ARCS.

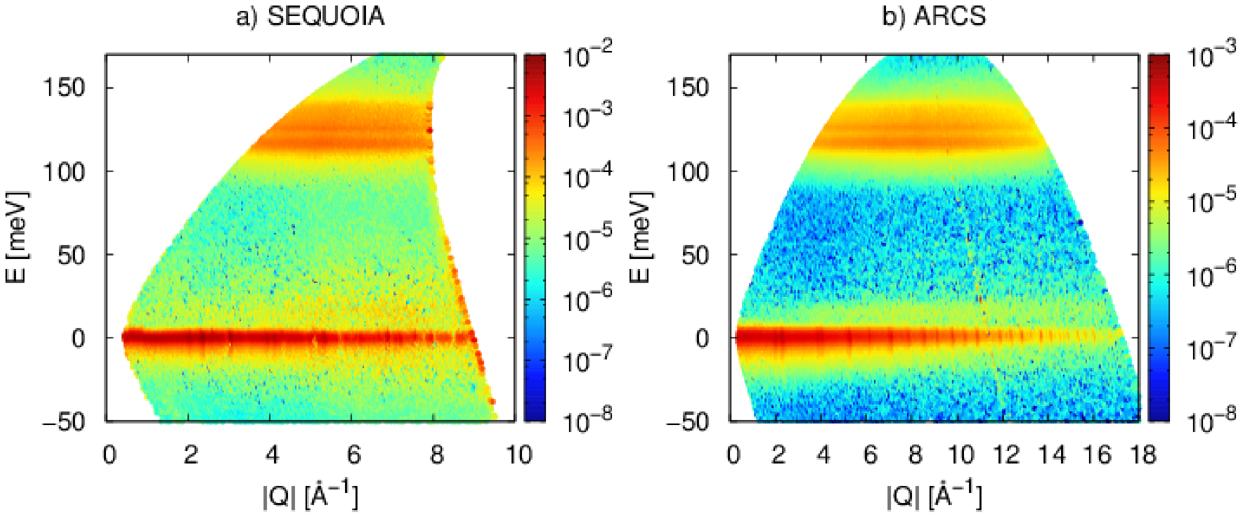

Figure 10. Instrument comparison of the 2D mesh of the dynamic structure factors at 295 K measured for E_i=180 meV neutrons of (a) $YH_{1.86}$ at SEQUOIA and (b) $YH_{1.87}$ at ARCS.

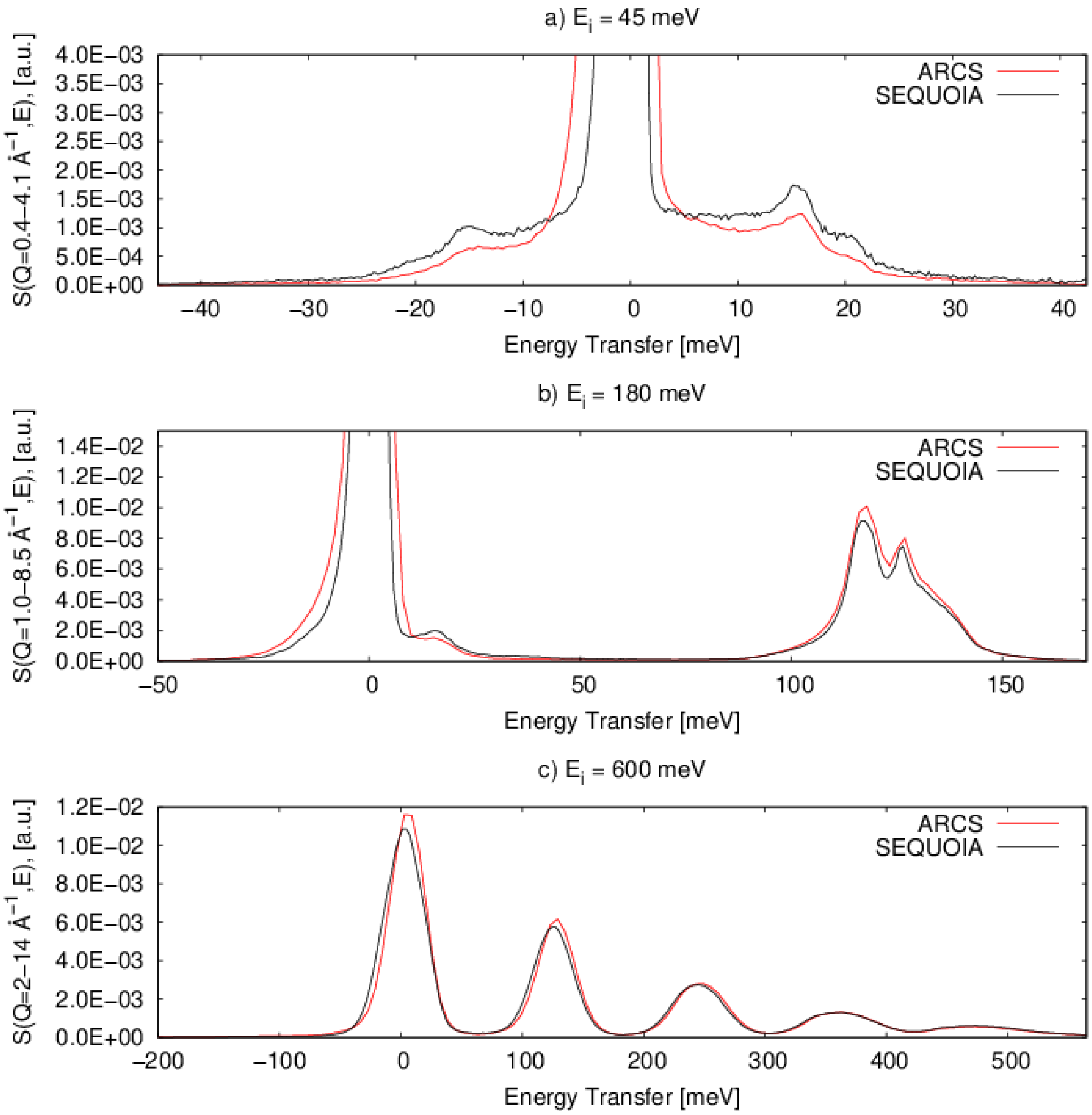

Figure 11. Instrument comparison of *Q*-integrated dynamic structure factors at 295 K for $YH_{1.86}$ at SEQUOIA and $YH_{1.87}$ at ARCS.

4.1.2 Simulation of Measured Data

To compare the experimental data, ENDF/B-VIII.0 library, and s-TDEP-calculated library, the SEQUOIA experimental setup was simulated in MCNP6.1 [37], as was done in Chapman et al. [20] and Ramić et al. [21, 22]. An improved resolution function was implemented in comparison with the previous model that used a Gaussian resolution function. A neutron beam profile at each incident energy was calculated by using MCViNE [38], which was used as an input to the MCNP6.1 calculation, and the respective resolution parameters for the SEQUOIA instrument were applied to the DDXS obtained from MCNP6.1. Thermal scattering libraries at different temperatures in ACE format for MCNP6.1 were calculated from respective phonon spectra with NJOY2016.

Figures 12, 13, 14, and 15 show the comparison between the experiments and MCNP-calculated DDXS from ENDF/B-VIII.0 and s-TDEP phonon spectra at 5, 295, 550, and 800 K. Figures 12(a), 13(a), 14(a), and 15(a) show that the acoustic peak locations are slightly under-calculated. This can also be observed in the comparison between ENDF/B-VIII.0 and the s-TDEP phonon spectra in Figure 5(b). From Figures 12(a), 13(a), 14(a), and 15(a), it can also be inferred that the locations of the acoustic peaks are shifted to lower energies with the rising temperature and thus are over-calculated by the ENDF/B-VIII.0 library at higher temperatures. The shifts in the acoustic phonon peak locations as a function temperature with $E_i = 45$ meV can be also observed in Figures 6(a) and 9(a). At 180 meV incident energy, Figures 6(b) and 9(b) also show shifts in the optical peaks to lower energy (i.e., “softening”) as the temperature increases from 295 to 1,200 K.

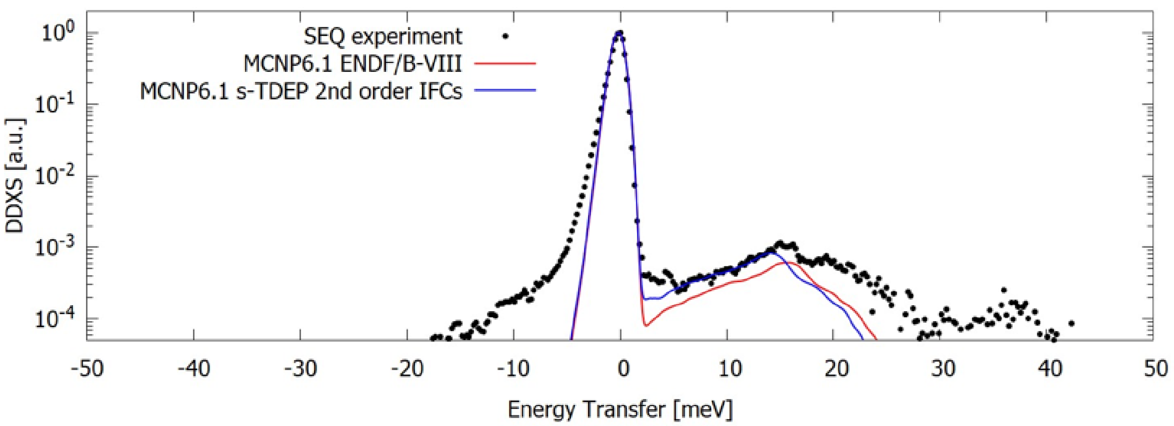
a) Comparison - E_i=45 Theta=25° T=5 Kelvin

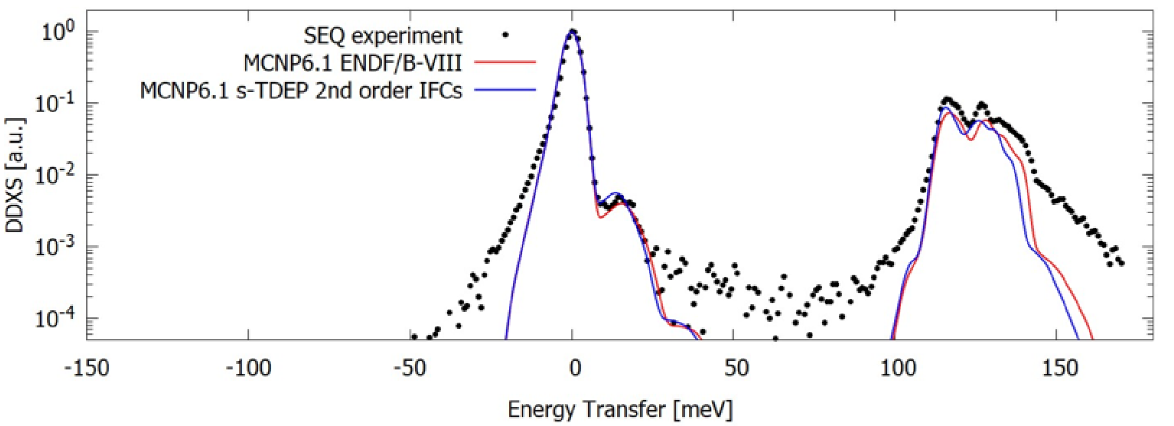
b) Comparison - E_i=180 Theta=25° T=5 Kelvin

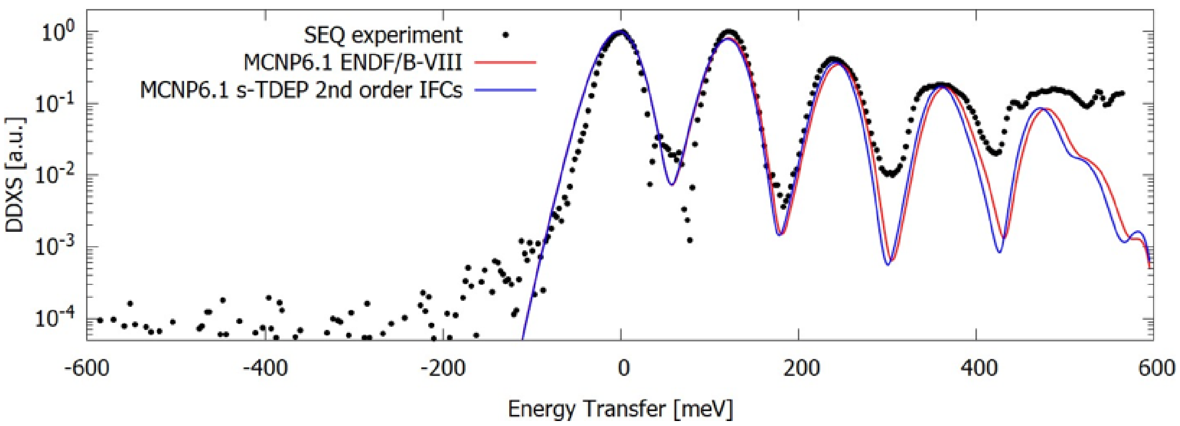
c) Comparison - E_i=600 Theta=25° T=5 Kelvin

Figure 12. DDXS comparison between ENDF/B-VIII.0 and s-TDEP at 5 K, 25° scattering angle, and 45, 180, and 600 meV incident energies.

a) Comparison - E_i=45 Theta=25° T=295 Kelvin

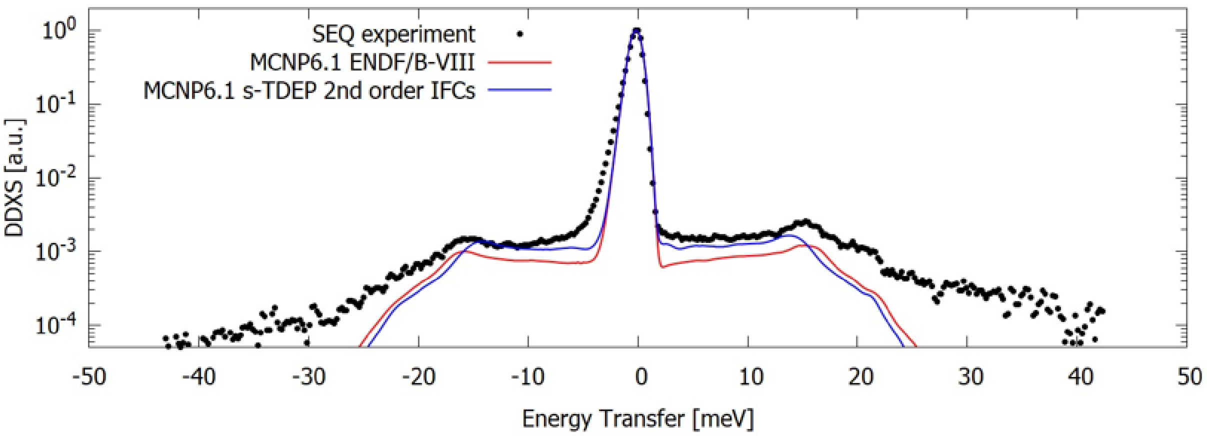

b) Comparison - E_i=180 Theta=25° T=295 Kelvin

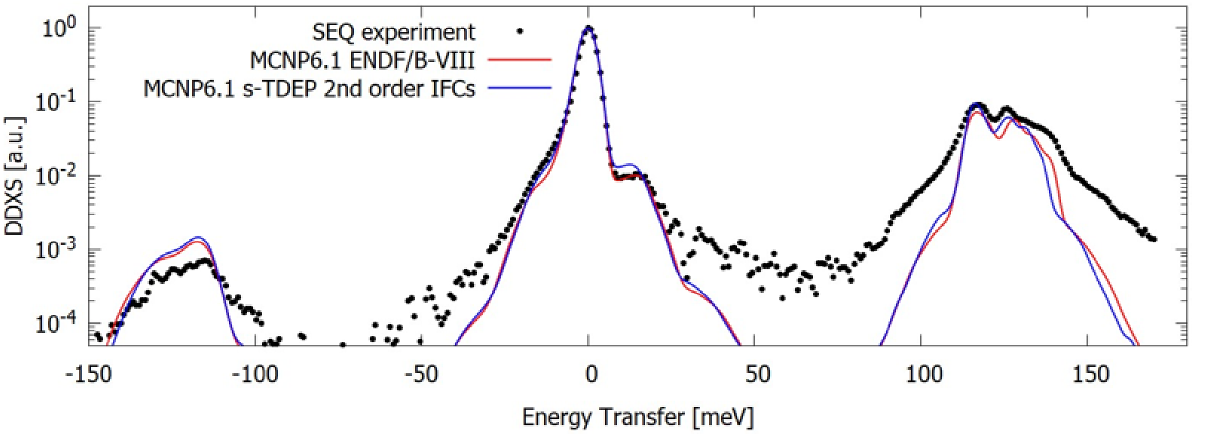

c) Comparison - E_i=600 Theta=25° T=295 Kelvin

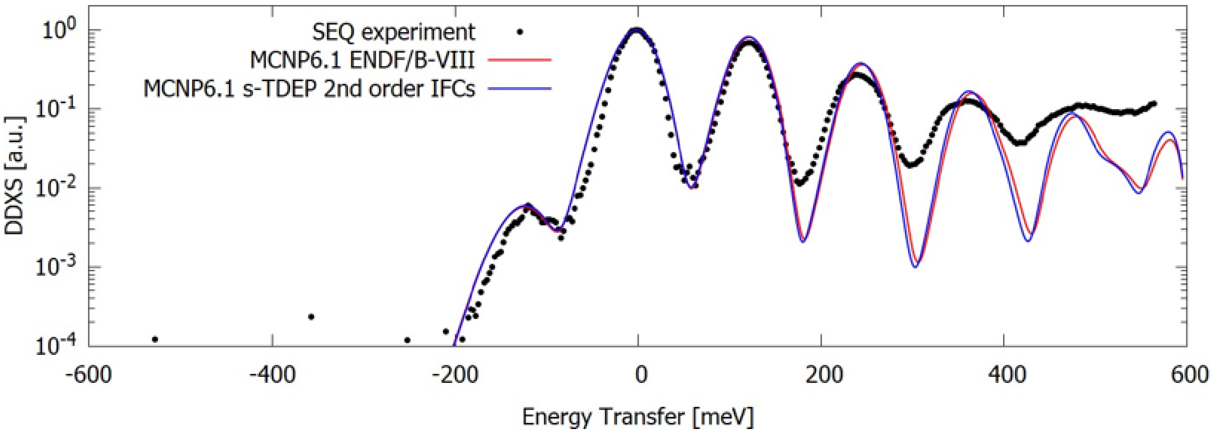

Figure 21. DDXS comparison between ENDF/B-VIII.0 and s-TDEP at 295 K, 25° scattering angle, and 45, 180, and 600 meV incident energies.

a) Comparison - E_i=45 Theta=25° T=550 Kelvin

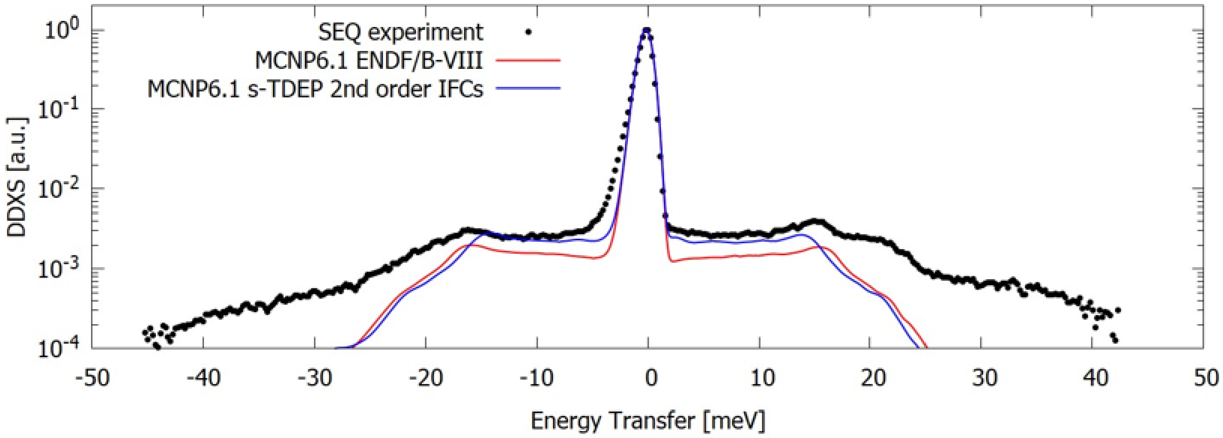

b) Comparison - E_i=180 Theta=25° T=550 Kelvin

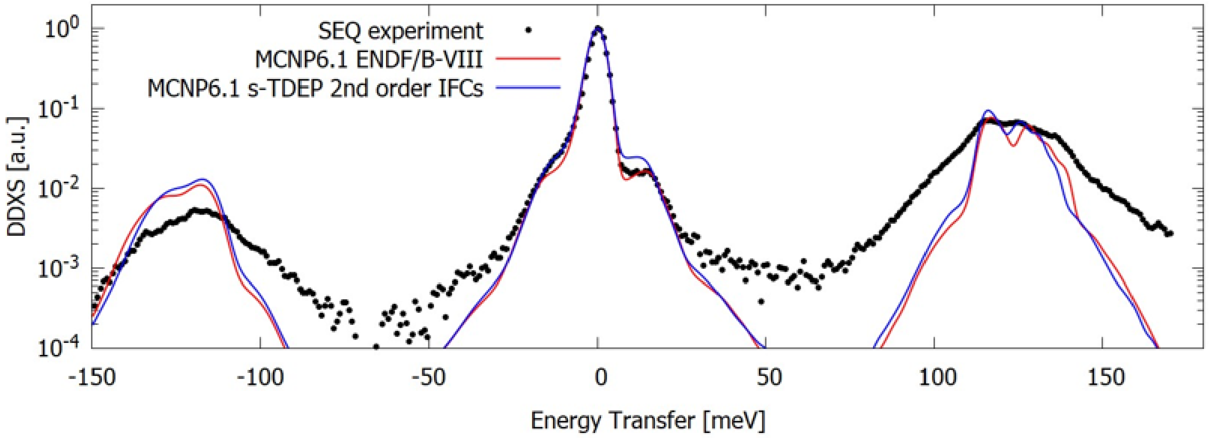

c) Comparison - E_i=600 Theta=25° T=550 Kelvin

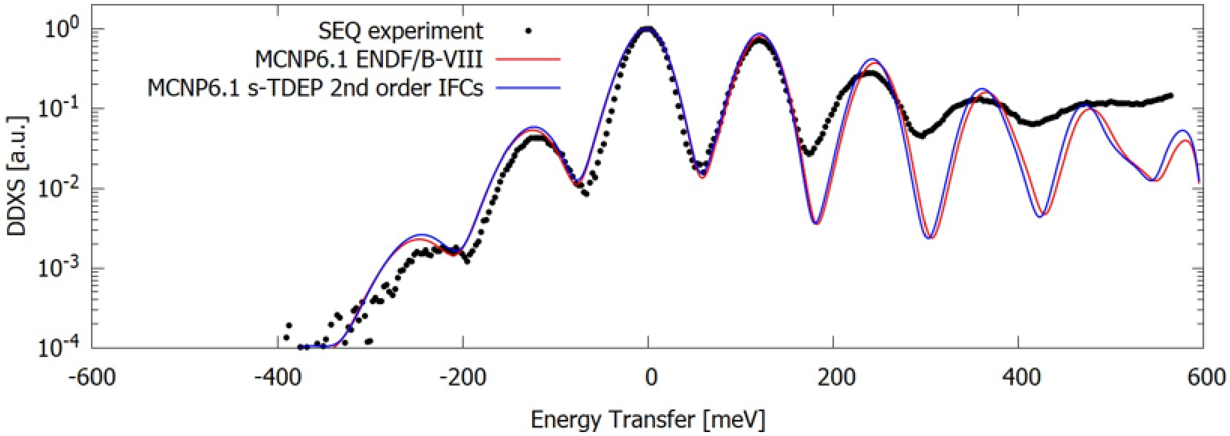

Figure 22. DDXS comparison between ENDF/B-VIII.0 and s-TDEP at 295 K, 25° scattering angle, and 45, 180, and 600 meV incident energies.

a) Comparison - E_i=45 Theta=25° T=800 Kelvin

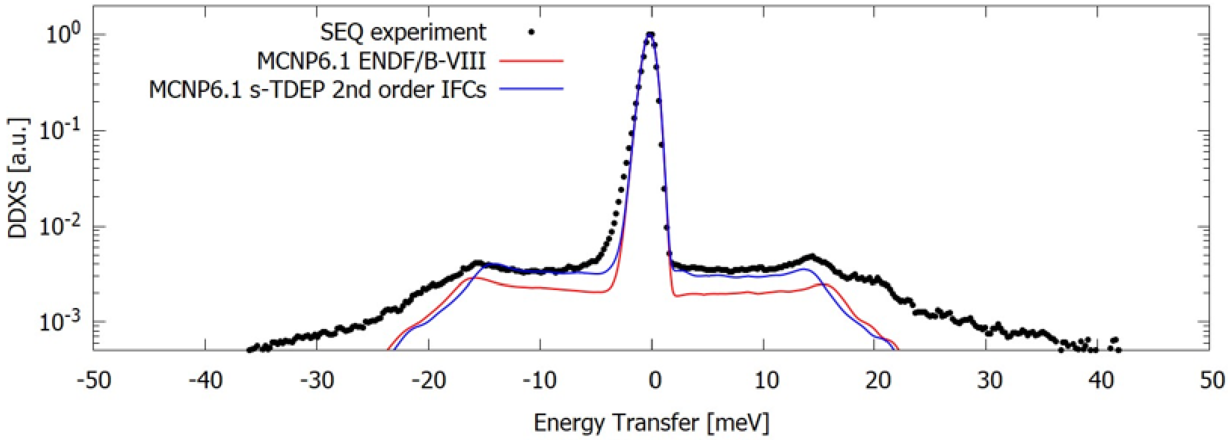

b) Comparison - E_i=180 Theta=25° T=800 Kelvin

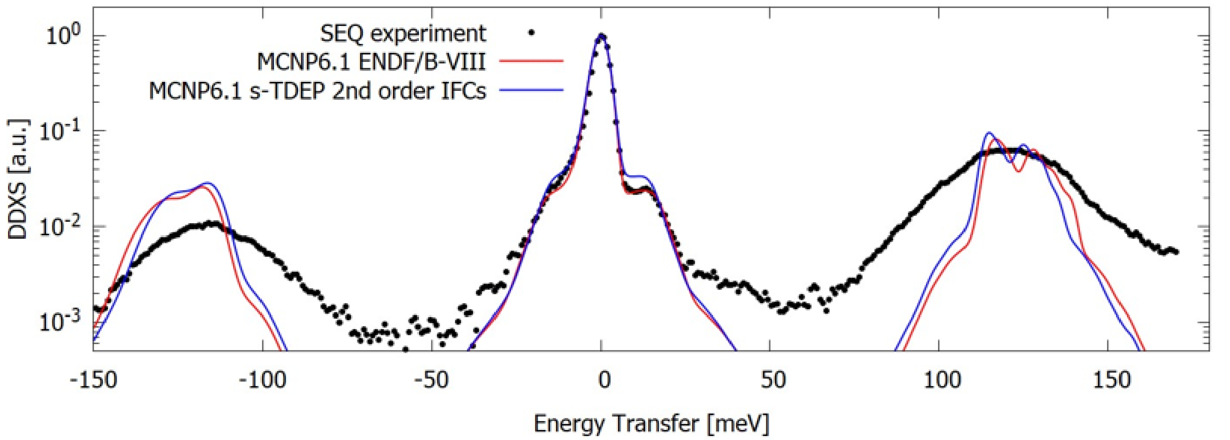

c) Comparison - E_i=600 Theta=25° T=800 Kelvin

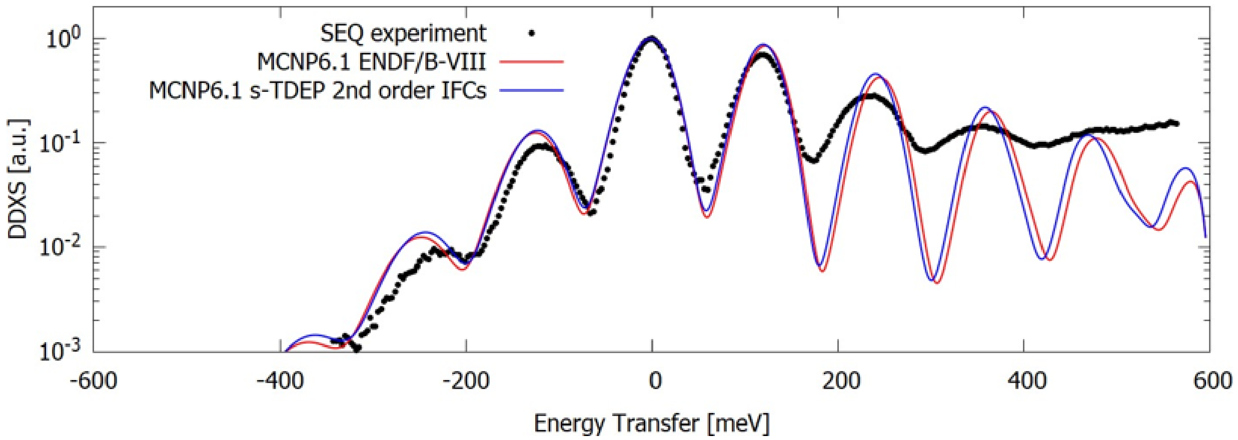

Figure 23. DDXS comparison between ENDF/B-VIII.0 and s-TDEP at 295 K, 25° scattering angle, and 45, 180, and 600 meV incident energies.

Each data trend, from 5 to 800 K, can be observed in s-TDEP-calculated phonon spectra in Figure 5(c)—although 5 and 295 K phonon spectra slightly under-calculate the location of the first peak in the optical region in comparison with the experimental data—and in the DDXS calculated data in Figures 12(b), 13(b), 14(b), and 15(b). At 600 meV incident energy, the multiple phonon scattering contributions to DDXS spectra are observed. From Figures 12(c), 13(c), 14(c), and 15(c), the fundamental mode with a peak around 130 meV is observed to be calculated correctly, whereas the overtones are slightly shifted to higher energies. This is mostly due to the anharmonicity of YH_x, which is not replicated by the LEAPR module of NJOY2016. When calculating multiple phonon contributions, LEAPR convolutes the fundamental mode phonon spectrum with itself. In Figures 12(b), 13(b), 14(b), and 15(b), the authors noted that they should be able to observe the shifts of optical peaks to lower energies as temperature increases, but that is even more pronounced in Figures 12(c), 13(c), 14(c), and 15(c). The trend can be observed in the first fundamental peak around 130 meV but is even more clear in the overtones in which the shift to lower energies is more pronounced.

An χ^2 test with respect to the experimental data was performed at each incident energy and temperature combination for MCNP-calculated DDXS for which the MCNP calculations were performed for 11 scattering angles from 5 to 55°, and the average values for χ^2 summed over all angles at respective combinations of incident energies and temperatures are presented in Table 5. Averaged over all combinations of incident energies and temperatures, ENDF/B-VIII.0 χ^2 is slightly lower than the s-TDEP χ^2 value, but that is mainly due to χ^2 contributions at 180 meV incident energies, which are consistently higher for s-TDEP than ENDF/B-VIII.0. For 45 and 600 meV incident energies, the χ^2 value for s-TDEP is lower than for ENDF/B-VIII.0 across all the temperatures except the outlier for 45 meV at 5 K. The biggest discrepancy in χ^2 at 180 meV incident energies is at 295 K, and χ^2 contributions at each individual data point can be observed in Figure 16.

Table 5. The summary of χ^2 values calculated for ENDF/B-VIII.0 and s-TDEP DDXS curves with respect to the experimental data across all combinations of temperatures and incident energies.

Temperature (K)	E_i (meV)	ENDF/B-VIII.0 χ^2	s-TDEP χ^2
5	45	0.10776	0.10878
	180	0.07133	0.08381
	600	0.41791	0.36023
295	45	0.15404	0.14944
	180	0.08614	0.43259
	600	0.24711	0.24260
550	45	0.16540	0.15563
	180	0.12711	0.15673
	600	0.23640	0.23091
800	45	0.16119	0.14555
	180	0.19037	0.23393
	600	0.26430	0.24877
	Average:	0.18575	0.21241

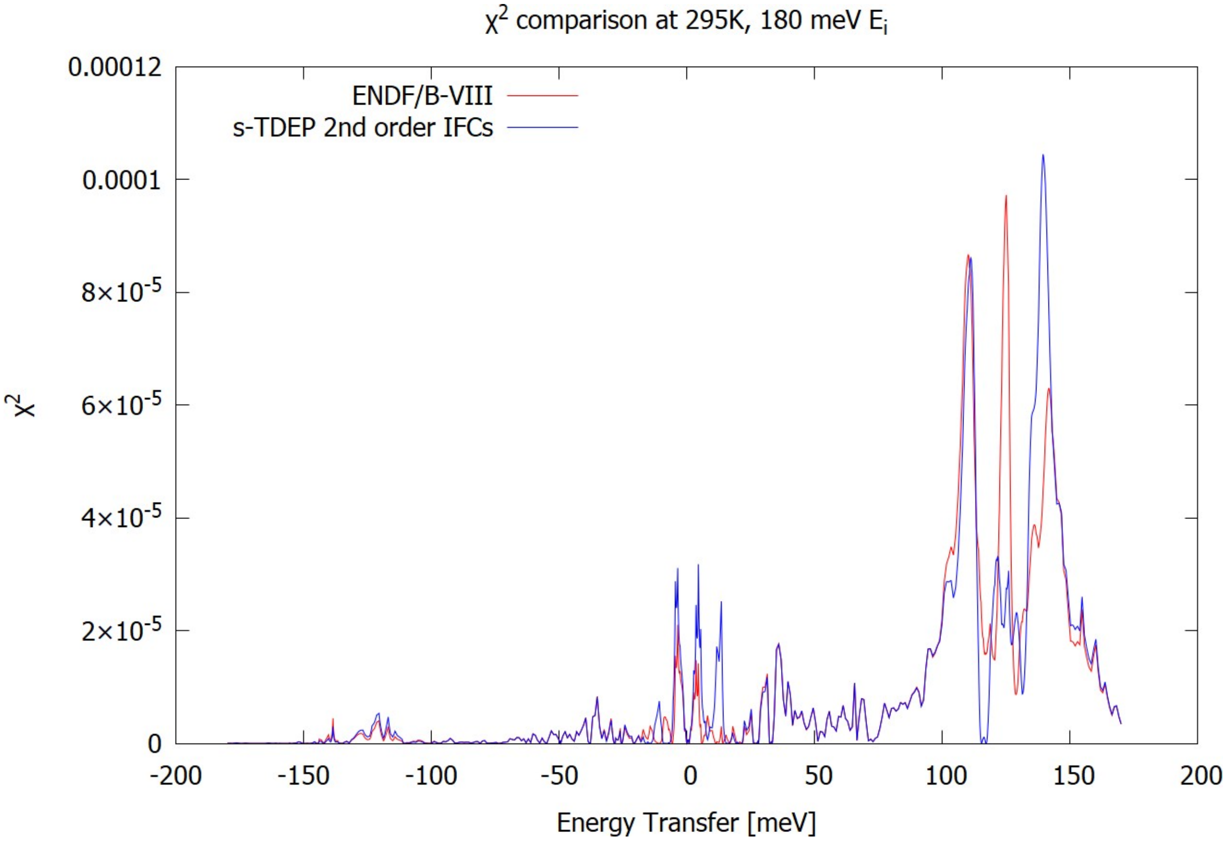

Figure 16. χ^2 individual data point comparison between ENDF/B-VIII.0 and s-TDEP at 295 K, 25° scattering angle, and 180 meV incident energy.

As shown in Figure 16, the biggest contribution for s-TDEP χ^2 comes in the 0–20 meV range in which the acoustic peak is being under-calculated and in the 130–150 meV range in which the width of the optical vibrational region is narrower than in ENDF/B-VIII.0 phonon spectrum. Figures 12(b) and 13(b) show that s-TDEP is better at calculating the location of the second peak in the optical region (around 126 meV), which ENDF/B-VIII.0 places around 128.2 meV. This means that the reason for better χ^2 values at 180 meV (i.e., the bigger width of the optical region in ENDF/B-VIII.0) is not physically accurate. The authors' preliminary work on the phonon spectra from third- and fourth-order IFCs, which will be published in the follow-up paper that is in preparation, shows that those contributions from higher order terms in Taylor expansion for potential energy account for the increased width of the vibrational region, and hence the χ^2 test by itself should not be used as the final measure of performance for these thermal scattering libraries in neutron transport calculations for the DDXS calculated from the phonon spectra from second-order IFCs. In the authors' previous works [21, 22], they show that how these libraries calculate the total cross section it is more important. The authors are currently planning total cross section measurements to be performed at the Rensselaer Polytechnic Institute Linear Accelerator for different hydrogen concentrations in YH_x and across a similar temperature range as performed in this work. Although s-TDEP and ENDF/B-VIII.0 perform similarly at lower temperatures, s-TDEP does a better job at higher temperatures, especially at 800 K, due to the shifts of acoustical and optical regions to lower energies. This is also pronounced at higher temperatures up to 1,200 K, and s-TDEP in the preliminary results at these temperatures also leads to improvement compared with ENDF/B-VIII.0.

4.2 VISION

4.2.1 Experimental Data

Results from the VISION experiment at 5 K as a function of the hydrogen concentration are shown in Figure 17. A plot that shows the change in spectra as a function of temperature is shown in Figure 18. In these plots, each dataset is normalized to a proton charge, which correlates to the number of neutrons impinging on the sample.

a) High-Q

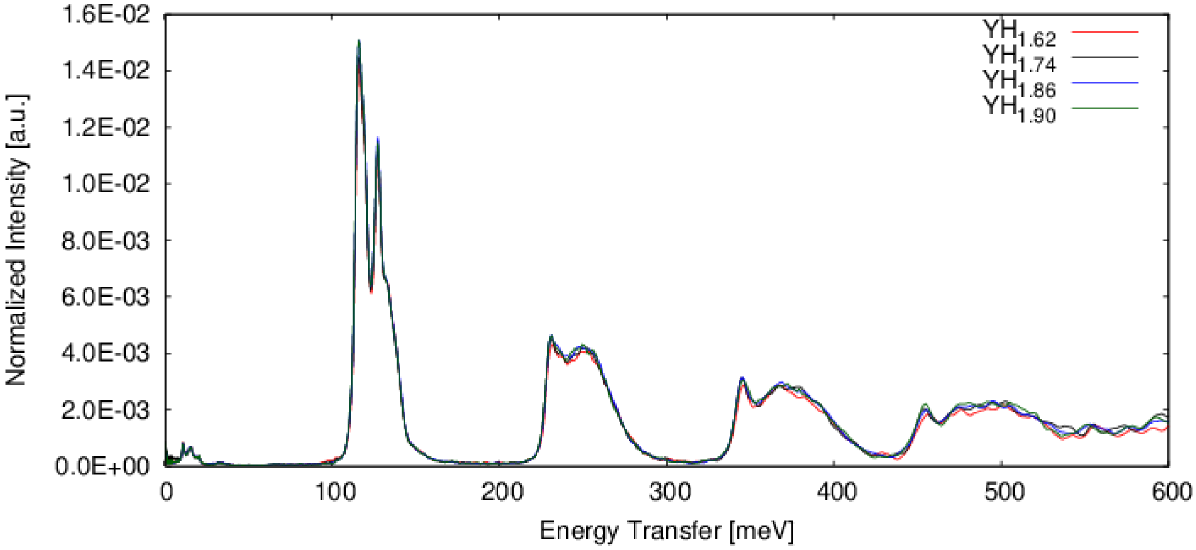

b) Low-Q

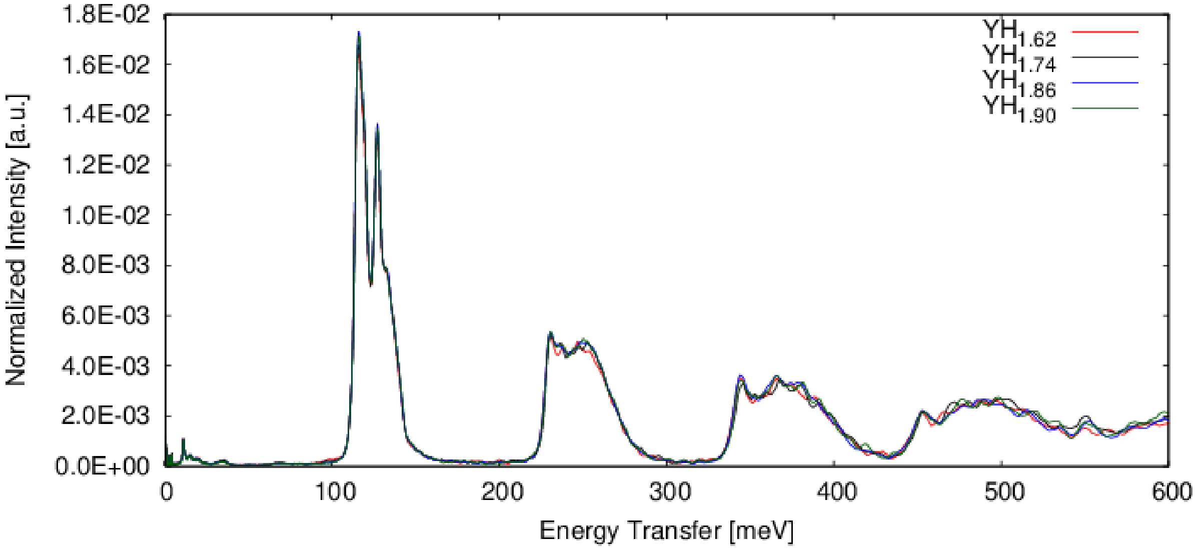

Figure 17. Hydrogen concentration comparison of VISION data of YH_x for $x = 1.62, 1.74, 1.86$, and 1.90 at 5 K.

a) High-Q

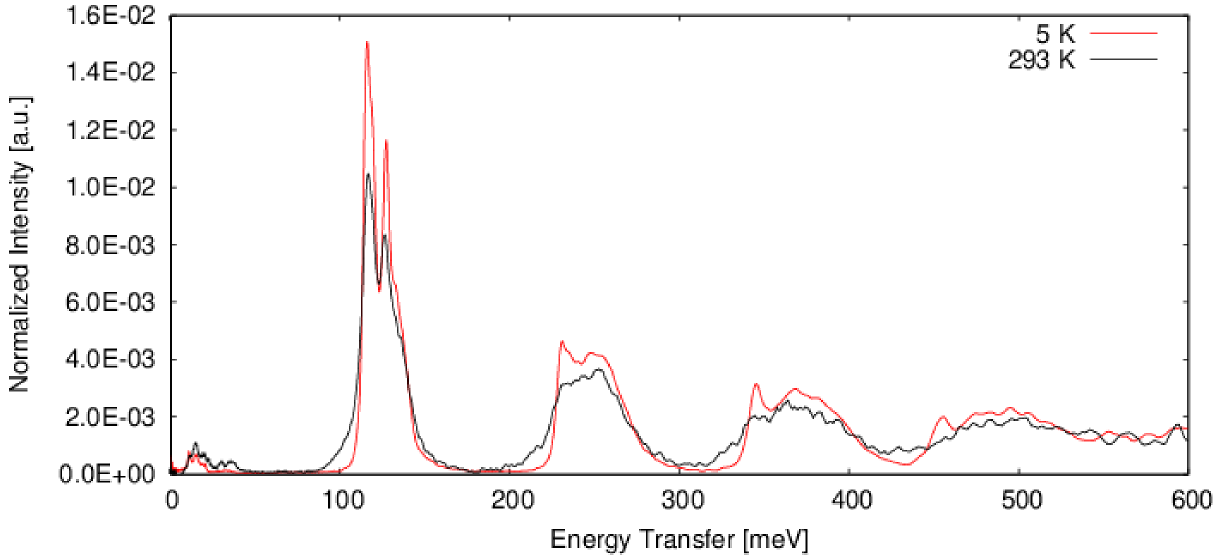

b) Low-Q

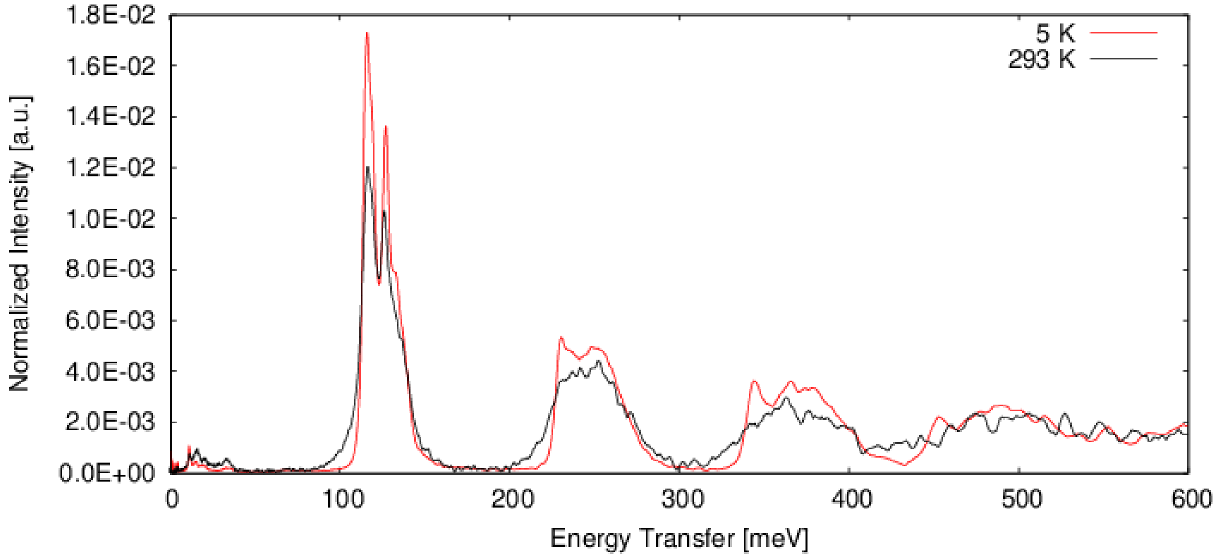

Figure 18. Temperature comparison of VISION data of $YH_{1.86}$ at 5 and 293 K.

From these plots, there is no noticeable difference between the samples as a function of hydrogen concentration in the magnitude of the peaks or their location. This was also seen in the SEQUOIA data in Figure 8 but is more prominently shown in Figure 17. One reason for this is due to the yttrium hydride phase diagram, shown in Figure 19. The phases at 0°C and 5 K are the same, and the hydrogen concentrations of YH_x for $x = 1.62$, 1.74, 1.86, and 1.90 correspond to an atomic percent of hydrogen of 61.8, 63.5, 65.0, and 65.5 %, respectively. All of these samples are within the mixed alpha-yttrium and delta-YH_2 phase, and it does not appear that the small change in atomic percent hydrogen makes a significant difference in these measurements.

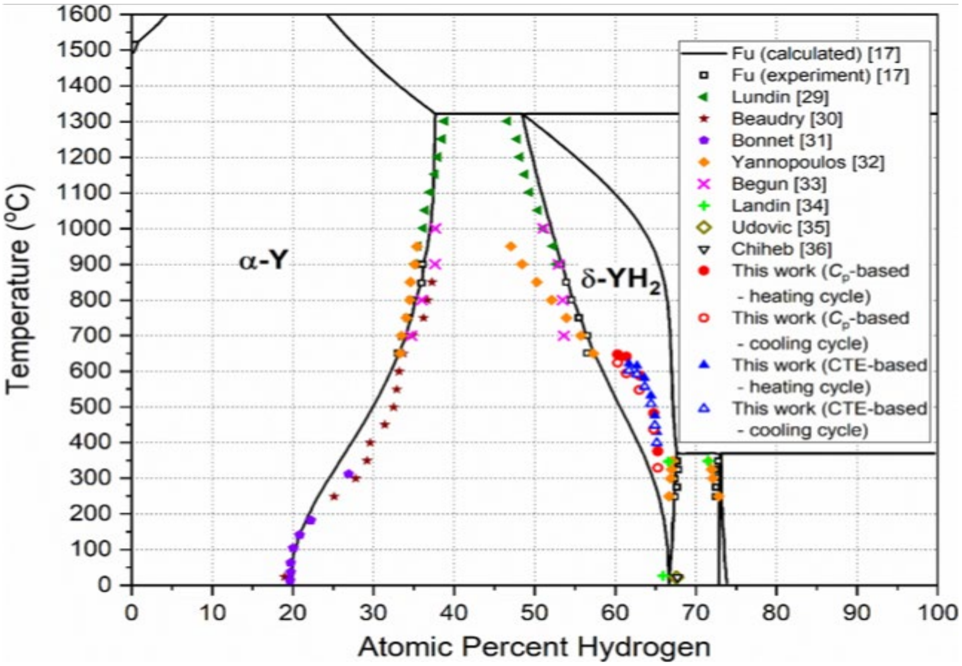

Figure 19. Yttrium hydride phase diagram.

There is evidence to suggest that the potential well for hydrogen in YH_x is anharmonic at energy transfers greater than 300 meV. To further show this, the high-*Q* data at 5 K are plotted against multiphohon spectra calculated in the harmonic approximation [39] and the Sjölander approximation [40] by using the spectra in the range of the fundamental modes (i.e., the spectra between *E* = 0 to 150 meV) in Figure 19. There is a significant red shift of the lower peaks, as indicated by the arrows, compared with the harmonic approximation calculations.

4.2.2 Simulation of Measured Data

Unlike the ARCS and SEQUOIA simulations, the VISION spectra can be extracted directly from the dynamic structure factor calculated for analysis in Section 4.1.2. After applying the VISION detector resolution function, the resulting spectrum can be directly compared with the experimental data. These results are shown in Figure 20. The magnitudes of the simulated peaks agree favorably with the VISION data with two notable exceptions: (1) the second peak of the fundamental mode near *E* = 130 meV and (2) the magnitude of the anharmonic peaks denoted by the arrows in Figure 19. Overall, there is a slight shift of the s-TDEP results toward the correct location of the peaks; however, much like the ARCS and SEQUOIA comparison, the differences between the ENDF/B-VIII.0 and s-TDEP results are small. This could indicate that more advanced methods are needed to calculate the multiphonon scattering contributions to the overall spectra. Figure 21 shows a comparison of VISION data against ENDF/B-VIII.0 and s-TDEP for $YH_{1.86}$ at 5 K.

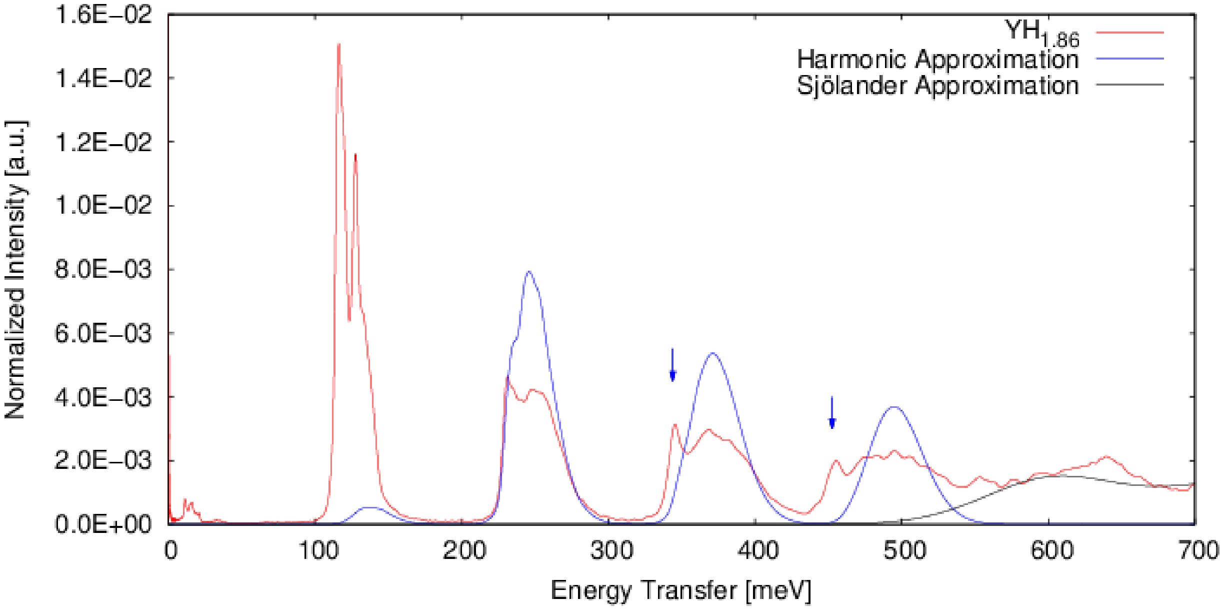

Figure 20. Comparison of VISION high-*Q* 5 K experimental data with multiphonon harmonic and Sjölander approximations.

a) High–Q

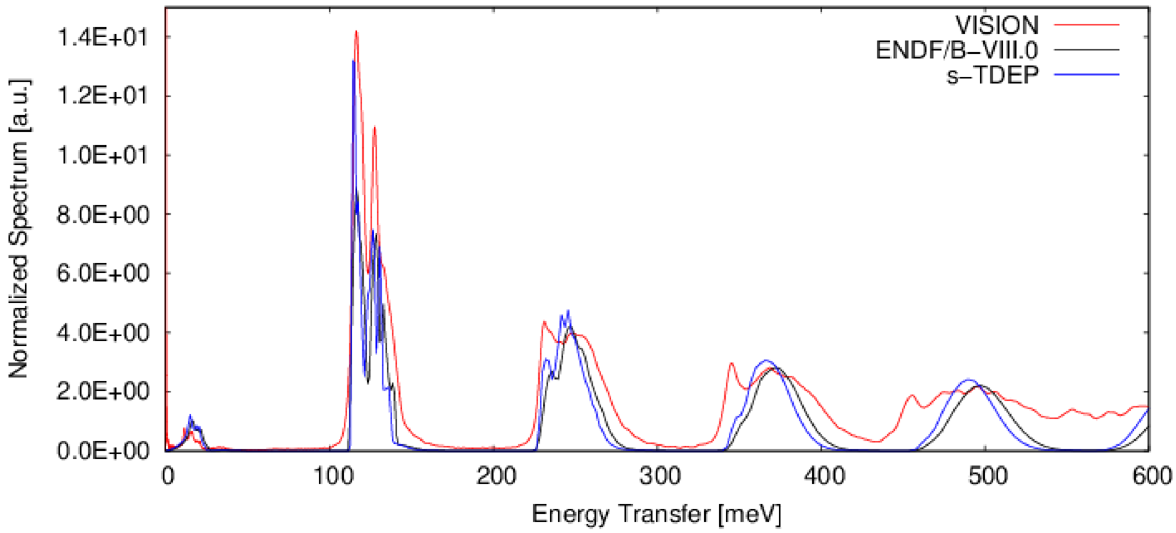

b) Low–Q

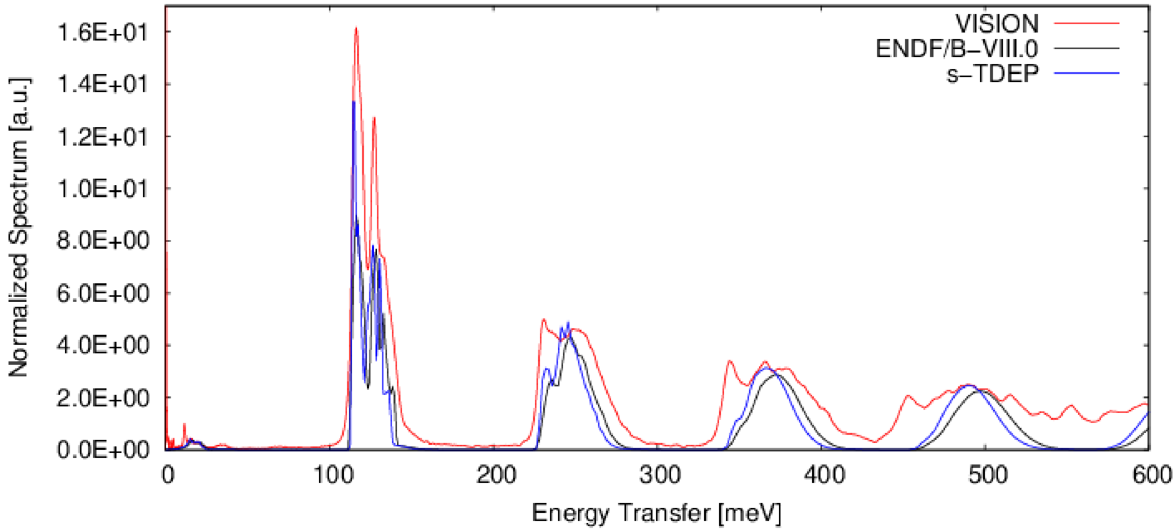

Figure 21. Comparison of VISION data against ENDF/B-VIII.0 and s-TDEP for $YH_{1.86}$ at 5 K.

5. CONCLUSIONS AND FUTURE WORK

The dynamic structure factors of yttrium hydride with H/Y atomic ratios from 1.62 to 1.90 were measured with the SEQUOIA, ARCS, and VISION instruments at SNS in the temperature range of 5 to 1,200 K to capture the temperature and hydrogen concentration dependence. The VISION measurement of the selected YH_x samples indicated anharmonic effects. These experiments provide a platform to validate the currently available ENDF/B-VIII.0 thermal scattering files and demonstrate the need for more accurate thermal scattering files to capture the temperature broadening and anharmonic effects. This work showed that the s-TDEP method can be used to calculate the temperature dependence of the phonon spectrum for $YH_{\sim 2}$ samples. The method correctly predicts the softening of optical peaks from 295 to 800 K.

The acoustic peaks are slightly under-calculated, and denser 7 × 7 × 7 k-points force calculations will be performed for the follow-up paper via VASP to check whether it will lead to improvement. The phonon spectra used in this work were calculated from only second-order IFCs. The follow-up work will present the results from phonon spectra obtained by using third- and fourth-order IFCs, which can be calculated via the TDEP method. A study on including nuclear quantum effects will also be performed with contributions from second-, third-, and fourth-order IFCs. Additionally, s-TDEP calculations will be performed for temperatures up to 1,200 K that are complementary to the ones done in this work up to 800 K. Modeling and comparison with ARCS experimental data will be also performed with an improved input file that will better replicate the full ARCS detector setup. Thermodynamic quantities will also be calculated at all temperatures, such as specific heat capacity, mode Gruneisen parameters, and lattice thermal conductivity.

One phenomena that was briefly mentioned involves the location of the hydrogen atom in the YH_x lattice. At room temperature, the location is known to favor the tetrahedral sites in the delta-YH_2 lattice, but it is unclear how this changes as a function of temperature. It is also possible that some of the higher temperature spectra might be described by new vibrational states in the phonon DOS. This will be investigated with the higher order, high-temperature s-TDEP calculations.

REFERENCES

[1] W.-E. Wang and D. R. Olander, “Thermodynamics of the Zr-H System,” *Journal of the American Ceramic Society*, **78**, *12*, 3323 (1995).

[2] G. M. Begun, J. F. Land, and J. T. Bell, “High temperature equilibrium measurements of the yttrium-hydrogen isotope (H2, D2, T2) systems.” *The Journal of Chemical Physics*, **72**, *5*, 2959 (1980); 10.1063/1.439496.

[3] *Advanced Small Modular Reactors, Department of Energy.* https://www.energy.gov/ne/nuclear-reactor-technologies/small-modular-nuclear-reactors .

[4] *Transformational Challenge Reactor,* (n.d.). tcr.ornl.gov.

[5] D. Brown, M. Chadwick, R. Capote, A. Kahler, A. Trkov, M. Herman, A. Sonzogni, Y. Danon, A. Carlson, M. Dunn, D. Smith, G. Hale, G. Arbanas, R. Arcilla, C. Bates, B. Beck, B. Becker, F. Brown, R. Casperson, J. Conlin, D. Cullen, M.- A. Descalle, R. Firestone, T. Gaines, K. Guber, A. Hawari, J. Holmes, T. Johnson, T. Kawano, B. Kiedrowski, A. Koning, S. Kopecky, L. Leal, J. Lestone, C. Lubitz, J. Márquez Damián, C. Mattoon, E. McCutchan, S. Mughabghab, P. Navratil, D. Neudecker, G. Nobre, G. Noguere, M. Paris, M. Pigni, A. Plompen, B. Pritychenko, V. Pronyaev, D. Roubtsov, D. Rochman, P. Romano, P. Schillebeeckx, S. Simakov, M. Sin, I. Sirakov, B. Sleaford, V. Sobes, E. Soukhovitskii, I. Stetcu, P. Talou, I. Thompson, S. van der Marck, L. Welser-Sherrill, D. Wiarda, M. White, J. Wormald, R. Wright, M. Zerkle, G. Žerovnik, and Y. Zhu, “ENDF/BVIII. 0: The 8th Major Release of the Nuclear Reaction Data Library with CIELO-project Cross Sections, New Standards and Thermal Scattering Data,” *Nuclear Data Sheets*, 148, 1 (2018); https://doi.org/10.1016/j.nds.2018.02.001. https://www.sciencedirect.com/science/article/pii/S0090375218300206.

[6] Zerkle, Michael and Holmes, Jesse, “A Thermal Neutron Scattering Law for Yttrium Hydride,” *EPJ Web Conf.*, 146, 13005 (2017); 10.1051/epjconf/201714613005. https://www.epj-conferences.org/articles/epjconf/abs/2017/15/epjconf-nd2016_13005/epjconf-nd2016_13005.html.

[7] C. Elsässer, S. Schweizer, and M. Fähnle, “Hydrogen Vibration in Cubic Dihydrides MH2 (M=Ti, Zr), and Localization in Cubic Laves Phases ZrM2H1/2 (M=V, Cr, Fe, Co),” *MRS Proceedings*, **453**, 221 (1996); 10.1557/PROC-453-221.

[8] O. Hellman, I. A. Abrikosov, and S. I. Simak, “Lattice dynamics of anharmonic solids from first principles,” *Phys. Rev. B*, **84**, 180301 (2011); 10.1103/PhysRevB.84.180301. https://link.aps.org/doi/10.1103/PhysRevB.84.180301.

[9] O. Hellman and I. A. Abrikosov, “Temperature-dependent effective third-order inter-atomic force constants from first principles,” *Phys. Rev. B*, **88**, 144301 (2013); 10.1103/Phys- RevB.88.144301. https://link.aps.org/doi/10.1103/PhysRevB.88.144301.

[10] O. Hellman, P. Steneteg, I. A. Abrikosov, and S. I. Simak, “Temperature dependent effective potential method for accurate free energy calculations of solids,” *Phys. Rev. B*, **87**, 104111 (2013); 10.1103/PhysRevB.87.104111. https://link.aps.org/doi/10.1103/ PhysRevB.87.104111.

[11] N. Shulumba, O. Hellman, and A. J. Minnich, “Intrinsic localized mode and low thermal conductivity of PbSe,” *Phys. Rev. B*, **95**, 014302 (2017); 10.1103/PhysRevB.95.014302. https://link.aps.org/doi/10.1103/PhysRevB.95.014302.

[12] X. Hu, D.Schappel, C. M.Silva, and K. A.Terrani, “Fabrication of yttrium hydride for high-temperature moderator application,” *Journal of Nuclear Materials*, **539**, 152335 (2020); https://doi.org/10.1016/j.jnucmat.2020.152335. http://www.sciencedirect.com/science/article/pii/S0022311520305456.

[13] D. Khatamian, C. Stassis, and B. J. Beaudry, “Location of deuterium in *α*-yttrium,” *Phys. Rev. B*, **23**, 624 (1981); 10.1103/PhysRevB.23.624. https://link.aps.org/doi/10.1103/PhysRevB.23.624.

[14] D. Khatamian, W. A. Kamitakahara, R. G. Barnes, and D. T. Peterson, “Crys- tal structure of $YD_{1.96}$ and $YH_{1.98}$ by neutron diffraction,” *Phys. Rev. B*, **21**, 2622 (1980); 10.1103/PhysRevB.21.2622. https://link.aps.org/doi/10.1103/PhysRevB.21.2622.

[15] B. Fultz and D. Abernathy, “ARCS A wide-Anglular Range Chopper Spectrometer at the SNS,” (2005); 10.2172/835574.

[16] G. E. Granroth, A. I. Kolesnikov, T. E.Sherline, J. P.Clancy, K. A. Ross, J. P. C. Ruff, B. D. Gaulin, and S. E. Nagler, “SEQUOIA: A Newly Operating Chopper Spectrometer at the SNS,” *Journal of Physics: Conference Series*, **251**, 012058 (2010); 10.1088/1742-6596/251/1/012058. https://doi.org/10.1088%2F1742-6596% 2F251%2F1%2F012058.

[17] P. A. Seeger, L. L. Daemen, and J. Z. Larese, “Resolution of VISION, a Crystal- Analyzer Spectrometer,” *Nuclear Instruments and Methods in Physics Research Section A: Accelerators, Spectrometers, Detectors and Associated Equipment*, **604**, *3*, 719 (2009); https://doi.org/10.1016/j.nima.2009.03.204. http://www.sciencedirect.com/science/article/pii/S0168900209006871.

[18] J. L. Niedziela, R. Mills, M. J. Loguillo, H. D. Skorpenske, D. Armitage, H. L. Smith, J. Y. Y. Lin, M. S. Lucas, M. B. Stone, and D. L. Abernathy, “Design and operating characteristic of a vacuum furnace for time-of-flight inelastic neutron scattering measurements,” *Review of Scientific Instruments*, **88**, *10*, 105116 (2017); 10.1063/1.5007089.

[19] R. MacFarlane and A. Kahler, “Methods for Processing ENDF/B-VII with NJOY,” *Nuclear Data Sheets*, **111**, *12*, 2739 (2010); https://doi.org/10.1016/j.nds.2010.11.001. http://www.sciencedirect.com/science/article/pii/S0090375210001006.

[20] C. W. Chapman, G. Arbanas, A. I. Kolesnikov, L. Leal, Y. Danon, C. Wendorff, K. Ramic, L. Liu, and F. Rahnema, “Methodology for Generating Covariance Data of Thermal Neutron Scattering Cross Sections,” *Nuclear Science and Engineering* (2020).

[21] K. Ramic, C. Wendorff, Y. Cheng, A. I. Kolesnikov, D. L. Abernathy, L. Daemen, G. Arbanas, L. Leal, Y. Danon, and L. E. Liu, “Thermal scattering law of C2H4n : Integrating experimental data

with DFT calculations," *Annals of Nuclear Energy*, **120**, 778 (2018); https://doi.org/10.1016/j.anucene.2018.06.029. http://www.sciencedirect.com/science/article/pii/S030645491830330X.

[22] K. Ramic, C. Wendorff, Y. Cheng, A. I. Kolesnikov, D. L. Abernathy, L. Daemen, G. Arbanas, L. Leal, Y. Danon, and L. E. Liu, "Toward a better thermal scattering law of (C5O2H8)n: Inelastic neutron scattering and oClimax + NJOY2016," *Annals of Nuclear Energy*, **133**, 425 (2019); https://doi.org/10.1016/j.anucene.2019.05.042. http://www.sciencedirect.com/science/article/pii/S0306454919302956.

[23] T. J. Udovic, J. J. Rush, and I. S. Anderson, "Local-mode dynamics in YH_2 and YD_2 by isotope-dilution neutron spectroscopy," *Phys. Rev. B*, **50**, 15739 (1994); 10.1103/Phys- RevB.50.15739. https://link.aps.org/doi/10.1103/PhysRevB.50.15739.

[24] K. Parlinski, "First-principle lattice dynamics and thermodynamics of crystals," *Journal of Physics: Conference Series*, **92**, 012009 (2007); 10.1088/1742-6596/92/1/012009. https://doi.org/10.1088%2F1742-6596%2F92%2F1%2F012009.

[25] A. Togo and I. Tanaka, "First principles phonon calculations in materials science," *Scr. Mater.*, **108**, 1 (2015).

[26] G. Goret, B. Aoun, and E. Pellegrini, "MDANSE: An Interactive Analysis Environment for Molecular Dynamics Simulations," *Journal of Chemical Information and Modeling*, **57**, *1*, 1 (2017); 10.1021/acs.jcim.6b00571. https://pubs.acs.org/doi/10.1021/acs.jcim.6b00571.

[27] T. Tadano, Y. Gohda, and S. Tsuneyuki, "Anharmonic force constants extracted from first-principles molecular dynamics: applications to heat transfer simulations," *Journal of Physics: Condensed Matter*, **26**, *22*, 225402 (2014); 10.1088/0953-8984/26/22/225402. https://doi.org/10.1088%2F0953-8984%2F26%2F22%2F225402.

[28] K. Parlinski, "Ab initio determination of anharmonic phonon peaks," *Phys. Rev. B*, **98**, 054305 (2018); 10.1103/PhysRevB.98.054305. https://link.aps.org/doi/10.1103/PhysRevB.98.054305.

[29] D. S.Kim, O. Hellman, J.Herriman, H. L.Smith, J. Y. Y.Lin, N.Shulumba, J. L. Niedziela, C. W. Li, D. L. Abernathy, and B. Fultz, "Nuclear quantum effect with pure anharmonicity and the anomalous thermal expansion of silicon," *Proceedings of the National Academy of Sciences*, **115**, *9*, 1992 (2018); 10.1073/pnas.1707745115. https://www.pnas.org/content/115/9/1992.

[30] G. Kresse and J. Hafner, "Ab initio molecular dynamics for liquid metals," *Phys. Rev. B*, **47**, 558 (1993); 10.1103/PhysRevB.47.558. https://link.aps.org/doi/10.1103/PhysRevB.47.558.

[31] G. Kresse and J. Furthmüller, "Efficiency of ab-initio total energy calculations for metals and semiconductors using a plane-wave basis set," *Computational Materials Science*, **6**, *1*, 15 (1996); https://doi.org/10.1016/0927-0256(96)00008-0. http://www.sciencedirect.com/science/article/pii/0927025696000080.

[32] G. Kresse and J. Furthmüller, "Efficient iterative schemes for ab initio total-energy calculations using a plane-wave basis set," *Phys. Rev. B*, **54**, 11169 (1996); 10.1103/Phys- RevB.54.11169. https://link.aps.org/doi/10.1103/PhysRevB.54.11169.

[33] M. Hacene, A. Anciaux-Sedrakian, X. Rozanska, D. Klahr, T.Guignon, and P. Fleurat-Lessard, "Accelerating VASP electronic structure calculations us- ing graphic processing units," *Journal of Computational Chemistry*, **33**, *32*, 2581 (2012); 10.1002/jcc.23096. https://onlinelibrary.wiley.com/doi/abs/10.1002/jcc.23096.

[34] M. Hutchinson and M. Widom, "VASP on a GPU: Application to exact-exchange calcula- tions of the stability of elemental boron," *Computer Physics Communications*, **183**, *7*, 1422 (2012);

https://doi.org/10.1016/j.cpc.2012.02.017. http://www.sciencedirect.com/science/article/pii/S0010465512000707.

[35] "YH2 Crystal Structure: Datasheet from "PAULING FILE Multinaries Edition – 2012" in SpringerMaterials (https://materials.springer.com/isp/crystallographic/docs/sd_0559145)," URL https://materials.springer.com/isp/crystallographic/docs/sd_0559145, copyright 2016 Springer-Verlag Berlin Heidelberg & Material Phases Data System (MPDS), Switzerland & National Institute for Materials Science (NIMS), Japan.

[36] J. N. Daou and P. Vajda, "Hydrogen ordering and metal-semiconductor transitions in the system YH_{2+x}," *Phys. Rev. B*, **45**, 10907 (1992); 10.1103/PhysRevB.45.10907. https://link.aps.org/doi/10.1103/PhysRevB.45.10907.

[37] J. Goorley, M. James et al., "Initial MCNP6 Release Overview," LA-UR-13-22934, Los Alamos National Laboratory (2013).

[38] J. Y. Lin, H. L. Smith, G. E. Granroth, D. L. Abernathy, M. D. Lumsden, B. Winn, A. A. Aczel, M. Aivazis, and B. Fultz, "MCViNE – An object oriented Monte Carlo neutron ray tracing simulation package," *Nuclear Instruments and Methods in Physics Research Section A: Accelerators, Spectrometers, Detectors and Associated Equipment*, **810**, 86 (2016); https://doi.org/10.1016/j.nima.2015.11.118. http://www.sciencedirect.com/science/article/pii/S0168900215015053.

[39] J. Li and A.I. Kolesnikov, "Neutron spectroscopic investigation of dynamics of water ice," *Journal of Molecular Liquids*, **100**, *1*, 1 (2002).

[40] A. Sjölander, "Multi-phonon Processes in Slow Neutron Scattering by Crystals," *Arkiv för Fysik*, **14**, *4*, 315 (1958)

APPENDIX A. ADDITIONAL PLOTS OF EXPERIMENTAL DATA

APPENDIX A: ADDITIONAL PLOTS OF EXPERIMENTAL DATA

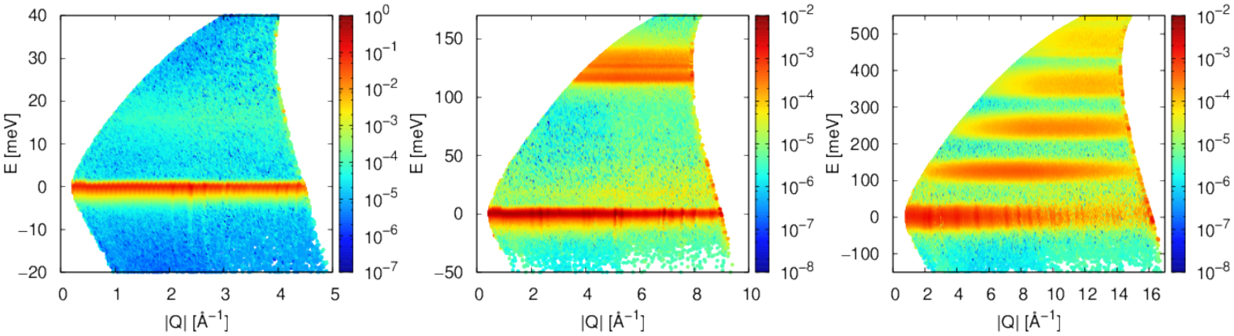

Figure 22. 2D mesh of the dynamic structure factors of $YH_{1.62}$ measured at SEQUOIA at 5 K for three incident energy measurements.

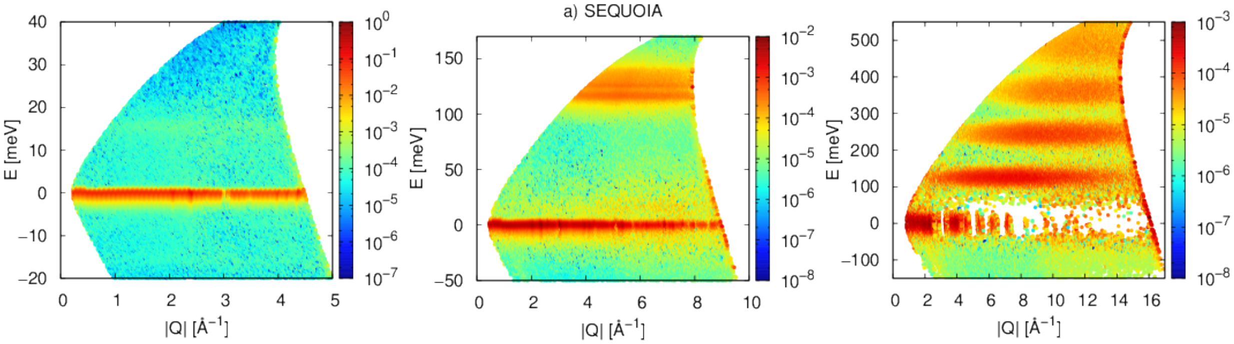

Figure 23. 2D mesh of the dynamic structure factors of $YH_{1.86}$ measured at SEQUOIA at 295 K for three incident energy measurements.

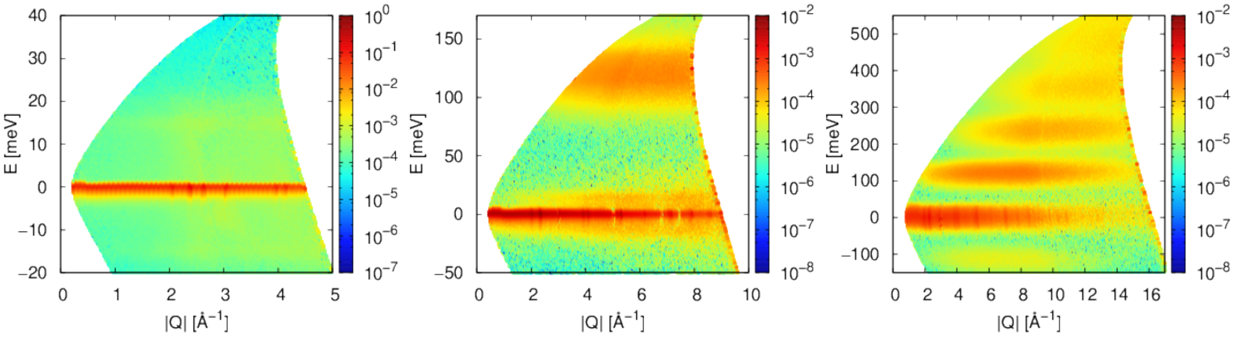

Figure 24. 2D mesh of the dynamic structure factors of $YH_{1.86}$ measured at SEQUOIA at 800 K for three incident energy measurements.

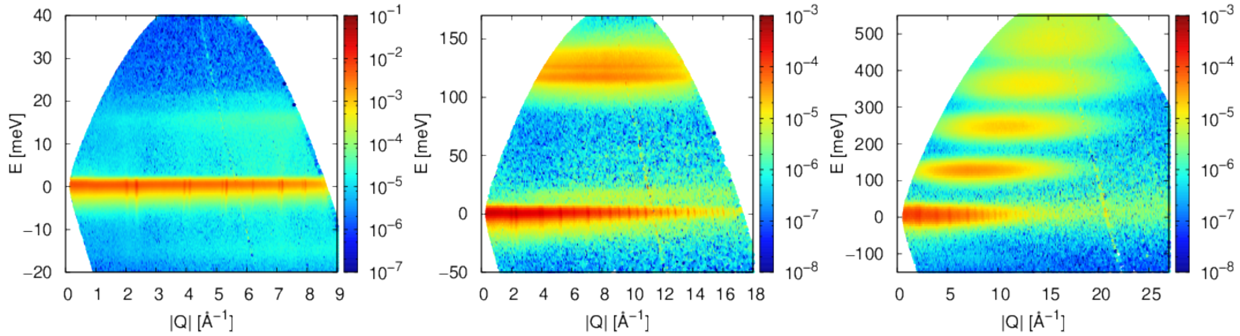

Figure 25. 2D mesh of the dynamic structure factors of $YH_{1.87}$ measured at ARCS at 295 K for three incident energy measurements.

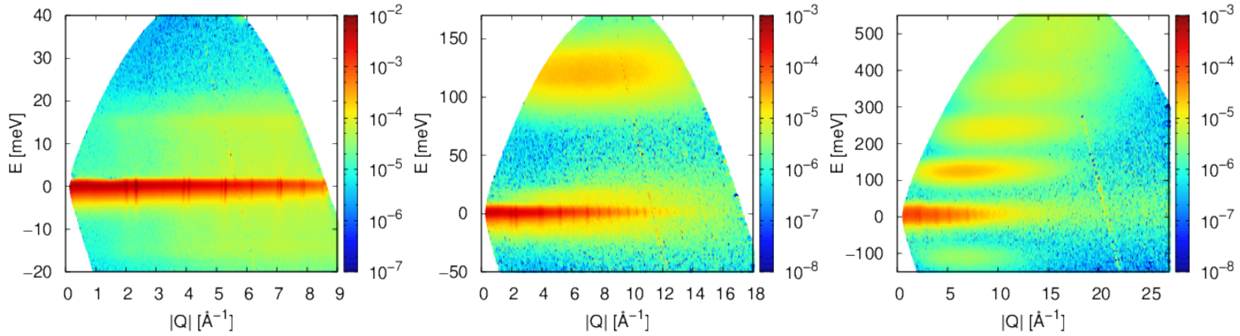

Figure 26. 2D mesh of the dynamic structure factors of $YH_{1.87}$ measured at ARCS at 800 K for three incident energy measurements.

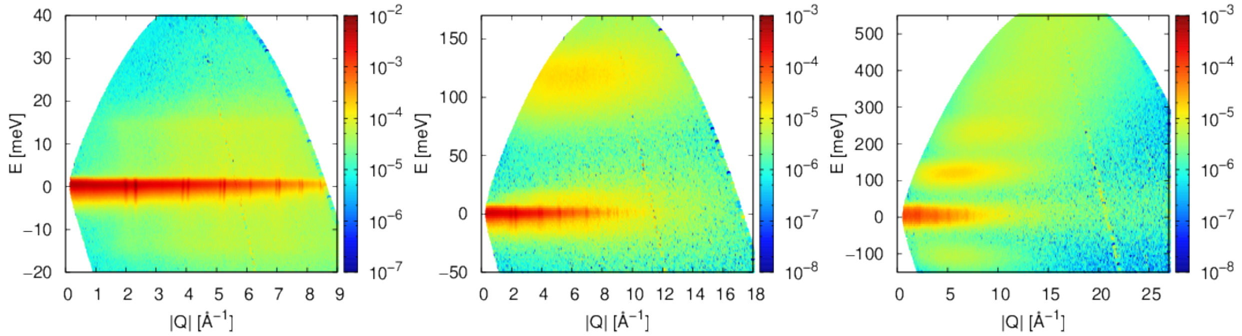

Figure 27. 2D mesh of the dynamic structure factors of $YH_{1.87}$ measured at ARCS at 1200 K for three incident energy measurements.

APPENDIX B. SAMPLE VASP INPUT

APPENDIX B: SAMPLE VASP INPUT

```
PREC    = Accurate
IBRION  = -1
ENCUT   = 500
EDIFF   = 1.0e-08
ISMEAR  = 2
SIGMA   = 0.01
IALGO   = 38
LREAL   = Auto
LWAVE   = .FALSE.
LCHARG  = .FALSE.
GGA     = AM
ISIF    = 2
ADDGRID = TRUE
KPAR    = 5
```

APPENDIX C. NJOY2016 INPUTS

APPENDIX C: NJOY2016 INPUTS

```
leapr
30
'H in YH2, all temperatures, s-TDEP'/
8 1 100/
5 105/
.9991673 20.43634 2 0 0 0/
0/
107 401 1/
1.00000E-3 1.25893E-3 1.58489E-3 1.99526E-3 2.51189E-3
3.16228E-3 3.98107E-3 5.01187E-3 6.30957E-3 7.94328E-3
1.00000E-2 1.25893E-2 1.58489E-2 1.99526E-2 2.51189E-2
3.16228E-2 3.98107E-2 5.01187E-2 6.30957E-2 7.94328E-2
1.00000E-1 1.25893E-1 1.58489E-1 1.99526E-1 2.51189E-1
3.16228E-1 3.98107E-1 5.01187E-1 6.30957E-1 7.94328E-1
1.00000E+0 1.12202E+0 1.25893E+0 1.41254E+0 1.58489E+0
1.77828E+0 1.99526E+0 2.23872E+0 2.51189E+0 2.81838E+0
3.16228E+0 3.54813E+0 3.98107E+0 4.46684E+0 5.01187E+0
5.62341E+0 6.30957E+0 7.07946E+0 7.94328E+0 8.91251E+0
1.00000E+1 1.12202E+1 1.25893E+1 1.41254E+1 1.58489E+1
1.77828E+1 1.99526E+1 2.23872E+1 2.51189E+1 2.81838E+1
3.16228E+1 3.54813E+1 3.98107E+1 4.46684E+1 5.01187E+1
5.62341E+1 6.30957E+1 7.07946E+1 7.94328E+1 8.91251E+1
1.00000E+2 1.12202E+2 1.25893E+2 1.41254E+2 1.58489E+2
1.77828E+2 2.00000E+2 2.20000E+2 2.40000E+2 2.60000E+2
2.80000E+2 3.00000E+2 3.20000E+2 3.40000E+2 3.60000E+2
3.80000E+2 4.00000E+2 4.20000E+2 4.40000E+2 4.60000E+2
4.80000E+2 5.00000E+2 5.20000E+2 5.40000E+2 5.60000E+2
5.80000E+2 6.00000E+2 6.20000E+2 6.40000E+2 6.60000E+2
6.80000E+2 7.00000E+2 7.20000E+2 7.40000E+2 7.60000E+2
7.80000E+2 8.00000E+2 / alpha grid
0.00000E+0 3.95257E-2 7.90514E-2 1.18577E-1 1.58103E-1
1.97628E-1 2.37154E-1 2.76680E-1 3.16206E-1 3.55731E-1
3.95257E-1 4.34783E-1 4.74308E-1 5.13834E-1 5.53360E-1
5.92885E-1 6.32411E-1 6.71937E-1 7.11462E-1 7.50988E-1
7.90514E-1 8.30040E-1 8.69565E-1 9.09091E-1 9.48617E-1
9.88142E-1 1.02767E+0 1.06719E+0 1.10672E+0 1.18577E+0
1.34387E+0 1.66008E+0 2.29249E+0 2.92490E+0 3.55731E+0
3.87352E+0 4.18972E+0 4.34783E+0 4.42688E+0 4.46640E+0
4.50593E+0 4.54545E+0 4.58498E+0 4.62451E+0 4.66403E+0
4.70356E+0 4.74308E+0 4.78261E+0 4.82213E+0 4.86166E+0
4.90119E+0 4.94071E+0 4.98024E+0 5.01976E+0 5.05929E+0
5.09881E+0 5.13834E+0 5.17787E+0 5.21739E+0 5.25692E+0
5.29644E+0 5.33597E+0 5.37549E+0 5.41502E+0 5.45455E+0
5.49407E+0 5.53360E+0 5.57312E+0 5.61265E+0 5.69170E+0
5.84980E+0 6.16601E+0 6.79842E+0 7.43083E+0 8.06324E+0
8.37945E+0 8.61660E+0 8.77470E+0 8.85375E+0 8.93281E+0
9.01186E+0 9.09091E+0 9.16996E+0 9.24901E+0 9.32806E+0
9.40711E+0 9.48617E+0 9.56522E+0 9.64427E+0 9.72332E+0
9.80237E+0 9.88142E+0 9.96047E+0 1.00395E+1 1.01186E+1
1.01976E+1 1.02767E+1 1.03557E+1 1.04348E+1 1.05138E+1
1.05929E+1 1.06719E+1 1.07510E+1 1.08300E+1 1.09091E+1
```

```
1.09881E+1 1.10672E+1 1.11462E+1 1.12253E+1 1.13834E+1
1.16996E+1 1.23320E+1 1.29644E+1 1.32806E+1 1.33992E+1
1.35178E+1 1.36364E+1 1.37549E+1 1.38735E+1 1.39921E+1
1.41107E+1 1.42292E+1 1.43478E+1 1.44664E+1 1.45850E+1
1.47036E+1 1.48221E+1 1.49407E+1 1.50593E+1 1.51779E+1
1.52964E+1 1.54150E+1 1.55336E+1 1.56522E+1 1.57708E+1
1.58893E+1 1.60079E+1 1.61265E+1 1.62451E+1 1.63636E+1
1.64822E+1 1.66008E+1 1.67194E+1 1.68379E+1 1.71542E+1
1.74704E+1 1.77075E+1 1.78656E+1 1.80237E+1 1.81818E+1
1.83399E+1 1.84980E+1 1.86561E+1 1.88142E+1 1.89723E+1
1.91304E+1 1.92885E+1 1.94466E+1 1.96047E+1 1.97628E+1
1.99209E+1 2.00791E+1 2.02372E+1 2.03953E+1 2.05534E+1
2.07115E+1 2.08696E+1 2.10277E+1 2.11858E+1 2.13439E+1
2.15020E+1 2.16601E+1 2.18182E+1 2.19763E+1 2.21344E+1
2.22925E+1 2.24506E+1 2.26482E+1 2.28458E+1 2.30435E+1
2.32411E+1 2.34387E+1 2.36364E+1 2.38340E+1 2.40316E+1
2.42292E+1 2.44269E+1 2.46245E+1 2.48221E+1 2.50198E+1
2.52174E+1 2.54150E+1 2.56126E+1 2.58103E+1 2.60079E+1
2.62055E+1 2.64032E+1 2.66008E+1 2.67984E+1 2.69960E+1
2.71937E+1 2.73913E+1 2.75889E+1 2.77866E+1 2.79842E+1
2.82213E+1 2.84585E+1 2.86957E+1 2.89328E+1 2.91700E+1
2.94071E+1 2.96443E+1 2.98814E+1 3.01186E+1 3.03557E+1
3.05929E+1 3.08300E+1 3.10672E+1 3.13043E+1 3.15415E+1
3.17787E+1 3.20158E+1 3.22530E+1 3.24901E+1 3.27273E+1
3.29644E+1 3.32016E+1 3.34387E+1 3.36759E+1 3.39526E+1
3.42292E+1 3.45059E+1 3.47826E+1 3.50593E+1 3.53360E+1
3.56126E+1 3.58893E+1 3.61660E+1 3.64427E+1 3.67194E+1
3.69960E+1 3.72727E+1 3.75494E+1 3.78261E+1 3.81028E+1
3.83794E+1 3.86561E+1 3.89328E+1 3.92095E+1 3.95257E+1
3.98419E+1 4.01581E+1 4.04743E+1 4.07905E+1 4.11067E+1
4.14229E+1 4.17391E+1 4.20553E+1 4.23715E+1 4.26877E+1
4.30040E+1 4.33202E+1 4.36364E+1 4.39526E+1 4.42688E+1
4.45850E+1 4.49012E+1 4.52569E+1 4.56126E+1 4.59684E+1
4.63241E+1 4.66798E+1 4.70356E+1 4.73913E+1 4.77470E+1
4.81028E+1 4.84585E+1 4.88142E+1 4.91700E+1 4.95257E+1
4.98814E+1 5.02372E+1 5.05929E+1 5.09881E+1 5.13834E+1
5.17787E+1 5.21739E+1 5.25692E+1 5.29644E+1 5.33597E+1
5.37549E+1 5.41502E+1 5.45455E+1 5.49407E+1 5.53360E+1
5.57312E+1 5.61265E+1 5.69170E+1 5.77075E+1 5.84980E+1
5.92885E+1 6.00791E+1 6.08696E+1 6.16601E+1 6.24506E+1
6.32411E+1 6.40316E+1 6.48221E+1 6.56126E+1 6.64032E+1
6.71937E+1 6.79842E+1 6.87747E+1 6.95652E+1 7.03557E+1
7.11462E+1 7.19368E+1 7.27273E+1 7.35178E+1 7.43083E+1
7.50988E+1 7.58893E+1 7.66798E+1 7.74704E+1 7.82609E+1
7.90514E+1 8.06324E+1 8.22134E+1 8.37945E+1 8.53755E+1
8.69565E+1 8.85375E+1 9.01186E+1 9.16996E+1 9.32806E+1
9.48617E+1 9.64427E+1 9.80237E+1 9.96047E+1 1.01186E+2
1.02767E+2 1.04348E+2 1.05929E+2 1.07510E+2 1.09091E+2
1.10672E+2 1.12253E+2 1.13834E+2 1.15415E+2 1.16996E+2
1.18577E+2 1.20158E+2 1.21739E+2 1.23320E+2 1.24901E+2
1.26482E+2 1.28063E+2 1.29644E+2 1.31225E+2 1.32806E+2
1.34387E+2 1.35968E+2 1.37549E+2 1.39130E+2 1.40711E+2
1.42292E+2 1.43874E+2 1.45455E+2 1.47036E+2 1.48617E+2
1.50198E+2 1.51779E+2 1.53360E+2 1.54941E+2 1.56522E+2
```

```
1.58103E+2 1.59684E+2 1.61265E+2 1.62846E+2 1.64427E+2
1.66008E+2 1.67589E+2 1.69170E+2 1.70751E+2 1.72332E+2
1.73913E+2 1.75494E+2 1.77075E+2 1.78656E+2 1.80237E+2
1.81818E+2 1.83399E+2 1.84980E+2 1.86561E+2 1.88142E+2
1.89723E+2 1.91304E+2 1.92885E+2 1.94466E+2 1.96047E+2
1.97628E+2 / beta grid
20/ temperature (K)
0.0005 294/  phonon frequency distribution
0.00000E+00 2.89588E-07 3.78977E-06 1.34575E-05 2.11810E-05 2.94223E-05
5.46600E-05 6.45790E-05 6.86907E-05 1.11468E-04 1.37214E-04 1.40964E-04
1.93821E-04 2.12952E-04 2.48832E-04 3.09178E-04 3.19447E-04 3.69179E-04
4.38330E-04 4.68764E-04 5.33639E-04 5.88122E-04 6.55816E-04 7.25116E-04
7.96859E-04 8.88532E-04 1.01670E-03 1.16550E-03 1.36434E-03 1.41136E-03
1.36042E-03 1.21123E-03 9.60404E-04 7.76159E-04 6.50997E-04 5.66179E-04
4.97161E-04 4.58790E-04 4.19258E-04 3.37641E-04 2.72474E-04 2.42682E-04
2.37987E-04 2.00832E-04 1.29635E-04 8.43748E-05 5.76216E-05 3.60422E-05
1.84986E-05 6.27031E-06 7.65845E-07 4.12050E-08 3.88714E-11 0.00000E+00
0.00000E+00 0.00000E+00 0.00000E+00 0.00000E+00 0.00000E+00 0.00000E+00
0.00000E+00 0.00000E+00 0.00000E+00 0.00000E+00 0.00000E+00 0.00000E+00
0.00000E+00 0.00000E+00 0.00000E+00 0.00000E+00 0.00000E+00 0.00000E+00
0.00000E+00 0.00000E+00 0.00000E+00 0.00000E+00 0.00000E+00 0.00000E+00
0.00000E+00 0.00000E+00 0.00000E+00 0.00000E+00 0.00000E+00 0.00000E+00
0.00000E+00 0.00000E+00 0.00000E+00 0.00000E+00 0.00000E+00 0.00000E+00
0.00000E+00 0.00000E+00 0.00000E+00 0.00000E+00 0.00000E+00 0.00000E+00
0.00000E+00 0.00000E+00 0.00000E+00 0.00000E+00 0.00000E+00 0.00000E+00
0.00000E+00 0.00000E+00 0.00000E+00 0.00000E+00 0.00000E+00 0.00000E+00
0.00000E+00 0.00000E+00 0.00000E+00 0.00000E+00 0.00000E+00 0.00000E+00
0.00000E+00 0.00000E+00 0.00000E+00 0.00000E+00 0.00000E+00 0.00000E+00
0.00000E+00 0.00000E+00 0.00000E+00 0.00000E+00 0.00000E+00 0.00000E+00
0.00000E+00 0.00000E+00 0.00000E+00 0.00000E+00 0.00000E+00 0.00000E+00
0.00000E+00 0.00000E+00 0.00000E+00 0.00000E+00 0.00000E+00 0.00000E+00
0.00000E+00 0.00000E+00 0.00000E+00 0.00000E+00 0.00000E+00 0.00000E+00
0.00000E+00 0.00000E+00 0.00000E+00 0.00000E+00 0.00000E+00 0.00000E+00
0.00000E+00 0.00000E+00 0.00000E+00 0.00000E+00 0.00000E+00 0.00000E+00
0.00000E+00 0.00000E+00 0.00000E+00 0.00000E+00 0.00000E+00 0.00000E+00
0.00000E+00 0.00000E+00 0.00000E+00 0.00000E+00 0.00000E+00 0.00000E+00
0.00000E+00 0.00000E+00 0.00000E+00 0.00000E+00 0.00000E+00 0.00000E+00
0.00000E+00 0.00000E+00 0.00000E+00 0.00000E+00 0.00000E+00 0.00000E+00
0.00000E+00 0.00000E+00 0.00000E+00 0.00000E+00 0.00000E+00 0.00000E+00
0.00000E+00 0.00000E+00 0.00000E+00 0.00000E+00 0.00000E+00 0.00000E+00
0.00000E+00 0.00000E+00 0.00000E+00 0.00000E+00 0.00000E+00 0.00000E+00
0.00000E+00 0.00000E+00 0.00000E+00 0.00000E+00 0.00000E+00 0.00000E+00
0.00000E+00 0.00000E+00 0.00000E+00 0.00000E+00 0.00000E+00 0.00000E+00
0.00000E+00 0.00000E+00 0.00000E+00 0.00000E+00 0.00000E+00 0.00000E+00
0.00000E+00 0.00000E+00 2.41260E-07 3.75841E-05 6.14737E-03 6.63705E-02
2.21525E-01 3.02846E-01 3.05104E-01 2.90482E-01 2.37650E-01 1.69641E-01
1.58467E-01 1.84197E-01 1.77131E-01 1.50732E-01 1.29729E-01 1.13496E-01
9.38304E-02 7.52738E-02 6.19136E-02 5.31287E-02 5.84037E-02 8.48432E-02
1.07736E-01 1.21586E-01 1.30485E-01 1.31317E-01 1.38059E-01 1.50076E-01
1.58269E-01 1.68259E-01 1.79679E-01 1.64345E-01 1.11820E-01 7.53691E-02
6.78677E-02 7.80422E-02 1.04606E-01 1.31766E-01 1.36427E-01 1.31435E-01
1.33937E-01 1.24566E-01 7.75040E-02 4.96121E-02 4.69693E-02 4.69604E-02
4.92622E-02 4.91902E-02 5.11983E-02 4.94050E-02 3.99295E-02 2.51076E-02
```

```
1.19024E-02 2.93017E-03 1.29119E-04 2.89348E-06 0.00000E+00 0.00000E+00
0.00000E+00 0.00000E+00 0.00000E+00 0.00000E+00 0.00000E+00 0.00000E+00
0.00000E+00 0.00000E+00 0.00000E+00 0.00000E+00 0.00000E+00 0.00000E+00/
0. 0. 1./  weights
0/
295/ temperature (K)
0.0005 282/  phonon frequency distribution
0.00000E+00 3.43163E-07 4.28383E-06 1.43740E-05 2.21009E-05 3.15569E-05
5.97127E-05 6.70135E-05 7.46100E-05 1.21469E-04 1.42067E-04 1.55153E-04
2.07430E-04 2.24571E-04 2.68376E-04 3.27693E-04 3.35255E-04 4.04970E-04
4.58462E-04 4.99977E-04 5.62898E-04 6.19798E-04 6.89654E-04 7.64777E-04
8.37237E-04 9.38899E-04 1.07307E-03 1.23786E-03 1.44112E-03 1.46817E-03
1.39444E-03 1.22883E-03 9.72602E-04 7.92645E-04 6.65572E-04 5.83670E-04
5.14120E-04 4.72750E-04 4.36444E-04 3.65114E-04 2.95532E-04 2.58761E-04
2.53652E-04 2.49695E-04 1.78539E-04 1.08613E-04 7.40555E-05 4.88947E-05
2.78709E-05 1.20478E-05 2.86535E-06 1.88900E-07 3.48604E-09 0.00000E+00
0.00000E+00 0.00000E+00 0.00000E+00 0.00000E+00 0.00000E+00 0.00000E+00
0.00000E+00 0.00000E+00 0.00000E+00 0.00000E+00 0.00000E+00 0.00000E+00
0.00000E+00 0.00000E+00 0.00000E+00 0.00000E+00 0.00000E+00 0.00000E+00
0.00000E+00 0.00000E+00 0.00000E+00 0.00000E+00 0.00000E+00 0.00000E+00
0.00000E+00 0.00000E+00 0.00000E+00 0.00000E+00 0.00000E+00 0.00000E+00
0.00000E+00 0.00000E+00 0.00000E+00 0.00000E+00 0.00000E+00 0.00000E+00
0.00000E+00 0.00000E+00 0.00000E+00 0.00000E+00 0.00000E+00 0.00000E+00
0.00000E+00 0.00000E+00 0.00000E+00 0.00000E+00 0.00000E+00 0.00000E+00
0.00000E+00 0.00000E+00 0.00000E+00 0.00000E+00 0.00000E+00 0.00000E+00
0.00000E+00 0.00000E+00 0.00000E+00 0.00000E+00 0.00000E+00 0.00000E+00
0.00000E+00 0.00000E+00 0.00000E+00 0.00000E+00 0.00000E+00 0.00000E+00
0.00000E+00 0.00000E+00 0.00000E+00 0.00000E+00 0.00000E+00 0.00000E+00
0.00000E+00 0.00000E+00 0.00000E+00 0.00000E+00 0.00000E+00 0.00000E+00
0.00000E+00 0.00000E+00 0.00000E+00 0.00000E+00 0.00000E+00 0.00000E+00
0.00000E+00 0.00000E+00 0.00000E+00 0.00000E+00 0.00000E+00 0.00000E+00
0.00000E+00 0.00000E+00 0.00000E+00 0.00000E+00 0.00000E+00 0.00000E+00
0.00000E+00 0.00000E+00 0.00000E+00 0.00000E+00 0.00000E+00 0.00000E+00
0.00000E+00 0.00000E+00 0.00000E+00 0.00000E+00 0.00000E+00 0.00000E+00
0.00000E+00 0.00000E+00 0.00000E+00 0.00000E+00 0.00000E+00 0.00000E+00
0.00000E+00 0.00000E+00 0.00000E+00 0.00000E+00 0.00000E+00 0.00000E+00
0.00000E+00 0.00000E+00 0.00000E+00 0.00000E+00 0.00000E+00 0.00000E+00
0.00000E+00 0.00000E+00 0.00000E+00 0.00000E+00 0.00000E+00 0.00000E+00
0.00000E+00 0.00000E+00 0.00000E+00 0.00000E+00 0.00000E+00 0.00000E+00
0.00000E+00 0.00000E+00 0.00000E+00 0.00000E+00 0.00000E+00 0.00000E+00
0.00000E+00 0.00000E+00 0.00000E+00 0.00000E+00 0.00000E+00 0.00000E+00
0.00000E+00 0.00000E+00 0.00000E+00 0.00000E+00 0.00000E+00 0.00000E+00
0.00000E+00 0.00000E+00 0.00000E+00 0.00000E+00 0.00000E+00 0.00000E+00
0.00000E+00 0.00000E+00 0.00000E+00 2.61943E-07 2.60829E-04 8.53100E-03
7.65936E-02 2.60933E-01 3.60985E-01 3.28228E-01 2.59555E-01 1.91499E-01
1.62092E-01 1.72430E-01 1.74193E-01 1.55670E-01 1.35655E-01 1.20144E-01
1.07166E-01 9.34948E-02 7.55438E-02 6.26489E-02 5.28925E-02 4.98618E-02
6.61974E-02 9.69748E-02 1.23862E-01 1.35354E-01 1.40909E-01 1.57114E-01
1.72561E-01 1.82035E-01 1.88632E-01 1.81613E-01 1.51093E-01 1.00767E-01
7.73867E-02 7.79627E-02 9.46567E-02 1.16802E-01 1.29155E-01 1.19173E-01
1.09752E-01 1.06022E-01 9.83184E-02 7.52581E-02 5.04784E-02 4.51941E-02
4.53444E-02 4.70921E-02 4.78151E-02 4.98543E-02 4.87745E-02 4.08307E-02
2.66357E-02 1.36774E-02 3.85522E-03 2.50166E-04 7.36160E-06 0.00000E+00/
```

```
0. 0. 1./  weights
0/
550/ temperature (K)
0.0005 282/  phonon frequency distribution
0.00000E+00 3.69043E-07 4.51073E-06 1.48094E-05 2.25987E-05 3.22999E-05
6.16991E-05 6.77449E-05 7.67336E-05 1.25865E-04 1.43707E-04 1.60864E-04
2.11942E-04 2.29785E-04 2.78851E-04 3.34797E-04 3.42459E-04 4.18236E-04
4.68895E-04 5.18248E-04 5.79283E-04 6.41660E-04 7.13610E-04 7.93998E-04
8.69411E-04 9.84174E-04 1.13021E-03 1.31303E-03 1.50552E-03 1.50810E-03
1.43532E-03 1.23224E-03 9.72959E-04 7.98661E-04 6.78125E-04 5.91510E-04
5.22776E-04 4.81131E-04 4.33361E-04 3.56445E-04 2.93510E-04 2.57948E-04
2.60203E-04 2.56071E-04 1.81593E-04 1.17487E-04 8.14076E-05 5.50319E-05
3.31189E-05 1.52483E-05 4.17435E-06 5.40118E-07 1.13307E-08 0.00000E+00
0.00000E+00 0.00000E+00 0.00000E+00 0.00000E+00 0.00000E+00 0.00000E+00
0.00000E+00 0.00000E+00 0.00000E+00 0.00000E+00 0.00000E+00 0.00000E+00
0.00000E+00 0.00000E+00 0.00000E+00 0.00000E+00 0.00000E+00 0.00000E+00
0.00000E+00 0.00000E+00 0.00000E+00 0.00000E+00 0.00000E+00 0.00000E+00
0.00000E+00 0.00000E+00 0.00000E+00 0.00000E+00 0.00000E+00 0.00000E+00
0.00000E+00 0.00000E+00 0.00000E+00 0.00000E+00 0.00000E+00 0.00000E+00
0.00000E+00 0.00000E+00 0.00000E+00 0.00000E+00 0.00000E+00 0.00000E+00
0.00000E+00 0.00000E+00 0.00000E+00 0.00000E+00 0.00000E+00 0.00000E+00
0.00000E+00 0.00000E+00 0.00000E+00 0.00000E+00 0.00000E+00 0.00000E+00
0.00000E+00 0.00000E+00 0.00000E+00 0.00000E+00 0.00000E+00 0.00000E+00
0.00000E+00 0.00000E+00 0.00000E+00 0.00000E+00 0.00000E+00 0.00000E+00
0.00000E+00 0.00000E+00 0.00000E+00 0.00000E+00 0.00000E+00 0.00000E+00
0.00000E+00 0.00000E+00 0.00000E+00 0.00000E+00 0.00000E+00 0.00000E+00
0.00000E+00 0.00000E+00 0.00000E+00 0.00000E+00 0.00000E+00 0.00000E+00
0.00000E+00 0.00000E+00 0.00000E+00 0.00000E+00 0.00000E+00 0.00000E+00
0.00000E+00 0.00000E+00 0.00000E+00 0.00000E+00 0.00000E+00 0.00000E+00
0.00000E+00 0.00000E+00 0.00000E+00 0.00000E+00 0.00000E+00 0.00000E+00
0.00000E+00 0.00000E+00 0.00000E+00 0.00000E+00 0.00000E+00 0.00000E+00
0.00000E+00 0.00000E+00 0.00000E+00 0.00000E+00 0.00000E+00 0.00000E+00
0.00000E+00 0.00000E+00 0.00000E+00 0.00000E+00 0.00000E+00 0.00000E+00
0.00000E+00 0.00000E+00 0.00000E+00 0.00000E+00 0.00000E+00 0.00000E+00
0.00000E+00 0.00000E+00 0.00000E+00 0.00000E+00 0.00000E+00 0.00000E+00
0.00000E+00 0.00000E+00 0.00000E+00 0.00000E+00 0.00000E+00 0.00000E+00
0.00000E+00 0.00000E+00 0.00000E+00 0.00000E+00 0.00000E+00 0.00000E+00
0.00000E+00 0.00000E+00 0.00000E+00 0.00000E+00 0.00000E+00 0.00000E+00
0.00000E+00 0.00000E+00 0.00000E+00 0.00000E+00 0.00000E+00 0.00000E+00
0.00000E+00 0.00000E+00 0.00000E+00 0.00000E+00 0.00000E+00 0.00000E+00
0.00000E+00 0.00000E+00 1.03279E-08 3.25252E-06 9.63493E-04 2.12129E-02
1.30424E-01 3.00086E-01 3.31159E-01 3.06141E-01 2.64445E-01 2.06477E-01
1.87144E-01 1.82146E-01 1.76936E-01 1.56370E-01 1.34605E-01 1.15276E-01
9.71079E-02 8.15010E-02 6.50072E-02 5.01755E-02 4.95303E-02 6.49634E-02
9.53235E-02 1.26597E-01 1.44727E-01 1.51295E-01 1.60875E-01 1.71981E-01
1.78503E-01 1.78576E-01 1.72517E-01 1.49374E-01 9.96772E-02 7.40487E-02
7.25965E-02 8.76235E-02 1.11430E-01 1.28286E-01 1.20368E-01 1.11270E-01
1.08604E-01 1.04377E-01 8.90935E-02 5.98999E-02 4.90975E-02 4.90167E-02
5.07626E-02 5.19319E-02 5.32254E-02 4.77893E-02 3.34914E-02 1.80498E-02
6.06457E-03 7.68475E-04 1.12516E-05 0.00000E+00 0.00000E+00 0.00000E+00/
0. 0. 1./  weights
0/
800/ temperature (K)
```

```
0.0005 282/  phonon frequency distribution
0.00000E+00 4.76301E-07 5.28884E-06 1.59762E-05 2.36596E-05 3.66688E-05
6.70886E-05 6.83644E-05 8.83295E-05 1.36716E-04 1.46262E-04 1.83692E-04
2.22214E-04 2.42483E-04 3.09015E-04 3.42508E-04 3.66612E-04 4.48234E-04
4.86761E-04 5.47319E-04 6.05041E-04 6.69508E-04 7.44406E-04 8.20495E-04
9.00680E-04 1.02305E-03 1.16597E-03 1.37473E-03 1.52338E-03 1.50170E-03
1.40697E-03 1.15637E-03 9.18847E-04 7.65204E-04 6.59613E-04 5.73867E-04
5.18962E-04 4.78522E-04 4.25147E-04 3.45342E-04 2.89460E-04 2.67392E-04
2.84240E-04 2.58557E-04 1.62289E-04 1.02867E-04 6.85897E-05 4.28504E-05
2.15670E-05 6.78174E-06 1.11289E-06 4.49742E-08 0.00000E+00 0.00000E+00
0.00000E+00 0.00000E+00 0.00000E+00 0.00000E+00 0.00000E+00 0.00000E+00
0.00000E+00 0.00000E+00 0.00000E+00 0.00000E+00 0.00000E+00 0.00000E+00
0.00000E+00 0.00000E+00 0.00000E+00 0.00000E+00 0.00000E+00 0.00000E+00
0.00000E+00 0.00000E+00 0.00000E+00 0.00000E+00 0.00000E+00 0.00000E+00
0.00000E+00 0.00000E+00 0.00000E+00 0.00000E+00 0.00000E+00 0.00000E+00
0.00000E+00 0.00000E+00 0.00000E+00 0.00000E+00 0.00000E+00 0.00000E+00
0.00000E+00 0.00000E+00 0.00000E+00 0.00000E+00 0.00000E+00 0.00000E+00
0.00000E+00 0.00000E+00 0.00000E+00 0.00000E+00 0.00000E+00 0.00000E+00
0.00000E+00 0.00000E+00 0.00000E+00 0.00000E+00 0.00000E+00 0.00000E+00
0.00000E+00 0.00000E+00 0.00000E+00 0.00000E+00 0.00000E+00 0.00000E+00
0.00000E+00 0.00000E+00 0.00000E+00 0.00000E+00 0.00000E+00 0.00000E+00
0.00000E+00 0.00000E+00 0.00000E+00 0.00000E+00 0.00000E+00 0.00000E+00
0.00000E+00 0.00000E+00 0.00000E+00 0.00000E+00 0.00000E+00 0.00000E+00
0.00000E+00 0.00000E+00 0.00000E+00 0.00000E+00 0.00000E+00 0.00000E+00
0.00000E+00 0.00000E+00 0.00000E+00 0.00000E+00 0.00000E+00 0.00000E+00
0.00000E+00 0.00000E+00 0.00000E+00 0.00000E+00 0.00000E+00 0.00000E+00
0.00000E+00 0.00000E+00 0.00000E+00 0.00000E+00 0.00000E+00 0.00000E+00
0.00000E+00 0.00000E+00 0.00000E+00 0.00000E+00 0.00000E+00 0.00000E+00
0.00000E+00 0.00000E+00 0.00000E+00 0.00000E+00 0.00000E+00 0.00000E+00
0.00000E+00 0.00000E+00 0.00000E+00 0.00000E+00 0.00000E+00 0.00000E+00
0.00000E+00 0.00000E+00 0.00000E+00 0.00000E+00 0.00000E+00 0.00000E+00
0.00000E+00 0.00000E+00 0.00000E+00 0.00000E+00 0.00000E+00 0.00000E+00
0.00000E+00 0.00000E+00 0.00000E+00 0.00000E+00 0.00000E+00 0.00000E+00
0.00000E+00 0.00000E+00 0.00000E+00 0.00000E+00 0.00000E+00 0.00000E+00
0.00000E+00 0.00000E+00 0.00000E+00 0.00000E+00 0.00000E+00 0.00000E+00
0.00000E+00 0.00000E+00 0.00000E+00 0.00000E+00 0.00000E+00 0.00000E+00
0.00000E+00 0.00000E+00 0.00000E+00 0.00000E+00 0.00000E+00 0.00000E+00
0.00000E+00 0.00000E+00 3.59590E-07 1.11870E-04 5.66162E-03 5.15136E-02
2.03013E-01 3.35573E-01 3.34817E-01 2.92834E-01 2.25629E-01 2.06101E-01
2.00336E-01 1.92019E-01 1.68735E-01 1.44709E-01 1.24002E-01 1.04638E-01
8.97917E-02 7.20927E-02 5.90015E-02 5.95315E-02 8.60017E-02 1.31535E-01
1.62805E-01 1.72850E-01 1.79076E-01 1.92407E-01 1.96652E-01 1.83343E-01
1.68741E-01 1.38700E-01 9.30415E-02 7.41752E-02 7.50116E-02 8.94507E-02
1.12550E-01 1.17095E-01 1.10613E-01 1.02689E-01 9.83544E-02 9.47340E-02
7.20120E-02 4.79024E-02 4.44697E-02 4.63698E-02 4.81948E-02 4.98753E-02
5.13147E-02 5.31286E-02 4.91893E-02 3.56811E-02 1.91998E-02 6.30390E-03
6.33784E-04 1.52216E-05 0.00000E+00 0.00000E+00 0.00000E+00 0.00000E+00/
0. 0. 1./  weights
0/
900/ temperature (K)
0.0005 282/  phonon frequency distribution
0.00000E+00 5.36092E-07 5.62829E-06 1.63832E-05 2.36769E-05 3.74255E-05
6.88845E-05 6.93580E-05 9.04161E-05 1.38320E-04 1.48279E-04 1.89918E-04
```

```
2.23250E-04 2.46039E-04 3.13666E-04 3.45849E-04 3.75611E-04 4.47122E-04
4.96434E-04 5.53553E-04 6.11906E-04 6.74306E-04 7.55860E-04 8.30118E-04
9.13423E-04 1.04636E-03 1.20225E-03 1.40772E-03 1.50610E-03 1.48033E-03
1.35483E-03 1.11065E-03 8.84691E-04 7.43094E-04 6.46917E-04 5.64976E-04
5.13581E-04 4.67574E-04 4.02584E-04 3.30508E-04 2.80156E-04 2.59670E-04
2.71637E-04 2.43290E-04 1.53571E-04 9.60875E-05 6.57990E-05 4.11368E-05
2.09153E-05 7.06440E-06 8.82224E-07 3.95787E-08 0.00000E+00 0.00000E+00
0.00000E+00 0.00000E+00 0.00000E+00 0.00000E+00 0.00000E+00 0.00000E+00
0.00000E+00 0.00000E+00 0.00000E+00 0.00000E+00 0.00000E+00 0.00000E+00
0.00000E+00 0.00000E+00 0.00000E+00 0.00000E+00 0.00000E+00 0.00000E+00
0.00000E+00 0.00000E+00 0.00000E+00 0.00000E+00 0.00000E+00 0.00000E+00
0.00000E+00 0.00000E+00 0.00000E+00 0.00000E+00 0.00000E+00 0.00000E+00
0.00000E+00 0.00000E+00 0.00000E+00 0.00000E+00 0.00000E+00 0.00000E+00
0.00000E+00 0.00000E+00 0.00000E+00 0.00000E+00 0.00000E+00 0.00000E+00
0.00000E+00 0.00000E+00 0.00000E+00 0.00000E+00 0.00000E+00 0.00000E+00
0.00000E+00 0.00000E+00 0.00000E+00 0.00000E+00 0.00000E+00 0.00000E+00
0.00000E+00 0.00000E+00 0.00000E+00 0.00000E+00 0.00000E+00 0.00000E+00
0.00000E+00 0.00000E+00 0.00000E+00 0.00000E+00 0.00000E+00 0.00000E+00
0.00000E+00 0.00000E+00 0.00000E+00 0.00000E+00 0.00000E+00 0.00000E+00
0.00000E+00 0.00000E+00 0.00000E+00 0.00000E+00 0.00000E+00 0.00000E+00
0.00000E+00 0.00000E+00 0.00000E+00 0.00000E+00 0.00000E+00 0.00000E+00
0.00000E+00 0.00000E+00 0.00000E+00 0.00000E+00 0.00000E+00 0.00000E+00
0.00000E+00 0.00000E+00 0.00000E+00 0.00000E+00 0.00000E+00 0.00000E+00
0.00000E+00 0.00000E+00 0.00000E+00 0.00000E+00 0.00000E+00 0.00000E+00
0.00000E+00 0.00000E+00 0.00000E+00 0.00000E+00 0.00000E+00 0.00000E+00
0.00000E+00 0.00000E+00 0.00000E+00 0.00000E+00 0.00000E+00 0.00000E+00
0.00000E+00 0.00000E+00 0.00000E+00 0.00000E+00 0.00000E+00 0.00000E+00
0.00000E+00 0.00000E+00 0.00000E+00 0.00000E+00 0.00000E+00 0.00000E+00
0.00000E+00 0.00000E+00 0.00000E+00 0.00000E+00 0.00000E+00 0.00000E+00
0.00000E+00 0.00000E+00 0.00000E+00 0.00000E+00 0.00000E+00 0.00000E+00
0.00000E+00 0.00000E+00 0.00000E+00 0.00000E+00 0.00000E+00 0.00000E+00
0.00000E+00 0.00000E+00 0.00000E+00 0.00000E+00 0.00000E+00 0.00000E+00
0.00000E+00 0.00000E+00 0.00000E+00 0.00000E+00 0.00000E+00 0.00000E+00
0.00000E+00 0.00000E+00 0.00000E+00 0.00000E+00 6.56498E-10 4.86292E-07
1.43978E-04 4.70467E-03 3.51446E-02 1.27034E-01 2.35838E-01 2.74177E-01
2.41784E-01 2.10757E-01 1.92484E-01 2.02368E-01 2.18389E-01 1.90322E-01
1.81249E-01 1.73003E-01 1.47085E-01 1.23691E-01 1.03933E-01 7.94229E-02
5.71594E-02 5.11893E-02 6.88840E-02 1.04371E-01 1.33161E-01 1.49199E-01
1.52103E-01 1.54627E-01 1.62003E-01 1.67547E-01 1.74646E-01 1.78144E-01
1.54517E-01 9.89438E-02 7.12417E-02 7.69459E-02 9.89867E-02 1.30139E-01
1.36614E-01 1.29258E-01 1.32162E-01 1.33499E-01 8.62609E-02 4.96001E-02
4.65695E-02 4.69636E-02 4.86435E-02 5.03221E-02 5.17943E-02 5.24929E-02
4.55200E-02 3.07795E-02 1.63576E-02 5.13931E-03 5.27990E-04 7.83709E-06
0.00000E+00 0.00000E+00 0.00000E+00 0.00000E+00 0.00000E+00 0.00000E+00/
0. 0. 1./  weights
0/
1000/ temperature (K)
0.0005 282/  phonon frequency distribution
0.00000E+00 4.79179E-07 5.22499E-06 1.55916E-05 2.28922E-05 3.54593E-05
6.51952E-05 6.56694E-05 8.75372E-05 1.33389E-04 1.41247E-04 1.82450E-04
2.15100E-04 2.37509E-04 3.06331E-04 3.32261E-04 3.66536E-04 4.38139E-04
4.79869E-04 5.42061E-04 5.97815E-04 6.63154E-04 7.44236E-04 8.10759E-04
9.03222E-04 1.03205E-03 1.18396E-03 1.38256E-03 1.46739E-03 1.41197E-03
```

```
1.26959E-03 1.01489E-03 8.23379E-04 6.89266E-04 5.99837E-04 5.24302E-04
4.76827E-04 4.39725E-04 3.76809E-04 3.08207E-04 2.66189E-04 2.56893E-04
2.67921E-04 2.09887E-04 1.32784E-04 9.15376E-05 6.23454E-05 3.83761E-05
1.88808E-05 5.42797E-06 8.15507E-07 3.08223E-08 0.00000E+00 0.00000E+00
0.00000E+00 0.00000E+00 0.00000E+00 0.00000E+00 0.00000E+00 0.00000E+00
0.00000E+00 0.00000E+00 0.00000E+00 0.00000E+00 0.00000E+00 0.00000E+00
0.00000E+00 0.00000E+00 0.00000E+00 0.00000E+00 0.00000E+00 0.00000E+00
0.00000E+00 0.00000E+00 0.00000E+00 0.00000E+00 0.00000E+00 0.00000E+00
0.00000E+00 0.00000E+00 0.00000E+00 0.00000E+00 0.00000E+00 0.00000E+00
0.00000E+00 0.00000E+00 0.00000E+00 0.00000E+00 0.00000E+00 0.00000E+00
0.00000E+00 0.00000E+00 0.00000E+00 0.00000E+00 0.00000E+00 0.00000E+00
0.00000E+00 0.00000E+00 0.00000E+00 0.00000E+00 0.00000E+00 0.00000E+00
0.00000E+00 0.00000E+00 0.00000E+00 0.00000E+00 0.00000E+00 0.00000E+00
0.00000E+00 0.00000E+00 0.00000E+00 0.00000E+00 0.00000E+00 0.00000E+00
0.00000E+00 0.00000E+00 0.00000E+00 0.00000E+00 0.00000E+00 0.00000E+00
0.00000E+00 0.00000E+00 0.00000E+00 0.00000E+00 0.00000E+00 0.00000E+00
0.00000E+00 0.00000E+00 0.00000E+00 0.00000E+00 0.00000E+00 0.00000E+00
0.00000E+00 0.00000E+00 0.00000E+00 0.00000E+00 0.00000E+00 0.00000E+00
0.00000E+00 0.00000E+00 0.00000E+00 0.00000E+00 0.00000E+00 0.00000E+00
0.00000E+00 0.00000E+00 0.00000E+00 0.00000E+00 0.00000E+00 0.00000E+00
0.00000E+00 0.00000E+00 0.00000E+00 0.00000E+00 0.00000E+00 0.00000E+00
0.00000E+00 0.00000E+00 0.00000E+00 0.00000E+00 0.00000E+00 0.00000E+00
0.00000E+00 0.00000E+00 0.00000E+00 0.00000E+00 0.00000E+00 0.00000E+00
0.00000E+00 0.00000E+00 0.00000E+00 0.00000E+00 0.00000E+00 0.00000E+00
0.00000E+00 0.00000E+00 0.00000E+00 0.00000E+00 0.00000E+00 0.00000E+00
0.00000E+00 0.00000E+00 0.00000E+00 0.00000E+00 0.00000E+00 0.00000E+00
0.00000E+00 0.00000E+00 0.00000E+00 0.00000E+00 0.00000E+00 0.00000E+00
0.00000E+00 0.00000E+00 0.00000E+00 0.00000E+00 0.00000E+00 0.00000E+00
0.00000E+00 0.00000E+00 0.00000E+00 0.00000E+00 0.00000E+00 0.00000E+00
0.00000E+00 0.00000E+00 0.00000E+00 0.00000E+00 0.00000E+00 0.00000E+00
0.00000E+00 0.00000E+00 0.00000E+00 0.00000E+00 0.00000E+00 0.00000E+00
0.00000E+00 0.00000E+00 0.00000E+00 3.57609E-11 1.73185E-07 1.70739E-05
9.03519E-04 7.89538E-03 2.52396E-02 8.48743E-02 2.18207E-01 3.25562E-01
3.13464E-01 2.65180E-01 2.13071E-01 1.97799E-01 1.99149E-01 1.72614E-01
1.59917E-01 1.53147E-01 1.33725E-01 1.15969E-01 9.51859E-02 7.53447E-02
5.67054E-02 5.60039E-02 6.95879E-02 1.03814E-01 1.40725E-01 1.59651E-01
1.70648E-01 1.85622E-01 2.01506E-01 2.17405E-01 2.07288E-01 1.45896E-01
9.47601E-02 7.64337E-02 7.47376E-02 8.28885E-02 1.08733E-01 1.44554E-01
1.51016E-01 1.39958E-01 1.24585E-01 7.66727E-02 5.12654E-02 5.01320E-02
5.27718E-02 5.43894E-02 5.62614E-02 5.78375E-02 5.57670E-02 4.12193E-02
2.23482E-02 7.29417E-03 9.94646E-04 1.44154E-05 0.00000E+00 0.00000E+00
0.00000E+00 0.00000E+00 0.00000E+00 0.00000E+00 0.00000E+00 0.00000E+00/
0. 0. 1./  weights
0/
1100/ temperature (K)
0.0005 282/  phonon frequency distribution
0.00000E+00 5.18945E-07 5.54173E-06 1.62553E-05 2.37077E-05 3.71939E-05
6.76313E-05 6.71110E-05 9.39432E-05 1.38879E-04 1.44849E-04 1.92901E-04
2.21659E-04 2.50953E-04 3.22063E-04 3.40963E-04 3.87832E-04 4.54332E-04
4.99954E-04 5.64463E-04 6.19266E-04 6.89965E-04 7.75514E-04 8.41230E-04
9.42844E-04 1.06887E-03 1.23803E-03 1.44796E-03 1.50442E-03 1.44488E-03
1.31166E-03 1.06175E-03 8.52609E-04 7.13098E-04 6.19400E-04 5.41839E-04
4.95502E-04 4.54325E-04 3.85197E-04 3.17513E-04 2.72931E-04 2.68904E-04
2.81927E-04 2.16397E-04 1.34597E-04 8.97440E-05 6.03075E-05 3.54719E-05
```

```
1.58813E-05 4.28002E-06 3.05860E-07 5.42015E-09 0.00000E+00 0.00000E+00
0.00000E+00 0.00000E+00 0.00000E+00 0.00000E+00 0.00000E+00 0.00000E+00
0.00000E+00 0.00000E+00 0.00000E+00 0.00000E+00 0.00000E+00 0.00000E+00
0.00000E+00 0.00000E+00 0.00000E+00 0.00000E+00 0.00000E+00 0.00000E+00
0.00000E+00 0.00000E+00 0.00000E+00 0.00000E+00 0.00000E+00 0.00000E+00
0.00000E+00 0.00000E+00 0.00000E+00 0.00000E+00 0.00000E+00 0.00000E+00
0.00000E+00 0.00000E+00 0.00000E+00 0.00000E+00 0.00000E+00 0.00000E+00
0.00000E+00 0.00000E+00 0.00000E+00 0.00000E+00 0.00000E+00 0.00000E+00
0.00000E+00 0.00000E+00 0.00000E+00 0.00000E+00 0.00000E+00 0.00000E+00
0.00000E+00 0.00000E+00 0.00000E+00 0.00000E+00 0.00000E+00 0.00000E+00
0.00000E+00 0.00000E+00 0.00000E+00 0.00000E+00 0.00000E+00 0.00000E+00
0.00000E+00 0.00000E+00 0.00000E+00 0.00000E+00 0.00000E+00 0.00000E+00
0.00000E+00 0.00000E+00 0.00000E+00 0.00000E+00 0.00000E+00 0.00000E+00
0.00000E+00 0.00000E+00 0.00000E+00 0.00000E+00 0.00000E+00 0.00000E+00
0.00000E+00 0.00000E+00 0.00000E+00 0.00000E+00 0.00000E+00 0.00000E+00
0.00000E+00 0.00000E+00 0.00000E+00 0.00000E+00 0.00000E+00 0.00000E+00
0.00000E+00 0.00000E+00 0.00000E+00 0.00000E+00 0.00000E+00 0.00000E+00
0.00000E+00 0.00000E+00 0.00000E+00 0.00000E+00 0.00000E+00 0.00000E+00
0.00000E+00 0.00000E+00 0.00000E+00 0.00000E+00 0.00000E+00 0.00000E+00
0.00000E+00 0.00000E+00 0.00000E+00 0.00000E+00 0.00000E+00 0.00000E+00
0.00000E+00 0.00000E+00 0.00000E+00 0.00000E+00 0.00000E+00 0.00000E+00
0.00000E+00 0.00000E+00 0.00000E+00 0.00000E+00 0.00000E+00 0.00000E+00
0.00000E+00 0.00000E+00 0.00000E+00 0.00000E+00 0.00000E+00 0.00000E+00
0.00000E+00 0.00000E+00 0.00000E+00 0.00000E+00 0.00000E+00 0.00000E+00
0.00000E+00 0.00000E+00 0.00000E+00 0.00000E+00 0.00000E+00 0.00000E+00
0.00000E+00 0.00000E+00 0.00000E+00 0.00000E+00 0.00000E+00 0.00000E+00
0.00000E+00 0.00000E+00 0.00000E+00 0.00000E+00 0.00000E+00 0.00000E+00
0.00000E+00 0.00000E+00 0.00000E+00 0.00000E+00 0.00000E+00 0.00000E+00
0.00000E+00 0.00000E+00 0.00000E+00 0.00000E+00 0.00000E+00 5.68174E-06
4.10892E-04 1.05058E-02 8.44829E-02 2.29737E-01 3.36964E-01 3.39150E-01
2.81859E-01 2.57997E-01 2.40079E-01 2.01693E-01 1.88724E-01 1.57236E-01
1.28393E-01 1.07530E-01 9.22622E-02 7.30665E-02 5.47846E-02 4.94884E-02
6.06076E-02 9.20340E-02 1.31441E-01 1.57407E-01 1.58349E-01 1.57472E-01
1.74364E-01 1.87837E-01 1.91446E-01 1.88937E-01 1.55311E-01 9.63242E-02
7.05769E-02 7.30319E-02 9.63029E-02 1.31949E-01 1.37728E-01 1.29810E-01
1.22293E-01 1.16897E-01 8.78780E-02 6.14271E-02 5.63980E-02 5.86254E-02
6.01977E-02 6.25628E-02 5.87200E-02 4.20127E-02 2.06209E-02 5.65291E-03
4.47252E-04 5.67551E-06 0.00000E+00 0.00000E+00 0.00000E+00 0.00000E+00
0.00000E+00 0.00000E+00 0.00000E+00 0.00000E+00 0.00000E+00 0.00000E+00/
0. 0. 1./  weights
0/
1200/ temperature (K)
0.0005 282/  phonon frequency distribution
0.00000E+00 5.28932E-07 5.55188E-06 1.61606E-05 2.35805E-05 3.76707E-05
6.68001E-05 6.63863E-05 9.50867E-05 1.37348E-04 1.43284E-04 1.93726E-04
2.18151E-04 2.50582E-04 3.21611E-04 3.35547E-04 3.89040E-04 4.51975E-04
4.97723E-04 5.64606E-04 6.18979E-04 6.92095E-04 7.79384E-04 8.45617E-04
9.55569E-04 1.08769E-03 1.27365E-03 1.48054E-03 1.51483E-03 1.44429E-03
1.25473E-03 9.90328E-04 8.01701E-04 6.77506E-04 5.90202E-04 5.21696E-04
4.73336E-04 4.15717E-04 3.47606E-04 2.92115E-04 2.57801E-04 2.66296E-04
2.80887E-04 2.05189E-04 1.27841E-04 8.66563E-05 5.81040E-05 3.38601E-05
1.47606E-05 3.82474E-06 2.73074E-07 3.99024E-09 0.00000E+00 0.00000E+00
0.00000E+00 0.00000E+00 0.00000E+00 0.00000E+00 0.00000E+00 0.00000E+00
0.00000E+00 0.00000E+00 0.00000E+00 0.00000E+00 0.00000E+00 0.00000E+00
```

```
0.00000E+00 0.00000E+00 0.00000E+00 0.00000E+00 0.00000E+00 0.00000E+00
0.00000E+00 0.00000E+00 0.00000E+00 0.00000E+00 0.00000E+00 0.00000E+00
0.00000E+00 0.00000E+00 0.00000E+00 0.00000E+00 0.00000E+00 0.00000E+00
0.00000E+00 0.00000E+00 0.00000E+00 0.00000E+00 0.00000E+00 0.00000E+00
0.00000E+00 0.00000E+00 0.00000E+00 0.00000E+00 0.00000E+00 0.00000E+00
0.00000E+00 0.00000E+00 0.00000E+00 0.00000E+00 0.00000E+00 0.00000E+00
0.00000E+00 0.00000E+00 0.00000E+00 0.00000E+00 0.00000E+00 0.00000E+00
0.00000E+00 0.00000E+00 0.00000E+00 0.00000E+00 0.00000E+00 0.00000E+00
0.00000E+00 0.00000E+00 0.00000E+00 0.00000E+00 0.00000E+00 0.00000E+00
0.00000E+00 0.00000E+00 0.00000E+00 0.00000E+00 0.00000E+00 0.00000E+00
0.00000E+00 0.00000E+00 0.00000E+00 0.00000E+00 0.00000E+00 0.00000E+00
0.00000E+00 0.00000E+00 0.00000E+00 0.00000E+00 0.00000E+00 0.00000E+00
0.00000E+00 0.00000E+00 0.00000E+00 0.00000E+00 0.00000E+00 0.00000E+00
0.00000E+00 0.00000E+00 0.00000E+00 0.00000E+00 0.00000E+00 0.00000E+00
0.00000E+00 0.00000E+00 0.00000E+00 0.00000E+00 0.00000E+00 0.00000E+00
0.00000E+00 0.00000E+00 0.00000E+00 0.00000E+00 0.00000E+00 0.00000E+00
0.00000E+00 0.00000E+00 0.00000E+00 0.00000E+00 0.00000E+00 0.00000E+00
0.00000E+00 0.00000E+00 0.00000E+00 0.00000E+00 0.00000E+00 0.00000E+00
0.00000E+00 0.00000E+00 0.00000E+00 0.00000E+00 0.00000E+00 0.00000E+00
0.00000E+00 0.00000E+00 0.00000E+00 0.00000E+00 0.00000E+00 0.00000E+00
0.00000E+00 0.00000E+00 0.00000E+00 0.00000E+00 0.00000E+00 0.00000E+00
0.00000E+00 0.00000E+00 0.00000E+00 0.00000E+00 0.00000E+00 0.00000E+00
0.00000E+00 0.00000E+00 0.00000E+00 0.00000E+00 0.00000E+00 0.00000E+00
0.00000E+00 0.00000E+00 0.00000E+00 0.00000E+00 0.00000E+00 0.00000E+00
0.00000E+00 0.00000E+00 0.00000E+00 0.00000E+00 0.00000E+00 0.00000E+00
0.00000E+00 0.00000E+00 0.00000E+00 4.77844E-06 3.40461E-04 1.13983E-02
7.59785E-02 1.87233E-01 2.63106E-01 2.70506E-01 2.36191E-01 2.17897E-01
2.38064E-01 2.45919E-01 2.12900E-01 1.86788E-01 1.68332E-01 1.43576E-01
1.19720E-01 1.00174E-01 7.98782E-02 5.91167E-02 5.41711E-02 7.04651E-02
1.03711E-01 1.38719E-01 1.51423E-01 1.54630E-01 1.64948E-01 1.69640E-01
1.75420E-01 1.92607E-01 1.89094E-01 1.26178E-01 7.89972E-02 6.59293E-02
6.99258E-02 8.58563E-02 1.19590E-01 1.49629E-01 1.55287E-01 1.47728E-01
1.07641E-01 6.18422E-02 4.92906E-02 5.13642E-02 5.15193E-02 5.42561E-02
5.53872E-02 5.74447E-02 5.31832E-02 3.71295E-02 1.88287E-02 5.41676E-03
5.47047E-04 4.49151E-06 0.00000E+00 0.00000E+00 0.00000E+00 0.00000E+00
0.00000E+00 0.00000E+00 0.00000E+00 0.00000E+00 0.00000E+00 0.00000E+00/
0. 0. 1./  weights
0/
' H(YH2)    ORNL       EVAL-SEP20 CHAPMAN,RAMIC                    '/
' REF. 0 (2020)        DIST-                                       '/
'---- ENDF/B-VIII      MATERIAL 5                                  '/
'----- THERMAL NEUTRON SCATTERING DATA                             '/
'------ ENDF-6 FORMAT                                              '/
'                                                                  '/
' Temperatures (K)                                                 '/
' ---------------                                                  '/
'   20 295 550 800 900 1000 1100 1200                              '/
'                                                                  '/
' History                                                          '/
' -------                                                          '/
'                                                                  '/
' This evaluation was produced at Oak Ridge National Laboratory in '/
' September 2020 using the LEAPR module of NJOY21 [1]. The phonon  '/
' frequency distributions for H an dY in YH2 were caluclated using '/
```

```
' the stochastic Temperature Dependent Effective Potential [2] and '/
' the alpha and beta mesh were the same as those used for the ENDF8'/
' evaluation [3].                                                  '/
'                                                                  '/
' Theory                                                           '/
' ------                                                           '/
' YH2 has a fluorite type cubic crystal structure with the yttrium '/
' atoms forming a face-centered cubic sub-lattice and the hydrogen '/
' atoms situated in the tetrahedral interstices. The stochastic    '/
' Temperature Dependent Effective Potential (s-TDEP) method was    '/
' used with VASP to calculate the phonon spectra for H and Y in    '/
' YH2. The calculated double differential scattering cross section '/
' agrees with measurements.                                        '/
'                                                                  '/
' References                                                       '/
' ----------                                                       '/
' 1. A. C. Kahler Ed., LA-UR-12-27079 (December 20, 2012).         '/
' 2. N. Shulumba, O. Hellman, and A.J. Minnich, "Intrinsic         '/
'    localized mode and low thermal conductivity  of PbSe," Phys.  '/
'    Rev. B, 95, 014302 (2017)                                     '/
' 3. M. L. Zerkle and J. C. Holmes, "A Thermal Neutron Scattering  '/
'    Law for Yttrium Hydride," Int. Conf. Nucl. Data (September,   '/
'    2016).                                                        '/
/
stop


leapr
60
'Y in YH2, all temperatures, s-TDEP'/
8 1/
55 155/
88.1421 7.66 1 0 0 0/
0/
107 401 1/
1.00000E-3 1.25893E-3 1.58489E-3 1.99526E-3 2.51189E-3
3.16228E-3 3.98107E-3 5.01187E-3 6.30957E-3 7.94328E-3
1.00000E-2 1.25893E-2 1.58489E-2 1.99526E-2 2.51189E-2
3.16228E-2 3.98107E-2 5.01187E-2 6.30957E-2 7.94328E-2
1.00000E-1 1.25893E-1 1.58489E-1 1.99526E-1 2.51189E-1
3.16228E-1 3.98107E-1 5.01187E-1 6.30957E-1 7.94328E-1
1.00000E+0 1.12202E+0 1.25893E+0 1.41254E+0 1.58489E+0
1.77828E+0 1.99526E+0 2.23872E+0 2.51189E+0 2.81838E+0
3.16228E+0 3.54813E+0 3.98107E+0 4.46684E+0 5.01187E+0
5.62341E+0 6.30957E+0 7.07946E+0 7.94328E+0 8.91251E+0
1.00000E+1 1.12202E+1 1.25893E+1 1.41254E+1 1.58489E+1
1.77828E+1 1.99526E+1 2.23872E+1 2.51189E+1 2.81838E+1
3.16228E+1 3.54813E+1 3.98107E+1 4.46684E+1 5.01187E+1
5.62341E+1 6.30957E+1 7.07946E+1 7.94328E+1 8.91251E+1
1.00000E+2 1.12202E+2 1.25893E+2 1.41254E+2 1.58489E+2
1.77828E+2 2.00000E+2 2.20000E+2 2.40000E+2 2.60000E+2
2.80000E+2 3.00000E+2 3.20000E+2 3.40000E+2 3.60000E+2
3.80000E+2 4.00000E+2 4.20000E+2 4.40000E+2 4.60000E+2
4.80000E+2 5.00000E+2 5.20000E+2 5.40000E+2 5.60000E+2
```

```
5.80000E+2 6.00000E+2 6.20000E+2 6.40000E+2 6.60000E+2
6.80000E+2 7.00000E+2 7.20000E+2 7.40000E+2 7.60000E+2
7.80000E+2 8.00000E+2 / alpha grid
0.00000E+0 3.95257E-2 7.90514E-2 1.18577E-1 1.58103E-1
1.97628E-1 2.37154E-1 2.76680E-1 3.16206E-1 3.55731E-1
3.95257E-1 4.34783E-1 4.74308E-1 5.13834E-1 5.53360E-1
5.92885E-1 6.32411E-1 6.71937E-1 7.11462E-1 7.50988E-1
7.90514E-1 8.30040E-1 8.69565E-1 9.09091E-1 9.48617E-1
9.88142E-1 1.02767E+0 1.06719E+0 1.10672E+0 1.18577E+0
1.34387E+0 1.66008E+0 2.29249E+0 2.92490E+0 3.55731E+0
3.87352E+0 4.18972E+0 4.34783E+0 4.42688E+0 4.46640E+0
4.50593E+0 4.54545E+0 4.58498E+0 4.62451E+0 4.66403E+0
4.70356E+0 4.74308E+0 4.78261E+0 4.82213E+0 4.86166E+0
4.90119E+0 4.94071E+0 4.98024E+0 5.01976E+0 5.05929E+0
5.09881E+0 5.13834E+0 5.17787E+0 5.21739E+0 5.25692E+0
5.29644E+0 5.33597E+0 5.37549E+0 5.41502E+0 5.45455E+0
5.49407E+0 5.53360E+0 5.57312E+0 5.61265E+0 5.69170E+0
5.84980E+0 6.16601E+0 6.79842E+0 7.43083E+0 8.06324E+0
8.37945E+0 8.61660E+0 8.77470E+0 8.85375E+0 8.93281E+0
9.01186E+0 9.09091E+0 9.16996E+0 9.24901E+0 9.32806E+0
9.40711E+0 9.48617E+0 9.56522E+0 9.64427E+0 9.72332E+0
9.80237E+0 9.88142E+0 9.96047E+0 1.00395E+1 1.01186E+1
1.01976E+1 1.02767E+1 1.03557E+1 1.04348E+1 1.05138E+1
1.05929E+1 1.06719E+1 1.07510E+1 1.08300E+1 1.09091E+1
1.09881E+1 1.10672E+1 1.11462E+1 1.12253E+1 1.13834E+1
1.16996E+1 1.23320E+1 1.29644E+1 1.32806E+1 1.33992E+1
1.35178E+1 1.36364E+1 1.37549E+1 1.38735E+1 1.39921E+1
1.41107E+1 1.42292E+1 1.43478E+1 1.44664E+1 1.45850E+1
1.47036E+1 1.48221E+1 1.49407E+1 1.50593E+1 1.51779E+1
1.52964E+1 1.54150E+1 1.55336E+1 1.56522E+1 1.57708E+1
1.58893E+1 1.60079E+1 1.61265E+1 1.62451E+1 1.63636E+1
1.64822E+1 1.66008E+1 1.67194E+1 1.68379E+1 1.71542E+1
1.74704E+1 1.77075E+1 1.78656E+1 1.80237E+1 1.81818E+1
1.83399E+1 1.84980E+1 1.86561E+1 1.88142E+1 1.89723E+1
1.91304E+1 1.92885E+1 1.94466E+1 1.96047E+1 1.97628E+1
1.99209E+1 2.00791E+1 2.02372E+1 2.03953E+1 2.05534E+1
2.07115E+1 2.08696E+1 2.10277E+1 2.11858E+1 2.13439E+1
2.15020E+1 2.16601E+1 2.18182E+1 2.19763E+1 2.21344E+1
2.22925E+1 2.24506E+1 2.26482E+1 2.28458E+1 2.30435E+1
2.32411E+1 2.34387E+1 2.36364E+1 2.38340E+1 2.40316E+1
2.42292E+1 2.44269E+1 2.46245E+1 2.48221E+1 2.50198E+1
2.52174E+1 2.54150E+1 2.56126E+1 2.58103E+1 2.60079E+1
2.62055E+1 2.64032E+1 2.66008E+1 2.67984E+1 2.69960E+1
2.71937E+1 2.73913E+1 2.75889E+1 2.77866E+1 2.79842E+1
2.82213E+1 2.84585E+1 2.86957E+1 2.89328E+1 2.91700E+1
2.94071E+1 2.96443E+1 2.98814E+1 3.01186E+1 3.03557E+1
3.05929E+1 3.08300E+1 3.10672E+1 3.13043E+1 3.15415E+1
3.17787E+1 3.20158E+1 3.22530E+1 3.24901E+1 3.27273E+1
3.29644E+1 3.32016E+1 3.34387E+1 3.36759E+1 3.39526E+1
3.42292E+1 3.45059E+1 3.47826E+1 3.50593E+1 3.53360E+1
3.56126E+1 3.58893E+1 3.61660E+1 3.64427E+1 3.67194E+1
3.69960E+1 3.72727E+1 3.75494E+1 3.78261E+1 3.81028E+1
3.83794E+1 3.86561E+1 3.89328E+1 3.92095E+1 3.95257E+1
3.98419E+1 4.01581E+1 4.04743E+1 4.07905E+1 4.11067E+1
```

```
4.14229E+1 4.17391E+1 4.20553E+1 4.23715E+1 4.26877E+1
4.30040E+1 4.33202E+1 4.36364E+1 4.39526E+1 4.42688E+1
4.45850E+1 4.49012E+1 4.52569E+1 4.56126E+1 4.59684E+1
4.63241E+1 4.66798E+1 4.70356E+1 4.73913E+1 4.77470E+1
4.81028E+1 4.84585E+1 4.88142E+1 4.91700E+1 4.95257E+1
4.98814E+1 5.02372E+1 5.05929E+1 5.09881E+1 5.13834E+1
5.17787E+1 5.21739E+1 5.25692E+1 5.29644E+1 5.33597E+1
5.37549E+1 5.41502E+1 5.45455E+1 5.49407E+1 5.53360E+1
5.57312E+1 5.61265E+1 5.69170E+1 5.77075E+1 5.84980E+1
5.92885E+1 6.00791E+1 6.08696E+1 6.16601E+1 6.24506E+1
6.32411E+1 6.40316E+1 6.48221E+1 6.56126E+1 6.64032E+1
6.71937E+1 6.79842E+1 6.87747E+1 6.95652E+1 7.03557E+1
7.11462E+1 7.19368E+1 7.27273E+1 7.35178E+1 7.43083E+1
7.50988E+1 7.58893E+1 7.66798E+1 7.74704E+1 7.82609E+1
7.90514E+1 8.06324E+1 8.22134E+1 8.37945E+1 8.53755E+1
8.69565E+1 8.85375E+1 9.01186E+1 9.16996E+1 9.32806E+1
9.48617E+1 9.64427E+1 9.80237E+1 9.96047E+1 1.01186E+2
1.02767E+2 1.04348E+2 1.05929E+2 1.07510E+2 1.09091E+2
1.10672E+2 1.12253E+2 1.13834E+2 1.15415E+2 1.16996E+2
1.18577E+2 1.20158E+2 1.21739E+2 1.23320E+2 1.24901E+2
1.26482E+2 1.28063E+2 1.29644E+2 1.31225E+2 1.32806E+2
1.34387E+2 1.35968E+2 1.37549E+2 1.39130E+2 1.40711E+2
1.42292E+2 1.43874E+2 1.45455E+2 1.47036E+2 1.48617E+2
1.50198E+2 1.51779E+2 1.53360E+2 1.54941E+2 1.56522E+2
1.58103E+2 1.59684E+2 1.61265E+2 1.62846E+2 1.64427E+2
1.66008E+2 1.67589E+2 1.69170E+2 1.70751E+2 1.72332E+2
1.73913E+2 1.75494E+2 1.77075E+2 1.78656E+2 1.80237E+2
1.81818E+2 1.83399E+2 1.84980E+2 1.86561E+2 1.88142E+2
1.89723E+2 1.91304E+2 1.92885E+2 1.94466E+2 1.96047E+2
1.97628E+2 / beta grid
20/ temperature (K)
0.0005 294/  phonon frequency distribution
0.00000E+00 1.83201E-05 2.39790E-04 8.52822E-04 1.35045E-03 1.88938E-03
3.53833E-03 4.20386E-03 4.54912E-03 7.48153E-03 9.29764E-03 9.73278E-03
1.36714E-02 1.53297E-02 1.83595E-02 2.33317E-02 2.48376E-02 2.97629E-02
3.64045E-02 4.04736E-02 4.80793E-02 5.56461E-02 6.50780E-02 7.62677E-02
8.95173E-02 1.07073E-01 1.32994E-01 1.68757E-01 2.18537E-01 2.58640E-01
3.08222E-01 3.47956E-01 3.05865E-01 2.58914E-01 2.36824E-01 2.31654E-01
2.37674E-01 2.65759E-01 2.88565E-01 2.63647E-01 2.41951E-01 2.62423E-01
3.26708E-01 3.00841E-01 1.94236E-01 1.35102E-01 1.05490E-01 8.12790E-02
5.70094E-02 2.92759E-02 6.34040E-03 5.30256E-04 6.54571E-06 0.00000E+00
0.00000E+00 0.00000E+00 0.00000E+00 0.00000E+00 0.00000E+00 0.00000E+00
0.00000E+00 0.00000E+00 0.00000E+00 0.00000E+00 0.00000E+00 0.00000E+00
0.00000E+00 0.00000E+00 0.00000E+00 0.00000E+00 0.00000E+00 0.00000E+00
0.00000E+00 0.00000E+00 0.00000E+00 0.00000E+00 0.00000E+00 0.00000E+00
0.00000E+00 0.00000E+00 0.00000E+00 0.00000E+00 0.00000E+00 0.00000E+00
0.00000E+00 0.00000E+00 0.00000E+00 0.00000E+00 0.00000E+00 0.00000E+00
0.00000E+00 0.00000E+00 0.00000E+00 0.00000E+00 0.00000E+00 0.00000E+00
0.00000E+00 0.00000E+00 0.00000E+00 0.00000E+00 0.00000E+00 0.00000E+00
0.00000E+00 0.00000E+00 0.00000E+00 0.00000E+00 0.00000E+00 0.00000E+00
0.00000E+00 0.00000E+00 0.00000E+00 0.00000E+00 0.00000E+00 0.00000E+00
0.00000E+00 0.00000E+00 0.00000E+00 0.00000E+00 0.00000E+00 0.00000E+00
0.00000E+00 0.00000E+00 0.00000E+00 0.00000E+00 0.00000E+00 0.00000E+00
0.00000E+00 0.00000E+00 0.00000E+00 0.00000E+00 0.00000E+00 0.00000E+00
```

```
0.00000E+00 0.00000E+00 0.00000E+00 0.00000E+00 0.00000E+00 0.00000E+00
0.00000E+00 0.00000E+00 0.00000E+00 0.00000E+00 0.00000E+00 0.00000E+00
0.00000E+00 0.00000E+00 0.00000E+00 0.00000E+00 0.00000E+00 0.00000E+00
0.00000E+00 0.00000E+00 0.00000E+00 0.00000E+00 0.00000E+00 0.00000E+00
0.00000E+00 0.00000E+00 0.00000E+00 0.00000E+00 0.00000E+00 0.00000E+00
0.00000E+00 0.00000E+00 0.00000E+00 0.00000E+00 0.00000E+00 0.00000E+00
0.00000E+00 0.00000E+00 0.00000E+00 0.00000E+00 0.00000E+00 0.00000E+00
0.00000E+00 0.00000E+00 0.00000E+00 0.00000E+00 0.00000E+00 0.00000E+00
0.00000E+00 0.00000E+00 0.00000E+00 0.00000E+00 0.00000E+00 0.00000E+00
0.00000E+00 0.00000E+00 0.00000E+00 0.00000E+00 0.00000E+00 0.00000E+00
0.00000E+00 0.00000E+00 0.00000E+00 0.00000E+00 0.00000E+00 0.00000E+00
0.00000E+00 0.00000E+00 0.00000E+00 0.00000E+00 0.00000E+00 0.00000E+00
0.00000E+00 0.00000E+00 0.00000E+00 0.00000E+00 0.00000E+00 0.00000E+00
0.00000E+00 0.00000E+00 0.00000E+00 0.00000E+00 0.00000E+00 0.00000E+00
0.00000E+00 0.00000E+00 0.00000E+00 0.00000E+00 0.00000E+00 0.00000E+00
0.00000E+00 0.00000E+00 4.42806E-09 8.80776E-07 1.37711E-04 1.43478E-03
4.55821E-03 5.36768E-03 4.33151E-03 3.46662E-03 2.53730E-03 1.67517E-03
1.34876E-03 1.40070E-03 1.26686E-03 1.05687E-03 8.99659E-04 7.61987E-04
5.73464E-04 3.80815E-04 2.79738E-04 2.17693E-04 2.25697E-04 3.95083E-04
5.27174E-04 5.70929E-04 5.59940E-04 4.79168E-04 4.16252E-04 3.65699E-04
2.90942E-04 2.17499E-04 1.61848E-04 9.39549E-05 3.87435E-05 1.83609E-05
2.21588E-05 5.42697E-05 1.26730E-04 1.86021E-04 1.66122E-04 1.16421E-04
8.35776E-05 8.13244E-05 7.58855E-05 9.49951E-05 9.97768E-05 9.39511E-05
9.39927E-05 8.82097E-05 8.54355E-05 7.61568E-05 5.57639E-05 3.02813E-05
1.18376E-05 2.39076E-06 7.78195E-08 1.49802E-10 0.00000E+00 0.00000E+00
0.00000E+00 0.00000E+00 0.00000E+00 0.00000E+00 0.00000E+00 0.00000E+00
0.00000E+00 0.00000E+00 0.00000E+00 0.00000E+00 0.00000E+00 0.00000E+00/
0. 0. 1./  weights
0/
295/ temperature (K)
0.0005 282/  phonon frequency distribution
0.00000E+00 2.13570E-05 2.66701E-04 8.97182E-04 1.39023E-03 1.99633E-03
3.80413E-03 4.30107E-03 4.87140E-03 8.02661E-03 9.49344E-03 1.05850E-02
1.44254E-02 1.59654E-02 1.95425E-02 2.44256E-02 2.57783E-02 3.22257E-02
3.76321E-02 4.26633E-02 5.00749E-02 5.78896E-02 6.75410E-02 7.92755E-02
9.25103E-02 1.11097E-01 1.37093E-01 1.74134E-01 2.23205E-01 2.60465E-01
3.08160E-01 3.44024E-01 2.95807E-01 2.51620E-01 2.29578E-01 2.24564E-01
2.28413E-01 2.49587E-01 2.71823E-01 2.54843E-01 2.29581E-01 2.34855E-01
2.87702E-01 3.25195E-01 2.34791E-01 1.47724E-01 1.12816E-01 8.84201E-02
6.62076E-02 4.14992E-02 1.56547E-02 1.86377E-03 7.11647E-05 0.00000E+00
0.00000E+00 0.00000E+00 0.00000E+00 0.00000E+00 0.00000E+00 0.00000E+00
0.00000E+00 0.00000E+00 0.00000E+00 0.00000E+00 0.00000E+00 0.00000E+00
0.00000E+00 0.00000E+00 0.00000E+00 0.00000E+00 0.00000E+00 0.00000E+00
0.00000E+00 0.00000E+00 0.00000E+00 0.00000E+00 0.00000E+00 0.00000E+00
0.00000E+00 0.00000E+00 0.00000E+00 0.00000E+00 0.00000E+00 0.00000E+00
0.00000E+00 0.00000E+00 0.00000E+00 0.00000E+00 0.00000E+00 0.00000E+00
0.00000E+00 0.00000E+00 0.00000E+00 0.00000E+00 0.00000E+00 0.00000E+00
0.00000E+00 0.00000E+00 0.00000E+00 0.00000E+00 0.00000E+00 0.00000E+00
0.00000E+00 0.00000E+00 0.00000E+00 0.00000E+00 0.00000E+00 0.00000E+00
0.00000E+00 0.00000E+00 0.00000E+00 0.00000E+00 0.00000E+00 0.00000E+00
0.00000E+00 0.00000E+00 0.00000E+00 0.00000E+00 0.00000E+00 0.00000E+00
0.00000E+00 0.00000E+00 0.00000E+00 0.00000E+00 0.00000E+00 0.00000E+00
0.00000E+00 0.00000E+00 0.00000E+00 0.00000E+00 0.00000E+00 0.00000E+00
0.00000E+00 0.00000E+00 0.00000E+00 0.00000E+00 0.00000E+00 0.00000E+00
```

```
0.00000E+00 0.00000E+00 0.00000E+00 0.00000E+00 0.00000E+00 0.00000E+00
0.00000E+00 0.00000E+00 0.00000E+00 0.00000E+00 0.00000E+00 0.00000E+00
0.00000E+00 0.00000E+00 0.00000E+00 0.00000E+00 0.00000E+00 0.00000E+00
0.00000E+00 0.00000E+00 0.00000E+00 0.00000E+00 0.00000E+00 0.00000E+00
0.00000E+00 0.00000E+00 0.00000E+00 0.00000E+00 0.00000E+00 0.00000E+00
0.00000E+00 0.00000E+00 0.00000E+00 0.00000E+00 0.00000E+00 0.00000E+00
0.00000E+00 0.00000E+00 0.00000E+00 0.00000E+00 0.00000E+00 0.00000E+00
0.00000E+00 0.00000E+00 0.00000E+00 0.00000E+00 0.00000E+00 0.00000E+00
0.00000E+00 0.00000E+00 0.00000E+00 0.00000E+00 0.00000E+00 0.00000E+00
0.00000E+00 0.00000E+00 0.00000E+00 0.00000E+00 0.00000E+00 0.00000E+00
0.00000E+00 0.00000E+00 0.00000E+00 0.00000E+00 0.00000E+00 0.00000E+00
0.00000E+00 0.00000E+00 0.00000E+00 0.00000E+00 0.00000E+00 0.00000E+00
0.00000E+00 0.00000E+00 0.00000E+00 0.00000E+00 0.00000E+00 0.00000E+00
0.00000E+00 0.00000E+00 0.00000E+00 0.00000E+00 0.00000E+00 0.00000E+00
0.00000E+00 0.00000E+00 0.00000E+00 3.85342E-09 6.20646E-06 1.95209E-04
1.66342E-03 5.14459E-03 6.21120E-03 4.67623E-03 3.12457E-03 1.99778E-03
1.45153E-03 1.50452E-03 1.42416E-03 1.15877E-03 9.83065E-04 8.43037E-04
7.28964E-04 5.92511E-04 4.15755E-04 2.98488E-04 2.10887E-04 1.84035E-04
2.86874E-04 5.07077E-04 6.66023E-04 6.75664E-04 6.06888E-04 5.42058E-04
4.51820E-04 3.37909E-04 2.46395E-04 1.78096E-04 9.79893E-05 4.29663E-05
3.38847E-05 5.46715E-05 1.10875E-04 1.66445E-04 1.78499E-04 1.36252E-04
9.69675E-05 8.30333E-05 7.28823E-05 6.77647E-05 8.60438E-05 9.12244E-05
8.84116E-05 8.55743E-05 7.96776E-05 7.54901E-05 6.60065E-05 4.92475E-05
2.81186E-05 1.21435E-05 2.80306E-06 1.37121E-07 2.07107E-09 0.00000E+00/
0. 0. 1./  weights
0/
550/ temperature (K)
0.0005 282/  phonon frequency distribution
0.00000E+00 2.28657E-05 2.79533E-04 9.18961E-04 1.41100E-03 2.03839E-03
3.90764E-03 4.32977E-03 4.98511E-03 8.27312E-03 9.55621E-03 1.09127E-02
1.46511E-02 1.62429E-02 2.01727E-02 2.47925E-02 2.61581E-02 3.30157E-02
3.81927E-02 4.38005E-02 5.11082E-02 5.93103E-02 6.90548E-02 8.13956E-02
9.48524E-02 1.14842E-01 1.42756E-01 1.82226E-01 2.29689E-01 2.66879E-01
3.19806E-01 3.38868E-01 2.87350E-01 2.46221E-01 2.28416E-01 2.22709E-01
2.28431E-01 2.50846E-01 2.65387E-01 2.43197E-01 2.23357E-01 2.30918E-01
2.88388E-01 3.13762E-01 2.18207E-01 1.45149E-01 1.11360E-01 8.83090E-02
6.76260E-02 4.54044E-02 2.01277E-02 3.95878E-03 2.32257E-01 0.00000E+00
0.00000E+00 0.00000E+00 0.00000E+00 0.00000E+00 0.00000E+00 0.00000E+00
0.00000E+00 0.00000E+00 0.00000E+00 0.00000E+00 0.00000E+00 0.00000E+00
0.00000E+00 0.00000E+00 0.00000E+00 0.00000E+00 0.00000E+00 0.00000E+00
0.00000E+00 0.00000E+00 0.00000E+00 0.00000E+00 0.00000E+00 0.00000E+00
0.00000E+00 0.00000E+00 0.00000E+00 0.00000E+00 0.00000E+00 0.00000E+00
0.00000E+00 0.00000E+00 0.00000E+00 0.00000E+00 0.00000E+00 0.00000E+00
0.00000E+00 0.00000E+00 0.00000E+00 0.00000E+00 0.00000E+00 0.00000E+00
0.00000E+00 0.00000E+00 0.00000E+00 0.00000E+00 0.00000E+00 0.00000E+00
0.00000E+00 0.00000E+00 0.00000E+00 0.00000E+00 0.00000E+00 0.00000E+00
0.00000E+00 0.00000E+00 0.00000E+00 0.00000E+00 0.00000E+00 0.00000E+00
0.00000E+00 0.00000E+00 0.00000E+00 0.00000E+00 0.00000E+00 0.00000E+00
0.00000E+00 0.00000E+00 0.00000E+00 0.00000E+00 0.00000E+00 0.00000E+00
0.00000E+00 0.00000E+00 0.00000E+00 0.00000E+00 0.00000E+00 0.00000E+00
0.00000E+00 0.00000E+00 0.00000E+00 0.00000E+00 0.00000E+00 0.00000E+00
0.00000E+00 0.00000E+00 0.00000E+00 0.00000E+00 0.00000E+00 0.00000E+00
0.00000E+00 0.00000E+00 0.00000E+00 0.00000E+00 0.00000E+00 0.00000E+00
0.00000E+00 0.00000E+00 0.00000E+00 0.00000E+00 0.00000E+00 0.00000E+00
```

```
0.00000E+00 0.00000E+00 0.00000E+00 0.00000E+00 0.00000E+00 0.00000E+00
0.00000E+00 0.00000E+00 0.00000E+00 0.00000E+00 0.00000E+00 0.00000E+00
0.00000E+00 0.00000E+00 0.00000E+00 0.00000E+00 0.00000E+00 0.00000E+00
0.00000E+00 0.00000E+00 0.00000E+00 0.00000E+00 0.00000E+00 0.00000E+00
0.00000E+00 0.00000E+00 0.00000E+00 0.00000E+00 0.00000E+00 0.00000E+00
0.00000E+00 0.00000E+00 0.00000E+00 0.00000E+00 0.00000E+00 0.00000E+00
0.00000E+00 0.00000E+00 0.00000E+00 0.00000E+00 0.00000E+00 0.00000E+00
0.00000E+00 0.00000E+00 0.00000E+00 0.00000E+00 0.00000E+00 0.00000E+00
0.00000E+00 0.00000E+00 0.00000E+00 0.00000E+00 0.00000E+00 0.00000E+00
0.00000E+00 0.00000E+00 0.00000E+00 0.00000E+00 0.00000E+00 0.00000E+00
0.00000E+00 0.00000E+00 0.00000E+00 0.00000E+00 0.00000E+00 0.00000E+00
0.00000E+00 0.00000E+00 0.00000E+00 8.76870E-08 2.54303E-05 5.29589E-04
3.02686E-03 6.08879E-03 5.58279E-03 4.23679E-03 3.11818E-03 2.04602E-03
1.64242E-03 1.55168E-03 1.34450E-03 1.06678E-03 8.56044E-04 6.88327E-04
5.48429E-04 4.23969E-04 3.11497E-04 2.14464E-04 2.18072E-04 3.22472E-04
5.36724E-04 7.71774E-04 8.16213E-04 7.21731E-04 6.15645E-04 5.00019E-04
3.73161E-04 2.70321E-04 2.04043E-04 1.22391E-04 5.43668E-05 3.63321E-05
5.03206E-05 1.00100E-04 1.67339E-04 1.96316E-04 1.53862E-04 1.10540E-04
9.61313E-05 8.13409E-05 7.48251E-05 8.89023E-05 1.00146E-04 1.01296E-04
9.50041E-05 8.86581E-05 7.96925E-05 6.27564E-05 3.89057E-05 1.77156E-05
4.96691E-06 5.21019E-07 3.74771E-09 0.00000E+00 0.00000E+00 0.00000E+00/
0. 0. 1./  weights
0/
800/ temperature (K)
0.0005 282/  phonon frequency distribution
0.00000E+00 2.97817E-05 3.30771E-04 1.00096E-03 1.49306E-03 2.33534E-03
4.29398E-03 4.41294E-03 5.79650E-03 9.07791E-03 9.83539E-03 1.26187E-02
1.55438E-02 1.73758E-02 2.26240E-02 2.57169E-02 2.84536E-02 3.58626E-02
4.02985E-02 4.70312E-02 5.43851E-02 6.29628E-02 7.35962E-02 8.59197E-02
1.00473E-01 1.22660E-01 1.51424E-01 1.95318E-01 2.41407E-01 2.80197E-01
3.32925E-01 3.25902E-01 2.72033E-01 2.39219E-01 2.26303E-01 2.21833E-01
2.34774E-01 2.58716E-01 2.65128E-01 2.37656E-01 2.23430E-01 2.46888E-01
3.14689E-01 3.02437E-01 1.91396E-01 1.31986E-01 1.02097E-01 7.91290E-02
5.57579E-02 2.86287E-02 7.18514E-03 4.73020E-04 0.00000E+00 0.00000E+00
0.00000E+00 0.00000E+00 0.00000E+00 0.00000E+00 0.00000E+00 0.00000E+00
0.00000E+00 0.00000E+00 0.00000E+00 0.00000E+00 0.00000E+00 0.00000E+00
0.00000E+00 0.00000E+00 0.00000E+00 0.00000E+00 0.00000E+00 0.00000E+00
0.00000E+00 0.00000E+00 0.00000E+00 0.00000E+00 0.00000E+00 0.00000E+00
0.00000E+00 0.00000E+00 0.00000E+00 0.00000E+00 0.00000E+00 0.00000E+00
0.00000E+00 0.00000E+00 0.00000E+00 0.00000E+00 0.00000E+00 0.00000E+00
0.00000E+00 0.00000E+00 0.00000E+00 0.00000E+00 0.00000E+00 0.00000E+00
0.00000E+00 0.00000E+00 0.00000E+00 0.00000E+00 0.00000E+00 0.00000E+00
0.00000E+00 0.00000E+00 0.00000E+00 0.00000E+00 0.00000E+00 0.00000E+00
0.00000E+00 0.00000E+00 0.00000E+00 0.00000E+00 0.00000E+00 0.00000E+00
0.00000E+00 0.00000E+00 0.00000E+00 0.00000E+00 0.00000E+00 0.00000E+00
0.00000E+00 0.00000E+00 0.00000E+00 0.00000E+00 0.00000E+00 0.00000E+00
0.00000E+00 0.00000E+00 0.00000E+00 0.00000E+00 0.00000E+00 0.00000E+00
0.00000E+00 0.00000E+00 0.00000E+00 0.00000E+00 0.00000E+00 0.00000E+00
0.00000E+00 0.00000E+00 0.00000E+00 0.00000E+00 0.00000E+00 0.00000E+00
0.00000E+00 0.00000E+00 0.00000E+00 0.00000E+00 0.00000E+00 0.00000E+00
0.00000E+00 0.00000E+00 0.00000E+00 0.00000E+00 0.00000E+00 0.00000E+00
0.00000E+00 0.00000E+00 0.00000E+00 0.00000E+00 0.00000E+00 0.00000E+00
0.00000E+00 0.00000E+00 0.00000E+00 0.00000E+00 0.00000E+00 0.00000E+00
0.00000E+00 0.00000E+00 0.00000E+00 0.00000E+00 0.00000E+00 0.00000E+00
```

```
0.00000E+00 0.00000E+00 0.00000E+00 0.00000E+00 0.00000E+00 0.00000E+00
0.00000E+00 0.00000E+00 0.00000E+00 0.00000E+00 0.00000E+00 0.00000E+00
0.00000E+00 0.00000E+00 0.00000E+00 0.00000E+00 0.00000E+00 0.00000E+00
0.00000E+00 0.00000E+00 0.00000E+00 0.00000E+00 0.00000E+00 0.00000E+00
0.00000E+00 0.00000E+00 0.00000E+00 0.00000E+00 0.00000E+00 0.00000E+00
0.00000E+00 0.00000E+00 0.00000E+00 0.00000E+00 0.00000E+00 0.00000E+00
0.00000E+00 0.00000E+00 0.00000E+00 0.00000E+00 0.00000E+00 0.00000E+00
0.00000E+00 0.00000E+00 0.00000E+00 0.00000E+00 0.00000E+00 0.00000E+00
0.00000E+00 0.00000E+00 7.11868E-09 3.26090E-06 1.56863E-04 1.29517E-03
4.32965E-03 6.19172E-03 5.22776E-03 3.84533E-03 2.54611E-03 1.91571E-03
1.74613E-03 1.57960E-03 1.28275E-03 1.03428E-03 8.41729E-04 6.79609E-04
5.53326E-04 3.68288E-04 2.39145E-04 2.61200E-04 4.60154E-04 8.08396E-04
9.35632E-04 8.23856E-04 6.52042E-04 5.15844E-04 3.81632E-04 2.71446E-04
1.94426E-04 1.11549E-04 5.10420E-05 4.01602E-05 5.85182E-05 1.14590E-04
1.85273E-04 1.75497E-04 1.40009E-04 1.08753E-04 8.93974E-05 8.64296E-05
8.22069E-05 9.93569E-05 1.08028E-04 9.47848E-05 9.26174E-05 8.63720E-05
8.10966E-05 7.34129E-05 5.91956E-05 3.74180E-05 1.70800E-05 4.64889E-06
3.73060E-07 5.04561E-09 0.00000E+00 0.00000E+00 0.00000E+00 0.00000E+00/
0. 0. 1. /  weights
0/
900/ temperature (K)
0.0005 282/  phonon frequency distribution
0.00000E+00 3.34340E-05 3.51147E-04 1.02442E-03 1.48924E-03 2.38043E-03
4.39489E-03 4.47163E-03 5.93921E-03 9.17010E-03 9.96261E-03 1.30208E-02
1.56111E-02 1.76232E-02 2.29525E-02 2.59641E-02 2.91755E-02 3.58187E-02
4.11551E-02 4.77200E-02 5.52451E-02 6.36825E-02 7.52903E-02 8.76557E-02
1.03058E-01 1.27223E-01 1.59100E-01 2.04470E-01 2.45612E-01 2.86440E-01
3.37716E-01 3.18763E-01 2.64506E-01 2.36441E-01 2.25343E-01 2.22772E-01
2.36943E-01 2.58609E-01 2.53286E-01 2.29262E-01 2.18926E-01 2.47197E-01
3.20153E-01 3.01902E-01 1.88965E-01 1.26858E-01 9.97034E-02 7.71983E-02
5.45009E-02 2.80803E-02 6.09365E-03 4.45512E-04 3.06417E-06 0.00000E+00
0.00000E+00 0.00000E+00 0.00000E+00 0.00000E+00 0.00000E+00 0.00000E+00
0.00000E+00 0.00000E+00 0.00000E+00 0.00000E+00 0.00000E+00 0.00000E+00
0.00000E+00 0.00000E+00 0.00000E+00 0.00000E+00 0.00000E+00 0.00000E+00
0.00000E+00 0.00000E+00 0.00000E+00 0.00000E+00 0.00000E+00 0.00000E+00
0.00000E+00 0.00000E+00 0.00000E+00 0.00000E+00 0.00000E+00 0.00000E+00
0.00000E+00 0.00000E+00 0.00000E+00 0.00000E+00 0.00000E+00 0.00000E+00
0.00000E+00 0.00000E+00 0.00000E+00 0.00000E+00 0.00000E+00 0.00000E+00
0.00000E+00 0.00000E+00 0.00000E+00 0.00000E+00 0.00000E+00 0.00000E+00
0.00000E+00 0.00000E+00 0.00000E+00 0.00000E+00 0.00000E+00 0.00000E+00
0.00000E+00 0.00000E+00 0.00000E+00 0.00000E+00 0.00000E+00 0.00000E+00
0.00000E+00 0.00000E+00 0.00000E+00 0.00000E+00 0.00000E+00 0.00000E+00
0.00000E+00 0.00000E+00 0.00000E+00 0.00000E+00 0.00000E+00 0.00000E+00
0.00000E+00 0.00000E+00 0.00000E+00 0.00000E+00 0.00000E+00 0.00000E+00
0.00000E+00 0.00000E+00 0.00000E+00 0.00000E+00 0.00000E+00 0.00000E+00
0.00000E+00 0.00000E+00 0.00000E+00 0.00000E+00 0.00000E+00 0.00000E+00
0.00000E+00 0.00000E+00 0.00000E+00 0.00000E+00 0.00000E+00 0.00000E+00
0.00000E+00 0.00000E+00 0.00000E+00 0.00000E+00 0.00000E+00 0.00000E+00
0.00000E+00 0.00000E+00 0.00000E+00 0.00000E+00 0.00000E+00 0.00000E+00
0.00000E+00 0.00000E+00 0.00000E+00 0.00000E+00 0.00000E+00 0.00000E+00
0.00000E+00 0.00000E+00 0.00000E+00 0.00000E+00 0.00000E+00 0.00000E+00
0.00000E+00 0.00000E+00 0.00000E+00 0.00000E+00 0.00000E+00 0.00000E+00
0.00000E+00 0.00000E+00 0.00000E+00 0.00000E+00 0.00000E+00 0.00000E+00
0.00000E+00 0.00000E+00 0.00000E+00 0.00000E+00 0.00000E+00 0.00000E+00
```

```
0.00000E+00 0.00000E+00 0.00000E+00 0.00000E+00 0.00000E+00 0.00000E+00
0.00000E+00 0.00000E+00 0.00000E+00 0.00000E+00 0.00000E+00 0.00000E+00
0.00000E+00 0.00000E+00 0.00000E+00 0.00000E+00 0.00000E+00 0.00000E+00
0.00000E+00 0.00000E+00 0.00000E+00 0.00000E+00 0.00000E+00 0.00000E+00
0.00000E+00 0.00000E+00 0.00000E+00 0.00000E+00 0.00000E+00 9.40180E-09
4.30816E-06 1.37212E-04 9.62188E-04 2.97338E-03 4.66551E-03 4.72488E-03
3.50371E-03 2.66382E-03 2.34855E-03 2.17678E-03 2.02067E-03 1.71490E-03
1.51980E-03 1.31043E-03 1.06879E-03 9.22398E-04 7.55374E-04 4.99448E-04
2.76754E-04 2.33038E-04 3.75070E-04 6.28040E-04 8.01589E-04 8.26125E-04
7.12232E-04 5.77381E-04 4.75315E-04 3.70351E-04 2.78016E-04 2.12115E-04
1.26392E-04 5.31723E-05 3.36102E-05 5.38709E-05 1.17432E-04 2.05589E-04
2.01993E-04 1.49320E-04 1.08672E-04 9.15709E-05 9.70469E-05 1.21959E-04
1.38998E-04 1.26973E-04 1.22954E-04 1.14983E-04 1.06036E-04 9.34840E-05
7.10668E-05 4.27962E-05 1.91552E-05 4.99653E-06 4.19032E-07 9.43987E-10
0.00000E+00 0.00000E+00 0.00000E+00 0.00000E+00 0.00000E+00 0.00000E+00/
0. 0. 1./  weights
0/
1000/ temperature (K)
0.0005 282/  phonon frequency distribution
0.00000E+00 3.11473E-05 3.39770E-04 1.01629E-03 1.50031E-03 2.34514E-03
4.33775E-03 4.42023E-03 6.00873E-03 9.23619E-03 9.90590E-03 1.30966E-02
1.57513E-02 1.78180E-02 2.34872E-02 2.61627E-02 2.98968E-02 3.68476E-02
4.17850E-02 4.91925E-02 5.67949E-02 6.60048E-02 7.81845E-02 9.02755E-02
1.07712E-01 1.32592E-01 1.65934E-01 2.14000E-01 2.53760E-01 2.95112E-01
3.37002E-01 3.10785E-01 2.59931E-01 2.33701E-01 2.25005E-01 2.25260E-01
2.40734E-01 2.64015E-01 2.56126E-01 2.31742E-01 2.30545E-01 2.74239E-01
3.26976E-01 2.52136E-01 1.57507E-01 1.18333E-01 9.31792E-02 7.17190E-02
4.96455E-02 2.40847E-02 5.50382E-03 3.40501E-04 0.00000E+00 0.00000E+00
0.00000E+00 0.00000E+00 0.00000E+00 0.00000E+00 0.00000E+00 0.00000E+00
0.00000E+00 0.00000E+00 0.00000E+00 0.00000E+00 0.00000E+00 0.00000E+00
0.00000E+00 0.00000E+00 0.00000E+00 0.00000E+00 0.00000E+00 0.00000E+00
0.00000E+00 0.00000E+00 0.00000E+00 0.00000E+00 0.00000E+00 0.00000E+00
0.00000E+00 0.00000E+00 0.00000E+00 0.00000E+00 0.00000E+00 0.00000E+00
0.00000E+00 0.00000E+00 0.00000E+00 0.00000E+00 0.00000E+00 0.00000E+00
0.00000E+00 0.00000E+00 0.00000E+00 0.00000E+00 0.00000E+00 0.00000E+00
0.00000E+00 0.00000E+00 0.00000E+00 0.00000E+00 0.00000E+00 0.00000E+00
0.00000E+00 0.00000E+00 0.00000E+00 0.00000E+00 0.00000E+00 0.00000E+00
0.00000E+00 0.00000E+00 0.00000E+00 0.00000E+00 0.00000E+00 0.00000E+00
0.00000E+00 0.00000E+00 0.00000E+00 0.00000E+00 0.00000E+00 0.00000E+00
0.00000E+00 0.00000E+00 0.00000E+00 0.00000E+00 0.00000E+00 0.00000E+00
0.00000E+00 0.00000E+00 0.00000E+00 0.00000E+00 0.00000E+00 0.00000E+00
0.00000E+00 0.00000E+00 0.00000E+00 0.00000E+00 0.00000E+00 0.00000E+00
0.00000E+00 0.00000E+00 0.00000E+00 0.00000E+00 0.00000E+00 0.00000E+00
0.00000E+00 0.00000E+00 0.00000E+00 0.00000E+00 0.00000E+00 0.00000E+00
0.00000E+00 0.00000E+00 0.00000E+00 0.00000E+00 0.00000E+00 0.00000E+00
0.00000E+00 0.00000E+00 0.00000E+00 0.00000E+00 0.00000E+00 0.00000E+00
0.00000E+00 0.00000E+00 0.00000E+00 0.00000E+00 0.00000E+00 0.00000E+00
0.00000E+00 0.00000E+00 0.00000E+00 0.00000E+00 0.00000E+00 0.00000E+00
0.00000E+00 0.00000E+00 0.00000E+00 0.00000E+00 0.00000E+00 0.00000E+00
0.00000E+00 0.00000E+00 0.00000E+00 0.00000E+00 0.00000E+00 0.00000E+00
0.00000E+00 0.00000E+00 0.00000E+00 0.00000E+00 0.00000E+00 0.00000E+00
0.00000E+00 0.00000E+00 0.00000E+00 0.00000E+00 0.00000E+00 0.00000E+00
0.00000E+00 0.00000E+00 0.00000E+00 0.00000E+00 0.00000E+00 0.00000E+00
0.00000E+00 0.00000E+00 0.00000E+00 0.00000E+00 0.00000E+00 0.00000E+00
```

```
0.00000E+00 0.00000E+00 0.00000E+00 0.00000E+00 0.00000E+00 0.00000E+00
0.00000E+00 0.00000E+00 0.00000E+00 0.00000E+00 0.00000E+00 0.00000E+00
8.73905E-09 1.41796E-06 5.11525E-05 1.08625E-03 3.95841E-03 5.98038E-03
5.12076E-03 3.82595E-03 2.80214E-03 2.12815E-03 1.71864E-03 1.31363E-03
1.22000E-03 1.06781E-03 8.27832E-04 6.43218E-04 5.24976E-04 3.91884E-04
2.66359E-04 2.43137E-04 3.03847E-04 5.04281E-04 8.28854E-04 9.97922E-04
9.31444E-04 7.64631E-04 5.86196E-04 4.35115E-04 2.85719E-04 1.48448E-04
7.20213E-05 4.81145E-05 5.20783E-05 7.84010E-05 1.55733E-04 2.51645E-04
2.37581E-04 1.58808E-04 1.19260E-04 1.17080E-04 1.42608E-04 1.38123E-04
1.21985E-04 1.13280E-04 1.02542E-04 9.04442E-05 7.24438E-05 4.61925E-05
2.14559E-05 5.71622E-06 6.49749E-07 3.89844E-09 0.00000E+00 0.00000E+00
0.00000E+00 0.00000E+00 0.00000E+00 0.00000E+00 0.00000E+00 0.00000E+00/
0. 0. 1./  weights
0/
1100/ temperature (K)
0.0005 282/  phonon frequency distribution
0.00000E+00 3.30922E-05 3.53488E-04 1.03848E-03 1.52341E-03 2.41804E-03
4.41437E-03 4.42938E-03 6.30652E-03 9.42364E-03 9.97010E-03 1.35631E-02
1.58864E-02 1.84415E-02 2.41963E-02 2.62971E-02 3.09801E-02 3.74013E-02
4.26700E-02 5.01678E-02 5.75674E-02 6.72248E-02 7.96977E-02 9.16955E-02
1.09868E-01 1.34341E-01 1.69692E-01 2.17665E-01 2.54453E-01 2.93147E-01
3.39625E-01 3.14669E-01 2.63287E-01 2.35870E-01 2.26137E-01 2.25911E-01
2.42717E-01 2.64182E-01 2.53501E-01 2.30365E-01 2.27668E-01 2.77685E-01
3.33390E-01 2.52060E-01 1.56560E-01 1.14432E-01 8.98812E-02 6.79316E-02
4.45404E-02 1.86761E-02 2.42722E-03 9.54238E-05 0.00000E+00 0.00000E+00
0.00000E+00 0.00000E+00 0.00000E+00 0.00000E+00 0.00000E+00 0.00000E+00
0.00000E+00 0.00000E+00 0.00000E+00 0.00000E+00 0.00000E+00 0.00000E+00
0.00000E+00 0.00000E+00 0.00000E+00 0.00000E+00 0.00000E+00 0.00000E+00
0.00000E+00 0.00000E+00 0.00000E+00 0.00000E+00 0.00000E+00 0.00000E+00
0.00000E+00 0.00000E+00 0.00000E+00 0.00000E+00 0.00000E+00 0.00000E+00
0.00000E+00 0.00000E+00 0.00000E+00 0.00000E+00 0.00000E+00 0.00000E+00
0.00000E+00 0.00000E+00 0.00000E+00 0.00000E+00 0.00000E+00 0.00000E+00
0.00000E+00 0.00000E+00 0.00000E+00 0.00000E+00 0.00000E+00 0.00000E+00
0.00000E+00 0.00000E+00 0.00000E+00 0.00000E+00 0.00000E+00 0.00000E+00
0.00000E+00 0.00000E+00 0.00000E+00 0.00000E+00 0.00000E+00 0.00000E+00
0.00000E+00 0.00000E+00 0.00000E+00 0.00000E+00 0.00000E+00 0.00000E+00
0.00000E+00 0.00000E+00 0.00000E+00 0.00000E+00 0.00000E+00 0.00000E+00
0.00000E+00 0.00000E+00 0.00000E+00 0.00000E+00 0.00000E+00 0.00000E+00
0.00000E+00 0.00000E+00 0.00000E+00 0.00000E+00 0.00000E+00 0.00000E+00
0.00000E+00 0.00000E+00 0.00000E+00 0.00000E+00 0.00000E+00 0.00000E+00
0.00000E+00 0.00000E+00 0.00000E+00 0.00000E+00 0.00000E+00 0.00000E+00
0.00000E+00 0.00000E+00 0.00000E+00 0.00000E+00 0.00000E+00 0.00000E+00
0.00000E+00 0.00000E+00 0.00000E+00 0.00000E+00 0.00000E+00 0.00000E+00
0.00000E+00 0.00000E+00 0.00000E+00 0.00000E+00 0.00000E+00 0.00000E+00
0.00000E+00 0.00000E+00 0.00000E+00 0.00000E+00 0.00000E+00 0.00000E+00
0.00000E+00 0.00000E+00 0.00000E+00 0.00000E+00 0.00000E+00 0.00000E+00
0.00000E+00 0.00000E+00 0.00000E+00 0.00000E+00 0.00000E+00 0.00000E+00
0.00000E+00 0.00000E+00 0.00000E+00 0.00000E+00 0.00000E+00 0.00000E+00
0.00000E+00 0.00000E+00 0.00000E+00 0.00000E+00 0.00000E+00 0.00000E+00
0.00000E+00 0.00000E+00 0.00000E+00 0.00000E+00 0.00000E+00 0.00000E+00
0.00000E+00 0.00000E+00 0.00000E+00 0.00000E+00 0.00000E+00 0.00000E+00
0.00000E+00 0.00000E+00 0.00000E+00 0.00000E+00 0.00000E+00 9.61877E-08
7.57231E-06 1.93927E-04 1.49384E-03 3.86358E-03 5.52159E-03 5.51408E-03
```

```
4.26004E-03 3.09472E-03 2.31913E-03 1.77329E-03 1.48656E-03 1.13293E-03
8.76980E-04 7.02589E-04 5.83248E-04 4.52246E-04 3.09651E-04 2.58920E-04
3.16282E-04 5.29191E-04 8.20380E-04 9.54994E-04 8.70683E-04 7.10387E-04
6.03322E-04 4.89506E-04 3.55761E-04 2.55878E-04 1.45401E-04 5.80430E-05
3.45945E-05 5.27334E-05 1.28362E-04 2.41557E-04 2.29509E-04 1.70255E-04
1.20934E-04 1.07304E-04 1.01212E-04 1.26833E-04 1.38129E-04 1.34623E-04
1.27685E-04 1.19305E-04 9.92095E-05 6.29674E-05 2.63029E-05 6.08450E-06
3.94031E-07 9.67071E-10 0.00000E+00 0.00000E+00 0.00000E+00 0.00000E+00
0.00000E+00 0.00000E+00 0.00000E+00 0.00000E+00 0.00000E+00 0.00000E+00/
0. 0. 1./  weights
0/
1200/ temperature (K)
0.0005 282/  phonon frequency distribution
0.00000E+00 3.41469E-05 3.58542E-04 1.04625E-03 1.53882E-03 2.47596E-03
4.41340E-03 4.44207E-03 6.47024E-03 9.43300E-03 9.97961E-03 1.38053E-02
1.58470E-02 1.86549E-02 2.44724E-02 2.62565E-02 3.15092E-02 3.77371E-02
4.31153E-02 5.09629E-02 5.84656E-02 6.85970E-02 8.15766E-02 9.39765E-02
1.13818E-01 1.40050E-01 1.79297E-01 2.29609E-01 2.69076E-01 3.18302E-01
3.50436E-01 2.99078E-01 2.52877E-01 2.31729E-01 2.24963E-01 2.29875E-01
2.48572E-01 2.57415E-01 2.39004E-01 2.20863E-01 2.25942E-01 2.84490E-01
3.28373E-01 2.33091E-01 1.47096E-01 1.10074E-01 8.67818E-02 6.55266E-02
4.24214E-02 1.71260E-02 2.14806E-03 7.46782E-05 0.00000E+00 0.00000E+00
0.00000E+00 0.00000E+00 0.00000E+00 0.00000E+00 0.00000E+00 0.00000E+00
0.00000E+00 0.00000E+00 0.00000E+00 0.00000E+00 0.00000E+00 0.00000E+00
0.00000E+00 0.00000E+00 0.00000E+00 0.00000E+00 0.00000E+00 0.00000E+00
0.00000E+00 0.00000E+00 0.00000E+00 0.00000E+00 0.00000E+00 0.00000E+00
0.00000E+00 0.00000E+00 0.00000E+00 0.00000E+00 0.00000E+00 0.00000E+00
0.00000E+00 0.00000E+00 0.00000E+00 0.00000E+00 0.00000E+00 0.00000E+00
0.00000E+00 0.00000E+00 0.00000E+00 0.00000E+00 0.00000E+00 0.00000E+00
0.00000E+00 0.00000E+00 0.00000E+00 0.00000E+00 0.00000E+00 0.00000E+00
0.00000E+00 0.00000E+00 0.00000E+00 0.00000E+00 0.00000E+00 0.00000E+00
0.00000E+00 0.00000E+00 0.00000E+00 0.00000E+00 0.00000E+00 0.00000E+00
0.00000E+00 0.00000E+00 0.00000E+00 0.00000E+00 0.00000E+00 0.00000E+00
0.00000E+00 0.00000E+00 0.00000E+00 0.00000E+00 0.00000E+00 0.00000E+00
0.00000E+00 0.00000E+00 0.00000E+00 0.00000E+00 0.00000E+00 0.00000E+00
0.00000E+00 0.00000E+00 0.00000E+00 0.00000E+00 0.00000E+00 0.00000E+00
0.00000E+00 0.00000E+00 0.00000E+00 0.00000E+00 0.00000E+00 0.00000E+00
0.00000E+00 0.00000E+00 0.00000E+00 0.00000E+00 0.00000E+00 0.00000E+00
0.00000E+00 0.00000E+00 0.00000E+00 0.00000E+00 0.00000E+00 0.00000E+00
0.00000E+00 0.00000E+00 0.00000E+00 0.00000E+00 0.00000E+00 0.00000E+00
0.00000E+00 0.00000E+00 0.00000E+00 0.00000E+00 0.00000E+00 0.00000E+00
0.00000E+00 0.00000E+00 0.00000E+00 0.00000E+00 0.00000E+00 0.00000E+00
0.00000E+00 0.00000E+00 0.00000E+00 0.00000E+00 0.00000E+00 0.00000E+00
0.00000E+00 0.00000E+00 0.00000E+00 0.00000E+00 0.00000E+00 0.00000E+00
0.00000E+00 0.00000E+00 0.00000E+00 0.00000E+00 0.00000E+00 0.00000E+00
0.00000E+00 0.00000E+00 0.00000E+00 0.00000E+00 0.00000E+00 0.00000E+00
0.00000E+00 0.00000E+00 0.00000E+00 0.00000E+00 0.00000E+00 0.00000E+00
0.00000E+00 0.00000E+00 0.00000E+00 1.70417E-08 1.92605E-06 1.10748E-04
1.07184E-03 3.38347E-03 5.01761E-03 4.57171E-03 3.29774E-03 2.77777E-03
2.62221E-03 2.32141E-03 1.88475E-03 1.51378E-03 1.22570E-03 9.83410E-04
7.95089E-04 6.49162E-04 5.07756E-04 3.37129E-04 2.92360E-04 4.20917E-04
6.64427E-04 9.26986E-04 9.46990E-04 8.54531E-04 7.37269E-04 5.92735E-04
```

```
4.55549E-04 3.42590E-04 2.13636E-04 9.79052E-05 4.54441E-05 3.27991E-05
4.40304E-05 8.35811E-05 1.78684E-04 2.62357E-04 2.30653E-04 1.60475E-04
1.26839E-04 1.52728E-04 1.68939E-04 1.71305E-04 1.59809E-04 1.54576E-04
1.42363E-04 1.29787E-04 1.04655E-04 6.51305E-05 2.81486E-05 6.75016E-06
5.68214E-07 0.00000E+00 0.00000E+00 0.00000E+00 0.00000E+00 0.00000E+00
0.00000E+00 0.00000E+00 0.00000E+00 0.00000E+00 0.00000E+00 0.00000E+00/
0. 0. 1./  weights
0/
' Y(YH2)    ORNL       EVAL-SEP20 CHAPMAN,RAMIC                    '/
' REF. 0 (2020)        DIST-                                       '/
'---- ENDF/B-VIII      MATERIAL 55                                 '/
'----- THERMAL NEUTRON SCATTERING DATA                             '/
'------ ENDF-6 FORMAT                                              '/
'                                                                  '/
' Temperatures (K)                                                 '/
' ---------------                                                  '/
'   20 295 550 800 900 1000 1100 1200                             '/
'                                                                  '/
' History                                                          '/
' -------                                                          '/
'                                                                  '/
' This evaluation was produced at Oak Ridge National Laboratory in '/
' September 2020 using the LEAPR module of NJOY21 [1]. The phonon  '/
' frequency distributions for H an dY in YH2 were caluclated using '/
' the stochastic Temperature Dependent Effective Potential [2] and '/
' the alpha and beta mesh were the same as those used for the ENDF8'/
' evaluation [3].                                                  '/
'                                                                  '/
' Theory                                                           '/
' ------                                                           '/
' YH2 has a fluorite type cubic crystal structure with the yttrium '/
' atoms forming a face-centered cubic sub-lattice and the hydrogen '/
' atoms situated in the tetrahedral interstices. The stochastic    '/
' Temperature Dependent Effective Potential (s-TDEP) method was    '/
' used with VASP to calculate the phonon spectra for H and Y in    '/
' YH2. The calculated double differential scattering cross section '/
' agrees with measurements.                                        '/
'                                                                  '/
' References                                                       '/
' ----------                                                       '/
' 1. A. C. Kahler Ed., LA-UR-12-27079 (December 20, 2012).         '/
' 2. N. Shulumba, O. Hellman, and A.J. Minnich, "Intrinsic         '/
'    localized mode and low thermal conductivity  of PbSe," Phys.  '/
'    Rev. B, 95, 014302 (2017)                                     '/
' 3. M. L. Zerkle and J. C. Holmes, "A Thermal Neutron Scattering  '/
'    Law for Yttrium Hydride," Int. Conf. Nucl. Data (September,   '/
'    2016).                                                        '/
/
stop
```